Solar-Terrestrial Centre of Excellence

Annual Report 2022

belspo

Royal Observatory of Belgium

RMI

BIRA-IASB

.be

STCE

Solar-**T**errestrial **C**entre of **E**xcellence

https://stce.be/

Ringlaan 3

B-1180 Brussels

Tel.: +32 2 373 0211

Fax: + 32 2 374 9822

Front page - *The Space Pole opened its doors to the general public during the weekend of 24-25 September. Upon entering the premises, the visitors were greeted by house-sized mock-ups of the Earth and the Moon. The theme for this event was "Space for Climate". Credits: Olivier Boulvin*

Table of Contents

A word from the STCE coordinator 4

Structure of the STCE 5

Monitoring space weather: solar-terrestrial highlights in 2022 8

Public outreach meets Science 14

- A Touch of Space Weather - Bringing space weather to visually impaired students 14
- SUN @ Africa Museum 15
- Battle of the scientists 16
- Open Doors at the Space Pole 17

Fundamental research 21

- All Spatial Scales Great and Small 21
- Scale Transfer in 1849: Heinrich Schwabe to Rudolf Wolf 22
- The centennial TSI variation 24
- Solar wind observed close to the Sun by Parker Solar Probe 25
- Plasmasphere-Radiation belts interactions 26
- Ionospheric effects of the Hunga volcano eruption 28
- The global spatiotemporal variability of integrated water vapor 28

Instrumentation and experiments 32

- The Starlink incident as observed by PROBA2/LYRA 32
- Flight Acceptance Review of the Science Operations Centre for PROBA-3/ASPIICS 33
- SIMBA completes its mission 34

Applications, modeling and services 37

- FARSUN: Findability and Accessibility of historical Raw SUnspot Numbers 37
- PITHIA-NRF 39
- T-FORS: Forecasting of Travelling Ionospheric Disturbances 40

Publications 42

- Peer reviewed articles 42
- Presentations and posters at conference 47
- Public Outreach: talks and publications for the general public 56

List of abbreviations 59

A word from the STCE coordinator

Dear reader,

You see before you the annual report of the Solar-Terrestrial Centre of Excellence. It highlights some of the finest results that were achieved in 2022 through collaborations across teams, institutes and borders.

A special focus of this year's report lies on outreach projects. We firmly believe that it is pertinent for researchers to leave their ivory tower and share their research with the public in ways that they can understand it. Special attention was given this year not only to children, but also to the public that does not necessarily has an interest in solar and terrestrial science. Additionally, we developed new ways to teach space weather to blind and visually impaired people.

2022 was also a year of novel discoveries. The Solar Orbiter and Parker Solar Probe satellites are teaming up to revolutionize the knowledge of solar physics and the study of space weather. Nevertheless, older space instruments can still surprise us with new applications. On ground, scientists find clever new uses of old data, while also unlocking them for the future generations.

We look to the future as well, and work hard on preparing new missions and initiate new projects that will guarantee the future of the collaborations fostered by the STCE.

Besides what is highlighted in this report, much other progress was achieved in 2022 in the form of fresh ideas, new results, new collaborations, and new methods. For many of these projects, the details can be found through our elaborate list of presentations and publications that are listed at the very end of this report. Please contact us if you would like more information on any of those.

For now, happy reading!

Ronald Van der Linden
General Coordinator of the Solar-Terrestrial Centre of Excellence
Director General of the Royal Observatory of Belgium

Structure of the STCE

The Solar-Terrestrial Centre of Excellence is a project of scientific collaboration that focuses on the Sun, through interplanetary space, up to the Earth and its atmosphere.

The solid base of the STCE is the expertise that exists in the 3 Federal Scientific Institutes of the Brussels Space Pole: the Royal Observatory of Belgium, the Royal Meteorological Institute and the Royal Belgian Institute for Space Aeronomy. The STCE supports fundamental solar, terrestrial and atmospheric physics research, is involved in earth-based observations and space missions, offers a broad variety of services (mainly linked to space weather and space climate) and operates a fully established space weather application centre. The scientists act at different levels within the frame of local, national and international collaborations of scientific and industrial partners.

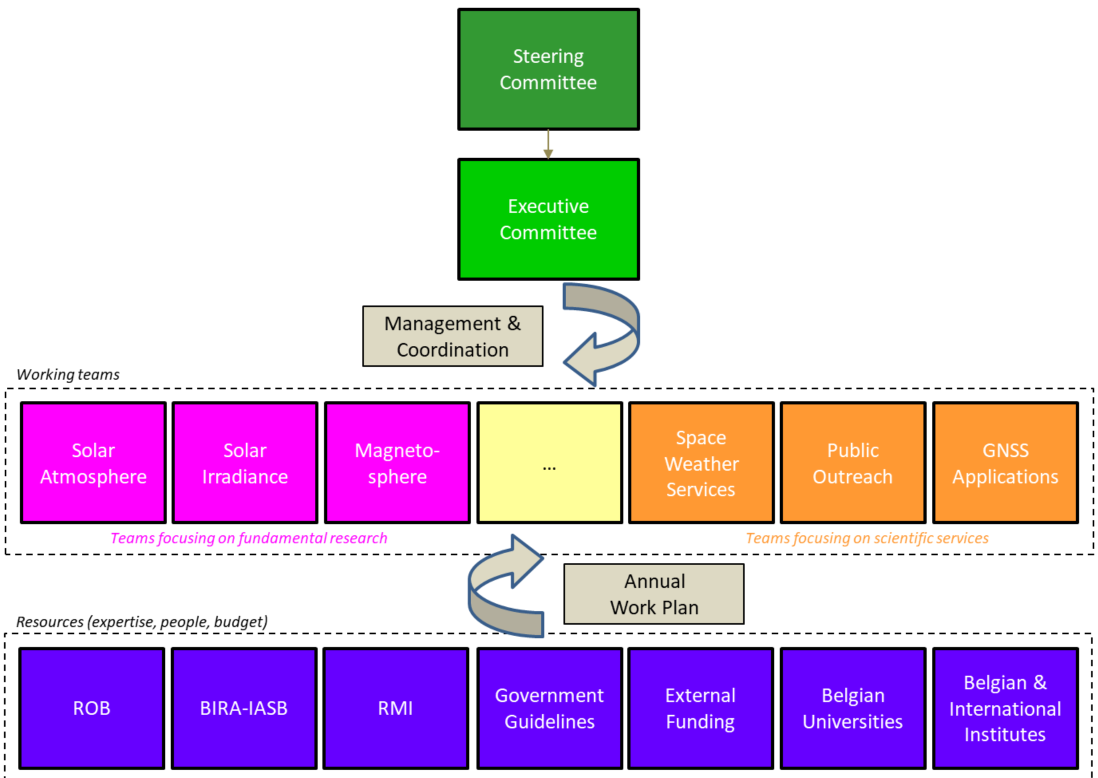

Figure 1: The STCE management structure

The STCE's strengths are based on sharing know-how, manpower, and infrastructure.

In order to optimize the coordination between the various working groups and institutions, as well as the available resources such as ICT, personnel and budget, a management structure for the STCE was put into place, consisting of a steering committee and an executive committee.

The ***steering committee*** takes all the final decisions on critical matters with regard to the STCE. It assures the integration of the STCE into the 3 institutions and the execution of the strategic plans. It is composed of:

- BELSPO General Director "Research and Space"

  Dr. Frank Monteny (BELSPO)

- Director General of each of the 3 institutions at the Space Pole

  Dr. Ronald Van der Linden (ROB)

  Dr. Daniel Gellens (RMI)

  Dr. Martine De Mazière (BIRA-IASB)

The ***executive committee*** assures the global coordination between the working groups and the correct use of the budgetary means for the various projects. It also identifies new opportunities and is the advisory body to the Steering Committee. It is composed of:

- STCE Coordinator

  Dr. Ronald Van der Linden

- Representatives of the research teams in the 3 institutes

  Dr. David Berghmans (ROB)
  Dr. Carine Bruyninx (ROB)
  Dr. Eric Pottiaux (ROB)
  Dr. Johan De Keyser (BIRA-IASB)
  Dr. Norma Crosby (BIRA-IASB)
  Dr. Stanimir Stankov (RMI)
  Dr. Stijn Nevens (RMI)
  Dr. Hugo De Backer (RMI)

A promotional movie giving a flavor of the STCE's tasks, interactions and various research programmes can be found via the STCE website (in English, and subtitled in French and Dutch). A concise and more recent introduction to the STCE can be found on the STCE's YouTube channel (English).

*A good portion of the Solar Influences Data analysis Center (SIDC) team of the Royal Observatory of Belgium during their Monthly Management Meeting on 14 October (Credits: Sergey Shestov). They are standing in front of a house-sized poster of the Sun made by Solar Orbiter's Extreme Ultraviolet Imager (EUI). Data processing was done by our very own Emil Kraaikamp with the final image containing more than 83 million pixels in a 9148 x 9112 pixel grid, making it the highest resolution mosaic image of the Sun's full disc and outer atmosphere, the corona, ever taken. Please check out the **ESA** and **SIDC** websites, it's crazy!*

Monitoring space weather: solar-terrestrial highlights in 2022

The official annual sunspot number (S_n) for 2022, as determined by the WDC-SILSO (World Data Center - Sunspot Index and Long-term Solar Observations), was 83.2. This is a significant increase compared to 2021 (29.6). Sunspot numbers rose during the March-May period, then remained relatively stable between 70 and 95 for the next 6 months. December brought a significant increase in sunspot activity, with the monthly sunspot number reaching 112.8 - the highest so far this solar cycle (SC25). The recorded sunspot numbers are about a third higher than initially predicted which - IF this trend continues - may indicate that SC25 maximum can be somewhat higher (around 150, but with a large uncertainty range) and earlier (in 2024) than the original prediction by the international SC25 panel of 115+/-10 in July 2025 +/- 8 months. The evolution of SC25 for various space weather (SWx) parameters can be followed on the STCE's SC25 Tracking page.

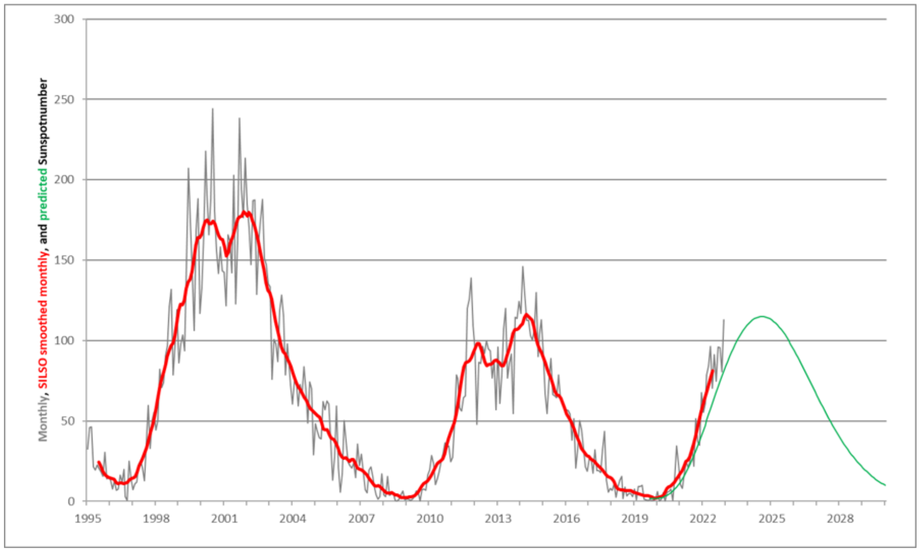

*Figure 2: The evolution of the monthly and SILSO smoothed monthly S_N (1995-2022 ; **SILSO formula**). The monthly sunspot numbers in 2022 remained higher than the expected values (depicted in green, with the predicted maximum advanced and occurring in August 2024).*

The highest daily sunspot number was observed on 4 October (164), but also in May, June, July and December there were days when the sunspot number was above 150. The observed 10.7cm radio flux (Penticton) reached its highest daily value for the entire year on 18 May (179.9 sfu, with 1 sfu = 10^{-22} W m^{-2} Hz^{-1}), up from 140.4 sfu recorded on 22 December the previous year. Several sunspot groups were visible with the protected naked eye (eclipse glasses), a few examples of which are shown in Figure 3. NOAA 2994 (April), 3014 (May) and 3153 (early December) belonged to the largest groups visible in 2022, reaching maximum sunspot areas of about 5 to 7 times the total surface area of the Earth.

Six of the 7 X-class flares produced in 2022 happened within a period of only 6 weeks. NOAA 2994 (on 17 and 30 April) and NOAA 3006 (on 3 and 10 May) produced 2 X-class events each, NOAA 2975 produced an X1.3 flare on 30 March, and NOAA 2992 produced the strongest event of the year on 20 April (X2.2). Only the coronal mass ejection (CME) associated with the first X-class event on 30 March was able to stir some geomagnetic unrest (minor storm on 2 April), the other CMEs didn't have an earth-directed component.

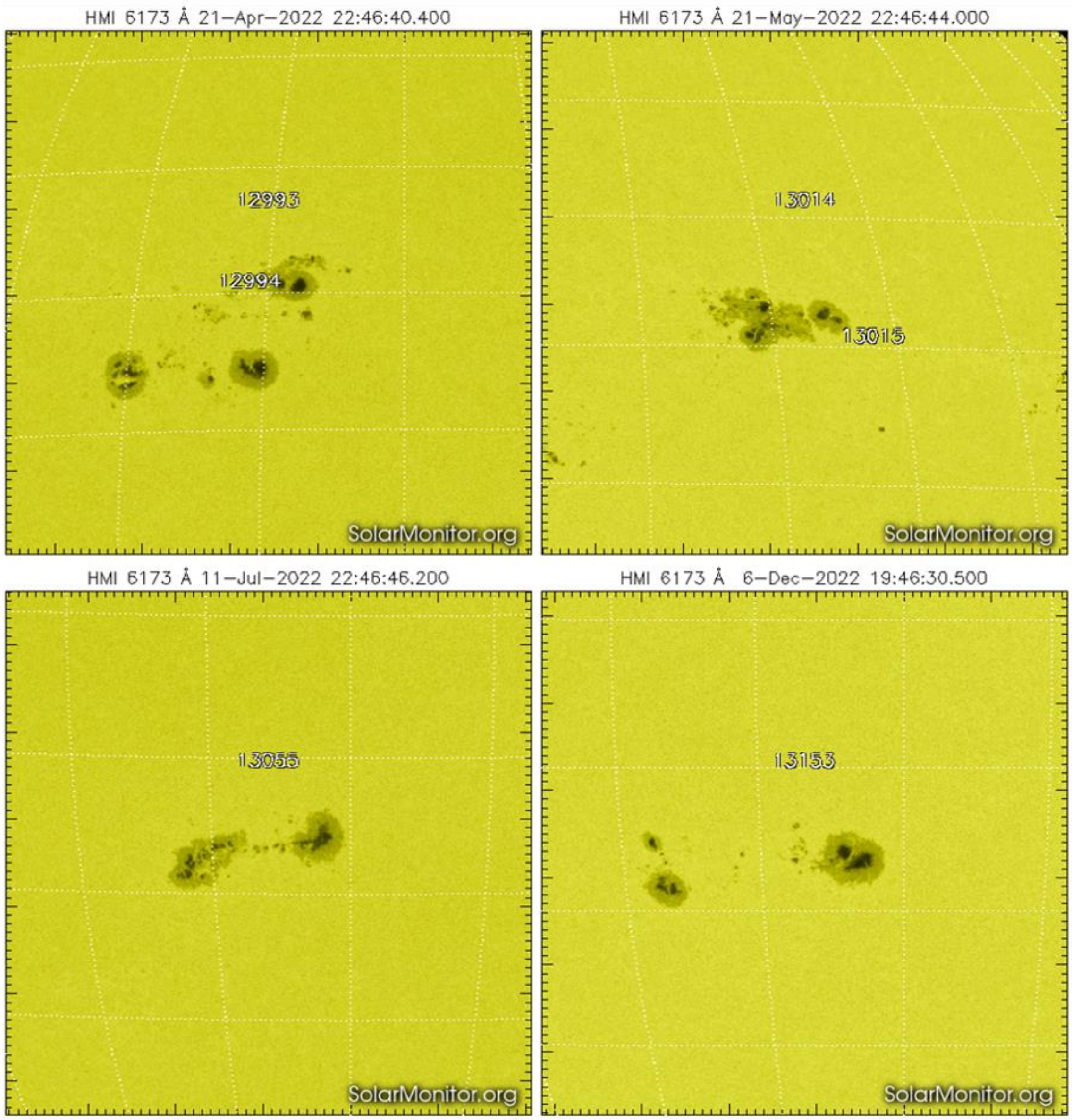

*Figure 3: A view on some of the largest sunspot groups so far this solar cycle. With a sunspot area of about 7 times the total surface area of the Earth, NOAA 3014 is the largest sunspot group so far in SC25. All of the sunspot groups in this compilation were visible with the protected naked eye. (Credits: **SDO/HMI** and **SolarMonitor.org**).*

The X-class flares were not associated with a proton event, i.e. the greater than 10 MeV proton flux did not pass the threshold of 10 pfu. The particle detector on board GOES-16 still recorded 5 such events in 2022, such as on 28 March when NOAA 2975 produced its first M-class flare (M4.0) resulting in a peak in the greater than 10 MeV proton flux of 18 pfu (Figure 4). During the long duration M3.9 flare generated by the same active region on 2 April, the proton flux peaked at 32 pfu, the highest of the year. The greater than 100 MeV proton flux briefly reached its alert threshold of 1 pfu during the events of 20 January and 28 March. No Ground Level Enhancements (GLE) were recorded by ground-based neutron monitors throughout the year.

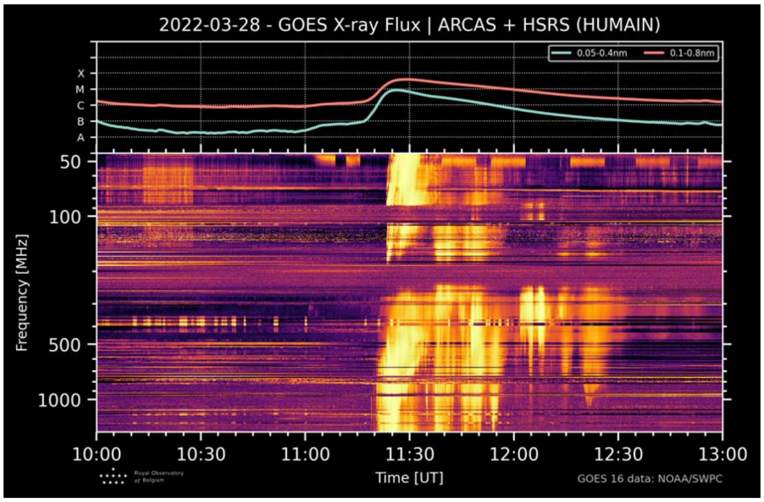

*Figure 4: Radio telescopes of the **Humain Radioastronomy Station** recorded the M4 eruption of 28 March in frequencies between 45 and 1495 MHz. Scanning continuously the intensity at these frequencies, disturbances can be discerned which are in this case associated with a CME-driven shock (Type II) and electrons trapped in closed magnetic field lines in the post-flare coronal loops (Type IV) - See the STCE's **SWx classification page** for more examples and info on Type II, Type IV and other radio bursts. Type IV bursts are strongly correlated with proton events, and indeed a small proton event was observed (18 pfu on 28 March). The top portion of the graph shows the evolution of the x-ray flux as measured by **GOES**.*

In 2022, the GOES recorded 185 M-class flares. NOAA 3165 produced 23 of those, and that in only 3 days (14-16 December). Also the duo NOAA 2992/2993, combining for 19 M-class events, NOAA 3088 (14, of which 13 in just 4 days) and 3112 (13) were notorious M-class flare producers. NOAA 3088 was the source of what was one of the visually most stunning flaring events of the year. On 28 August, it produced an M6.7 flare near the Sun's southwest limb. Extreme ultraviolet (EUV) images showed that the post-flare coronal loops reached a height of around 180.000 km, which is about half of the average Earth-Moon distance (Figure 5; STCE news item).

Another impressive event was the long duration M3.4 flare produced by NOAA 3032 on 13 June. The flare lasted for 2 hours and 14 minutes, but more importantly, it produced a very strong radio burst at GNSS frequencies (Global Navigation Satellite Systems, such as GPS or Galileo). The radio burst was recorded by the San Vito radio station in Italy, lasted for nearly an hour and reached an intensity of 98.000 sfu. Usually, the intensity at these frequencies during solar cycle maximum is only around 120 sfu, and there are typically only a handful of such strong bursts over an entire solar cycle!

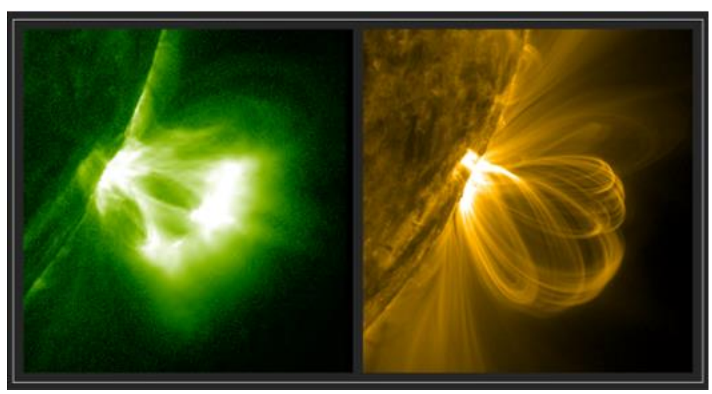

*Figure 5: The **SDO/AIA** extreme ultraviolet (EUV) images above show coronal loops in AIA 094 (multi-million degrees) on the left and in AIA 171 (temperatures around 700.000 degrees) on the right following the strong M6.7 flare on 28 August (peak time at 16:19 UTC). Note that the green and yellow colours are artificial and meant to distinguish between the different filters and temperatures. The images were taken on 29 August at resp. 00:09 and 07:57 UTC.*

The daily CME rate increased from about 3 at the beginning to well over 5 by the end of the year. Some of the source regions of these CMEs were already active while still behind the east limb, or continued their eruptive activity while having rounded the west limb. As a result, several farside CMEs were observed throughout the year. Such was the case for a full halo CME that was observed late on 15 February. The CME had a speed of 2200 km/s and was so violent that, despite the poor magnetic connection of the source location on the Sun with the Earth, GOES-16 still recorded a mild enhancement in the greater than 10 MeV proton flux. The Full

Sun Imager (FSI) on board Solar Orbiter, which was trailing the Earth by 17 degrees, was able to track the ejected prominence material in EUV (extreme ultraviolet) passbands for up to more than 6 solar radii, the first observed in 30.4 nm emission at such a great height (STCE news item ; see also pp. 21 of this annual report).

Solar Orbiter's FSI also helped to trace the source of another violent farside eruption, this time late on 23 July. The fast (1700 km/s) halo CME that was observed by SOHO and STEREO-A coronagraphs had its origin in the eruption of a long and solid filament, which is a cloud of ionized gas suspended above the solar surface squeezed between regions of opposite magnetic polarity. Becoming unstable somewhere between 17 and 18 UTC, the filament violently got ejected splitting into 2 during the process (Figure 6). This time, the proton flux as measured by GOES didn't become enhanced.

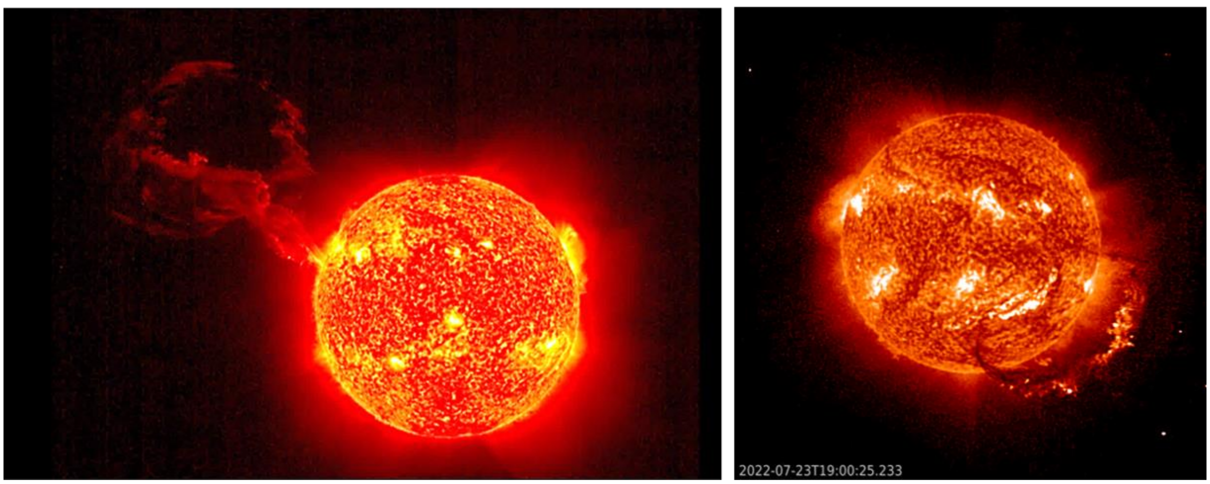

Figure 6: Solar Orbiter's view on the 2 major solar eruptions of 15 February and 23 July. From Earth's point of view, both events happened on the Sun's farside. For Solar Orbiter, the 23 July event took place on the solar hemisphere facing the satellite. Both EUV images (30.4 nm) are enhanced, in particular the left image (15 February) in order to bring out the faint features of the outer portions of the eruption.

Despite all the farside CME activity, there were also frontside CMEs that had an earth-directed component. The geomagnetic activity resulting from these interplanetary CMEs ("ICMEs") was not too impressive. K_p wise, the strongest geomagnetic storms took place on 10 April and 17 August, both reaching K_p = 7 (major storm). Contrary to 2021, the Dst index (Disturbance storm-time index) never went below -100 nT (Kyoto World Data Center for Geomagnetism). Low values were reached on 14 January (-91 nT), 13-14 March (-85 nT) and on 7 November (-92 nT). The magnetic shielding provided by the 13-14 March ICME resulted in a significant decrease in the harmful cosmic rays, as recorded by neutron monitors around the world (a so-called "Forbush decrease"). The neutron monitor in Oulu, Finland showed a decrease of 6-7% in the 1-hour count rates compared to undisturbed levels.

The source of the 7 November geomagnetic storm is unknown (a so-called "transient" in the solar wind). Though it was only a minor storm, the resulting disturbance of the ionosphere affected GNSS-based augmentation systems used in aviation (STCE news item). Figure 7 shows the impact on the GPS-based (WAAS: Wide Area Augmentation System) and the Galileo-based (EGNOS: European Geostationary Navigation Overlay Service) LPV-200 systems. LPV-200 (Localizer Performance with Vertical guidance) systems deliver accurate information on an aircraft's approach to a runway with the use of GNSS positioning technology. The redder the color in the plot, the better the LPV-200 service coverage. It is evident that on 7 November, which corresponds to the day of the aforementioned minor geomagnetic storm, the LPV-200 service was significantly disturbed over large portions of Canada and Northern Europe.

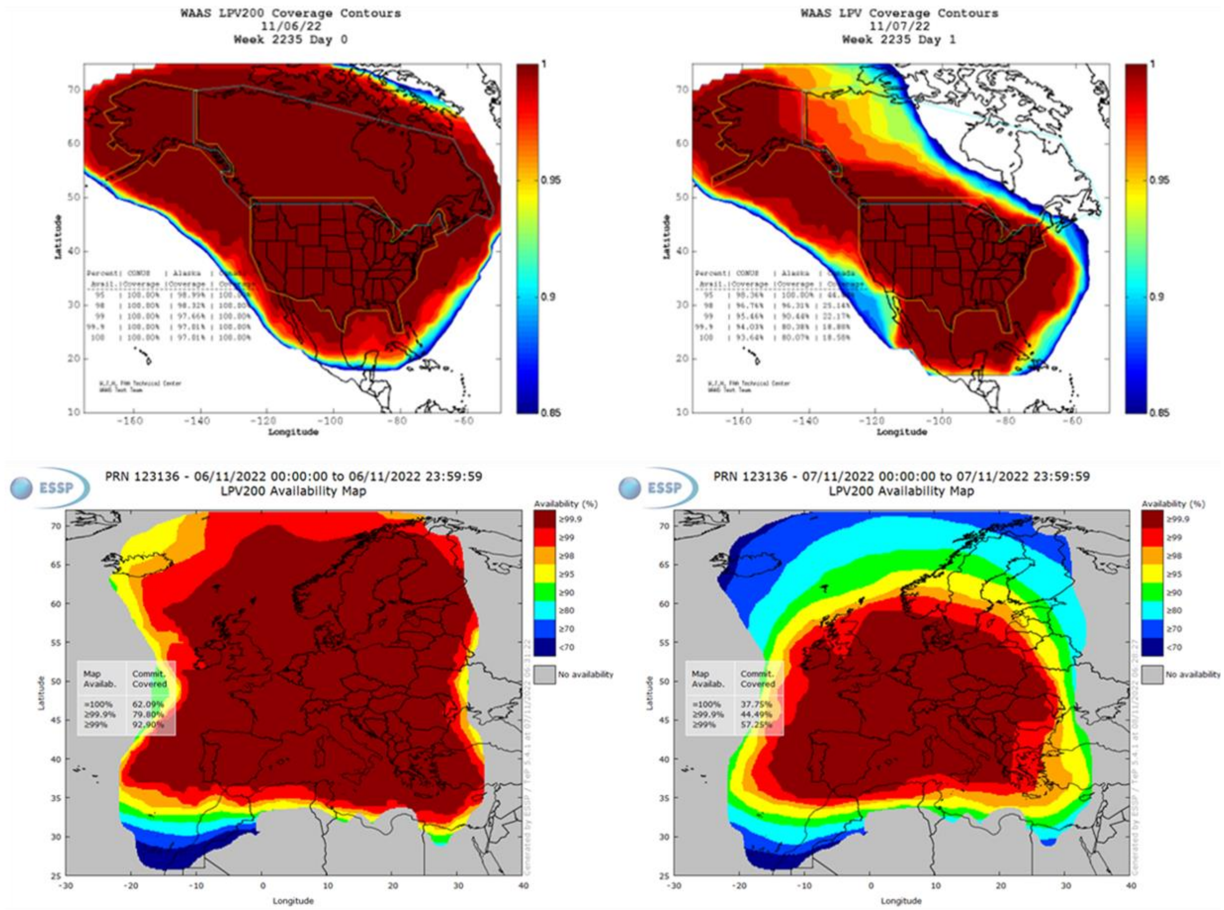

Figure 7: The effect of the minor geomagnetic storm of 7 November on GNSS-based navigation systems can well be seen in the plots above. They show on the left a typical, undisturbed coverage of the LPV-200 systems for WAAS (USA and Canada) and EGNOS (Europe) on 6 November, and the significantly reduced coverage of these systems over Canada and Northern Europe on 7 November (right plots).

Another minor geomagnetic storm with a major impact on our technology was the storm from 3-4 February, when SpaceX lost a large portion of its batch of satellites it had launched just a few hours earlier (STCE news item). Shortly after launch, the satellites were put -as usual- in a stand-by orbit with a perigee (point closest to Earth) of 210 km, before being transferred to their final orbit at 540 km altitude. Note that 210 km is just above the minimum orbit altitude for a satellite, which is grosso modo 180 +/-20 km pending size and shape of the satellite. SpaceX does this on purpose, because in the very rare case that a satellite does not pass the initial system checkouts, it will quickly be deorbited by atmospheric drag (friction between the atmosphere and the satellite - https://www.stce.be/news/452/welcome.html). As it happened, the satellites were at this low altitude portion of their orbit maneuver when the geomagnetic storm occurred. In this respect, PROBA2/LYRA made important density measurements of the Earth's atmosphere during this storm (see pp. 32 of this annual report). The increased drag encountered by the Starlink fleet resulted in the loss of 38 of the 49 satellites, which re-entered the Earth's atmosphere and burned up. Note that after this event, the SpaceX team launched the next series of Starlink satellites to a higher checkout orbit with an altitude of 300 km to evade the effects of intense drag.

High-speed streams from coronal holes (CHs) regularly disturbed the earth environment, but they were less prominent and had a smaller SWx impact than in 2021. High speed wind streams (HSS) related to these CHs drove the maximum solar wind speeds near Earth to values between 650 and 700 km/s around 26 June, 4 September (see Figure 8 for source CH) and 26-27 December. The passage of these HSS generated elevated levels of energetic (energies of more than 2 MeV) electrons in the Earth's outer radiation belt, as measured by the GOES. Daily maxima occasionally rose above the alert threshold of 1000 pfu (particle flux units; 1 pfu = 1 electron / cm^2 s sr). A maximum flux of just over 20.000 pfu was reached on 8 September, and the daily electron fluence was at its highest levels of the year on 7 and 8 September. It is known that sustained high levels of these electron fluences can lead to electrostatic discharges (ESD) resulting in malfunctions of a satellite and occasionally even in the satellite failure. The HSS that arrived on 4 September resulted in periods of enhanced (moderate to high) levels of electron fluence from 5 till 14 September 2022. Operators reported numerous satellite glitches at the end of the period, in particular a few days after maximum fluence on 8 September.

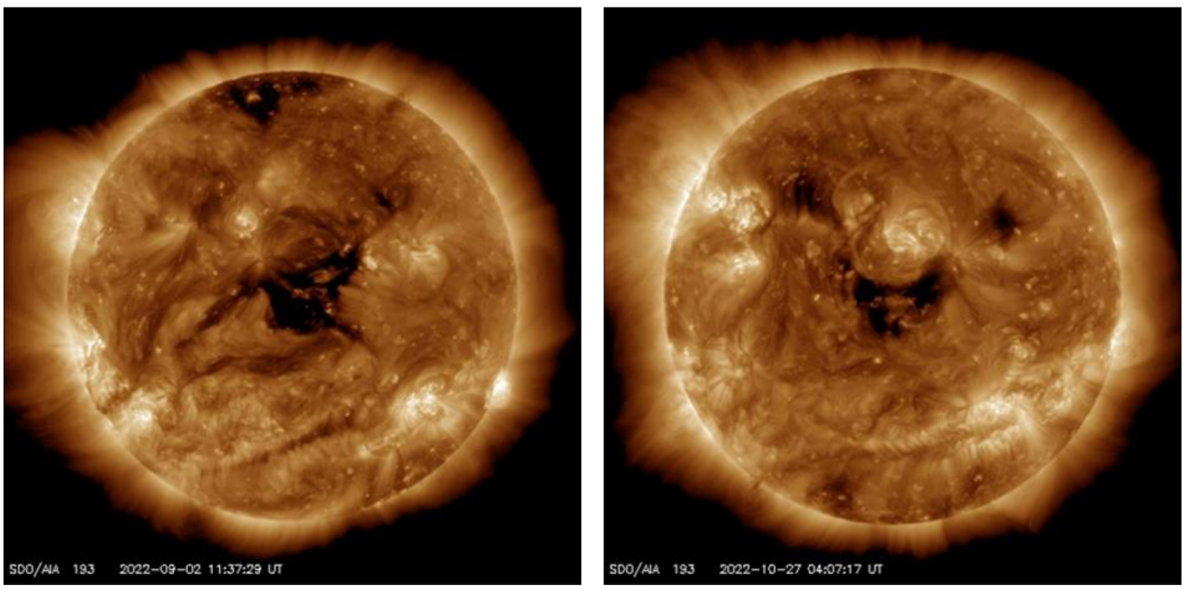

Figure 8: (left) The coronal hole that transited the central meridian on 1 and 2 September was responsible for a high-speed stream (HSS) that affected the earth environment for several days causing glitches in some satellites. (right) The fortunate locations of 3 rather small CHs gave the Sun a smiling face on 27 October.

Public outreach meets Science

A Touch of Space Weather - Bringing space weather to visually impaired students

A Touch of Space Weather is a new project that brings the captivating science of space weather to blind and visually impaired students in an engaging and accessible manner. By offering interactive workshops and a website, students can embark on a journey to explore the Sun, Earth's atmosphere, magnetic field, aurora, and other fascinating topics related to space weather, all through the senses of touch and sound.

Audio booklets - With the aim of making the field of space weather accessible to all, our "A Touch of Space Weather" team works on a series of audio booklets that explain various high-school scientific topics through the lenses of space weather. Collaborating closely with teachers and assistants of blind and visually impaired students, the project ensures that these audio resources seamlessly integrate into secondary school lessons, catering to students aged 11-16. The audio booklets will cover topics such as: The Sun, Space flight, Moon exploration, Animal magnetoreception, Mars, and many others.

Tactile images - Just like their sighted peers, blind and visually impaired children yearn to visualize and comprehend complex concepts that are often taken for granted. Terms like "magnetosphere" or "solar wind" may seem foreign and abstract at first, but with the help of "A Touch of Space Weather," these concepts become vivid and tangible. Through nine tactile images, that were developed during the project, students can imagine the space weather phenomena and effects through the sense of touch.

Figure 9: Blind and visually impaired students interact with the tactile images of space weather, assisted by teachers and researchers. Several tactile images are spread on grey tables in a brightly decorated room, in front of three students with two assistants, as they interact with the phenomena being described by the images.

Using affordable materials readily available at hobby shops, anyone - parents, friends, or teachers of blind and visually impaired children - can easily recreate these tactile images. Comprehensive instructions and video tutorials have been published on the project's website, ensuring that everyone can follow the instruction and make their own tactile images.

Visits to schools - To test the tactile images and get crucial feedback from visually impaired students, our team visited two specialized schools, De Kade and IRSA in Belgium. There, we presented the images and embarked on engaging discussions about space weather. The reactions were overwhelming, as students were moved by the experience of "feeling" the ethereal aurora for the first time and sensing the dynamic movement of the solar wind along Earth's magnetic field lines. The dedicated teachers and students at De Kade, led by representative Kris Paschen, have played an invaluable role in providing feedback on the educational material and offering support in understanding the unique challenges faced by blind and visually impaired children.

Inclusivity - The project doesn't stop there. It aims to foster inclusivity and raise awareness among children who are not blind or visually impaired. Through a series of workshops held at Astropolis Space Village, Open Days at The Royal Belgian Institute for Space Aeronomy, and visits to the European School and Bogaert International School, children were encouraged to create their own tactile images that will be later delivered to schools for blind and visually impaired. By doing so, these young learners not only delved into the world of space weather but also learned about inclusivity and diversity.

The project was awarded an EGU Public Engagement Grant in 2021. This grant has covered the physical costs of creating "A Touch of Space Weather" boxes, which will be distributed to schools and organizations providing a set of tactile images, usb with audio booklets, and several 3D printed models. The STCE framework provides support for further advancements in the project.

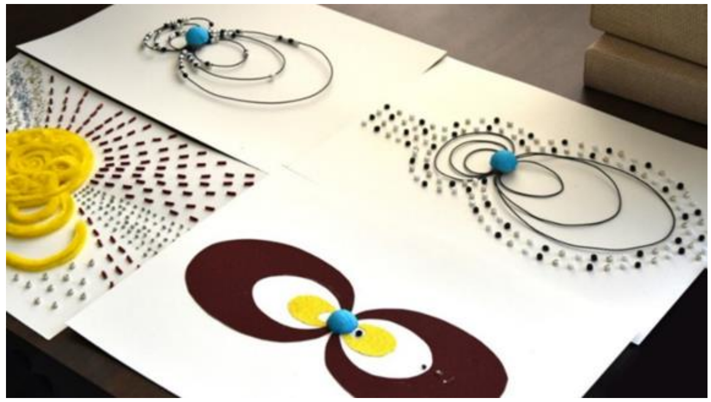

Figure 10: Examples of the tactile images developed within the project. The top image shows the Earth's magnetosphere and interaction with the solar wind particles. The bottom left image shows the Sun with two different types of solar wind, and energetic particles, and the bottom right image shows the radiation belts around Earth.

A Touch of Space Weather helps to revolutionize the way blind and visually impaired students engage with science. By incorporating tactile experiences, 3D printed models, and upcoming audio booklets, this project ensures that every student, regardless of their visual abilities, has the opportunity to explore and appreciate the wonders of space weather in a truly immersive and meaningful way. By actively involving the senses and promoting inclusivity, this project sets the stage for a future where the norm will be to experience science through all of our senses.

SUN @ Africa Museum

From 5 till 24 April 2022, the STCE brought SUN to the Africa Museum: a 3D projection with state-of-the-art images from the SDO/AIA telescope on a gigantic, hanging balloon 6 meter in diameter showing 10 weeks of the life of our Sun. Smoke and sound effects mimic the Sun's outer atmosphere to complete the unique experience. This spectacular piece of light art brings you closer to the Sun than you've ever been before.

SUN is an installation by British artist Alex Rinsler and solar expert Prof. Robert Walsh (University of Central Lancashire). With this installation in the AfricaMuseum, in cooperation with the STCE, the spectacular artwork was shown outside the United Kingdom for the very first time.

The Sun is the determining factor for life and climate on this globe. Through human activity, climate change is one of the most pressing issues faced by society today. This exhibit in the Small Rotunda of the AfricaMuseum also presented world-leading research on the Sun and Earth's climate carried out at both scientific institutions.

The AfricaMuseum presented projects on the impact of tropical rainforests on the climate, and on the impact of climate change on the spread of tropical diseases and natural hazards such as landslides. The STCE highlighted its studies on long-term variations of the Sun that affect Earth's climate. The difference between solar radiation that strikes the Earth and the radiation that is sent back into space, is key to climate change and subject of STCE research.

On Sunday, 10 April, inspired storytellers brought African and Scandinavian stories about the Sun to children and slightly older Sun-lovers. Seated by the light artwork, they dove into the world of aardvarks, bats and the northern lights during one of the storytelling moments.

Figure 11: The SUN at the AfricaMuseum.

Battle of the scientists

After having survived the preliminaries in December 2021, 5 scientists were selected to participate in the final round of the "Battle of the Scientists" ("Wetenschapsbattle" in Dutch). This event was held in the University Forum (UFO) in Ghent on 22 March. The main purpose of this initiative is to make girls and boys interested in science and technology already at a young age (6-12 years).

The Battle of the Scientists is a unique and interactive competition in which 5 scientists present their research in a 10' talk to a room filled with about 400 primary school children, while thousands (at least 5000 registered) watched the event from their classroom through a livestream.

The children organize the battle themselves and vote for the winning presentation. They do the preselection of the scientists, form a jury and present the show. They are time keepers and count the votes. Not only do they learn invaluable skills, they are also exposed to the coolest science.

Figure 12: The 5 participants in the 2022 edition of the Wetenschapsbattle. Petra and Elke are 2nd and 4th from the left.

The theme for the 2022 battle was "space", and so the STCE entered two applications: "Red alert: a solar storm is coming!" and "Dancing aurora: heavenly creatures and science?". Both proposals were selected by the organizing school! On 22 March, we had the chance to explain space weather in all its forms to these kids and hopefully motivate some of them to become scientists themselves, making use of the beautiful solar images and movies.

The battle took place during the Belgian Astronaut Week in March 2022. This event was organized to celebrate the 30th anniversary of Dirk Frimout's shuttle flight, as well as the 20th anniversary of Frank De Winne's trip to the International Space Station. Dirk Frimout attended the battle and answered some of the children's questions explaining what it is like to go to space.

The battle was won by Marijn Timmer (Universiteit Antwerpen) with his presentation "Marijn en de PlasGasFabriek", detailing his ongoing research on recycling urine from astronauts into breathable air during their future space mission to Mars.

Open Doors at the Space Pole

The doors of the Space Pole were open to the public during the weekend of 24-25 September. The theme for this event was "Space for Climate". The Open Days attracted thousands of visitors, who could for example visit the telescopes or the climatic park. Many discovered how a weather forecast is made, learned everything about climate change, or followed one of the many thematic lectures. Attending the launch of a weather balloon is always a highlight, as impressive as watching the formation of aurora in a dark room. The visitors could also learn everything about the study of the Earth, planets, moons and comets, from our own solar system to far beyond in the universe. Numerous scientists from the Space Pole were happy to assist the visitors at the various information stands and also organized workshops and live scientific experiments. There were also numerous activities put together for children. The next two pages provide a glimpse of the ongoings during the Open Doors 2022 (image credits: Olivier Boulvin and ROB).

*Frédéric Clette wrote a book on the Sun (in French). Nearly 500 pages long, this **book** is intended for a wide readership, providing a global panorama of the Sun, its multiple influences on our planet and us, humans, as well as the new dangers it may bring for our present society. He presented his book on numerous occasions, such as here during the -at that time still outdoors in the aftermath of Covid-19- monthly management meeting of the solar physics department.*

Fundamental research

All Spatial Scales Great and Small

The year 2022 was the first in the nominal mission phase of the ESA/NASA Solar Orbiter spacecraft, following its launch in February 2020 and subsequent commissioning and cruise phase. Solar Orbiter is on a 10-year mission to observe the Sun from close-by and discover the connection between processes in the solar atmosphere and the extended solar wind.

One of the cornerstone instruments aboard Solar Orbiter is the Extreme Ultraviolet Imager (EUI), built by an international consortium under the lead of the Centre Spatial de Liège, and now operated by the Royal Observatory of Belgium, as Principal Investigator institute. The EUI instrument consists of 3 telescopes, the Full Sun Imager (FSI) and two high-resolution imagers: the High-Resolution Imager in the EUV (HRIEUV) and the High-Resolution Imager in Lyman-alpha (HRILYA). Here we report on two spectacular observations of EUI that made it into the international press.

On 15 February, the FSI telescope of EUI captured the largest solar prominence eruption ever observed in a single image together with the full solar disc (see below, and this STCE press release). Solar prominences are large structures of tangled magnetic field lines that keep dense concentrations of solar plasma suspended above the Sun's surface. They are often associated with coronal mass ejections, which -if directed towards Earth- can wreak havoc on our technology and everyday life. This latest event took place on 15 February and extended millions of kilometers into space. The coronal mass ejection was not directed to Earth.

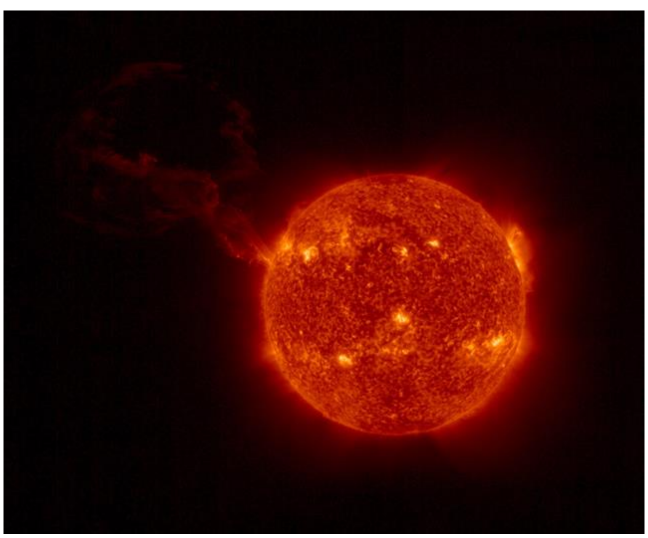

Figure 13: The largest prominence eruption ever observed together with the solar disc. The image was taken with the He II 30.4 nm channel of the FSI telescope of the Extreme Ultraviolet Imager aboard Solar Orbiter.

Other space telescopes, such as the ESA/NASA SOHO spacecraft, frequently see solar activity like this, but either closer to the Sun, or further out by means of an occulter, which blocks out the glare of the Sun's disc to enable detailed imagery of the corona itself. Thus, the prominence observed by Solar Orbiter is the largest ever event of its kind to be captured in a single field of view together with the solar disc, opening up new possibilities to see how events like these connect to the solar disc for the first time.

Another spectacular observation was taken with the HRIEUV telescope on 7 March. Over a period of more than 4 hours, the satellite aimed at different positions, each time capturing a small square of the Sun at very high resolution. Solar Orbiter was located halfway between the Sun and the Earth when this mosaic image was made. No less than 25 images were needed to get the full picture of the Sun. The EUI instrument cannot change its pointing independently, so for each image we had to slightly change the orientation of the full satellite. After the images were sent from the satellite to the ground, our scientists meticulously pieced them together. Not easy, because during those 4 hours and 30 minutes the Sun rotates a little on its own axis and the solar atmosphere changes in appearance.

The result is the sharpest image of the solar atmosphere ever taken consisting of 9000x9000 pixels. That resolution cannot be printed in this publication but can be found online (SIDC/EUI). Following an ESA press release, Forbes magazine wrote "If you only look at 1 space photo this year, then this one has to be it". An image was printed on a 7x7 m^2 canvas with each pixel still smaller than 1 mm^2, and put on display on an outside wall of the Royal Observatory of Belgium. A picture with the team of the Solar Influences Data analysis Center (SIDC) posing in front of this canvas can be found on page 7 of this annual report.

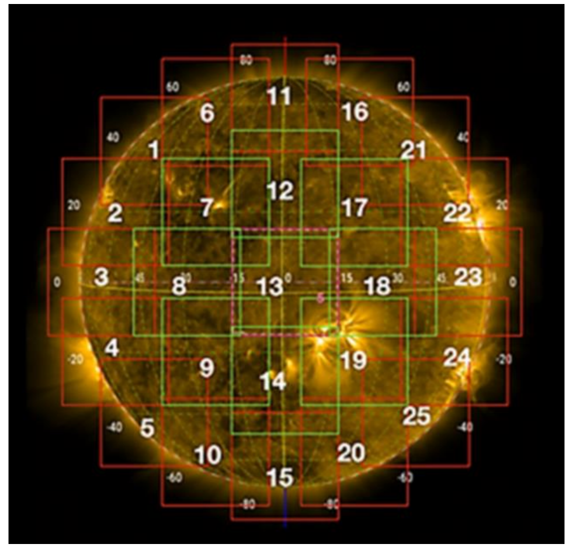

Figure 14: The 4h-lasting pointing-pattern of the Solar Orbiter spacecraft to produce the highest resolution image ever of the full coronal disc.

Scale Transfer in 1849: Heinrich Schwabe to Rudolf Wolf

The Sun is a fascinating and complex star that scientists have been studying for centuries. One of the ways they measure its activity is by counting sunspots. Scientists have been tracking the number of sunspots over time to understand how the Sun behaves and maintained the records in the form of a series called the International Sunspot Number (ISN). ISN is a widely used measure of solar activity that dates back to the 1600s. It is a count of the number of sunspots on the visible disk of the Sun, and it is used to track the 11-year solar cycle and its variability over longer periods of time. However, the historical record of sunspot observations is far from complete, with gaps and inconsistencies in the data that make it difficult to construct a reliable long-term record of solar activity. To overcome these limitations, scientists have developed methods to reconstruct the ISN using raw data counts which are being recovered from the archives from observers all over the world.

Overall, reconstructions of the ISN provide a valuable tool for understanding the long-term behavior of the Sun and its impact on Earth's climate and environment. However, uncertainties and limitations in the data mean that caution must be exercised when interpreting the results, and efforts are ongoing to improve the accuracy and consistency of the records.

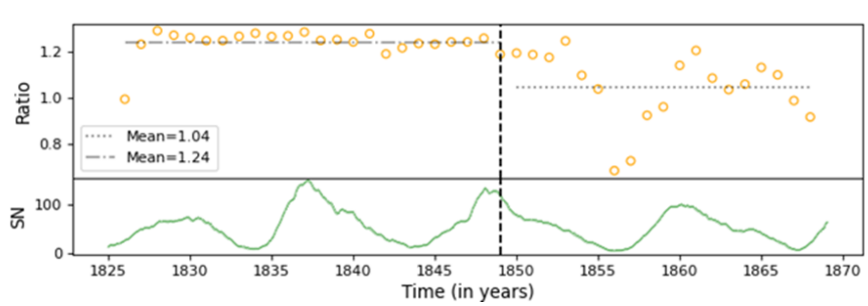

Figure 15: Yearly ratio for ISN versus Schwabe counts with vertical dashed line representing start of Wolf's observation as shown in Leussu et al. (2013).

The historical data on sunspot counts has been a challenge to analyze because there have been inconsistencies in the way observations were made and recorded. To overcome this difficulty, in 1859, Prof. Rudolf Wolf started to apply a parameter called the “k-factor” to other sunspot observers to bring them to his scale. In other words, he would adjust their observations to fit his own scale. This was a common practice back in the day, and it was essential to ensure that the data was consistent across all observers. Note that Prof. Wolf had started making his own observations from 1849 and was keeping records of his observations in his logbook called the Mittheilungen. Along with his own data he started collecting sunspot records from various other observers and included them in the Mittheilungen as well. The Royal Observatory of Belgium conducted a mission between 2017 and 2019 to digitize all the data contained in the published Mittheilungen.

From 1826 to 1848, Heinrich Schwabe was the primary observer of sunspots, as determined by Rudolf Wolf. In simple words, every observer in that period used to get scaled to Schwabe. But in 1849, Wolf took over the role of primary observer, and this shift caused an inconsistency in the Sunspot Number series as can be seen in Figure 15.

In this study, we focused on this specific issue with the International Sunspot Number series. We found that there was a significant jump in the sunspot counts around 1849, which had been a long-standing mystery for researchers. We discovered that this jump was caused by a mistake in the way the data was processed. Specifically, the k-factor, which is a scaling factor used to standardize observations made by different observers, was applied incorrectly to Schwabe’s data before 1849.

To address this issue, we carefully examined the available data and conducted statistical analyses to validate the k-factor used by Wolf to scale the observers. We were able to propose a corrected k-factor for Schwabe, which we believe will help to make the sunspot counts more accurate.

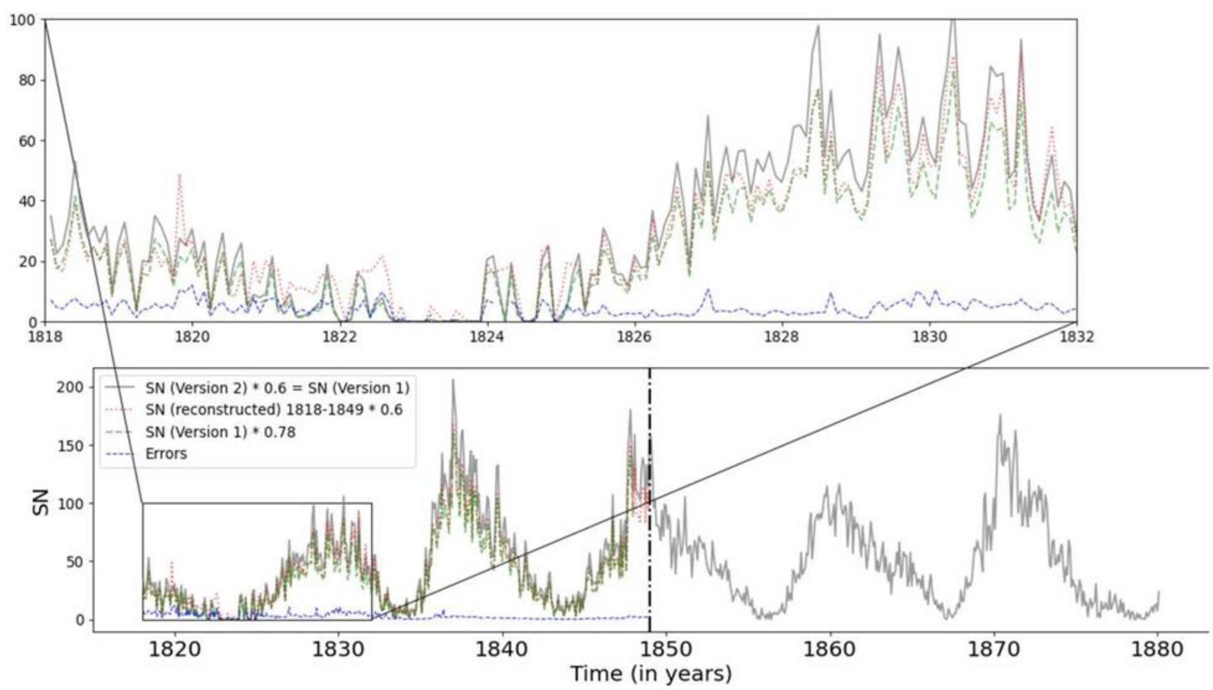

Figure 16: Monthly smoothed SN_Version 1, SN_Version 2, reconstructed SN_Version 1 spanning from 1818-1868 and 22% lowered SN_Version 1 from 1818-1848. The zoom in the plot is for easy comparisons, with SN in the y-axis and time (in years) in the x-axis.

Since all other observers were scaled to Schwabe before 1849, we reconstructed the ISN from the period from 1818 to 1848 as seen in Figure 16, using the data from the Mittheilungen but we plan to extend our analysis to other periods in the future. Ultimately, our goal is to reconstruct the sunspot data from raw historical records, which will help scientists to better understand the Sun and its impact on our world.

This study also highlights the importance of meticulous record-keeping, consistency in data collection, and the need for correcting historical data to maintain the accuracy of scientific datasets. It's fascinating to think that a small adjustment made over 170 years ago could affect our understanding of solar activity today. This study was published early 2023 in Solar Physics (Bhattacharya et al.; 2023).

The centennial TSI variation

Summary - A variation of the solar energy received by the Earth, quantified by the so-called Total Solar Irradiance (TSI), is a radiative forcing for climate changes on Earth. Since the 1976 Science paper by J. Eddy, solar-climate research has been dominated by the paradigm that solar activity and TSI have been slowly increasing since the Maunder Minimum -extending from about 1645 to 1715- to the present, which was believed to be a Modern Solar Maximum. If this paradigm were valid, over the last 50 years, when most of the global warming has occurred, this warming would be partly due to anthropogenic greenhouse gas warming, and partly due to natural solar warming.

However, evidence has been accumulating against the 'Modern Solar Maximum paradigm'. Based on this evidence, in 2022 researchers from ROB, VUB and LATMOS have published a new reconstruction of the centennial TSI variation from 1700 to 2020. This new centennial TSI reconstruction is nothing less than a paradigm shift compared to the 'Modern Solar Maximum paradigm'. Following the TSI reconstruction, the TSI did not gradually increase over the last 320 years, but rather varied with a long-term periodicity of 105 years, and currently we are near the *minimum* of this 105 year variation. Therefore, over the last 50 years, the Sun did not contribute to global warming, but rather tried to cool the Earth, partly counteracting greenhouse gas warming. Since we are near the minimum of the 105-year variation, we can expect a trend reversal and for the next 50 years we can expect that the Sun will contribute to global warming, making it more difficult for mankind to reach the goals of the Paris Climate Agreement, in order to avoid catastrophic climate change.

Detailed explanation - In 1612, Galileo Galilei started recording his telescopic observations of the surface of the Sun for the first time. He noticed the existence of small dark spots on the Sun -now called sunspots- and recorded their evolution. The observation of sunspots has continued from the 17th century to the present. As such, it can be considered as the longest running scientific experiment ever. Since 1981, the ROB started to host the World Data Center for the collection and analysis of sunspot observations. Continuous daily observations are available from 1700 to the present. From these observations, we know that the solar activity -measured by the number of sunspots- varies with an 11-year cycle, and that the amplitude of the cycle is variable. From joint sunspot and solar magnetogram observations, we also know that sunspots correspond to regions of strong magnetic fields on the solar surface.

In 2015, following a series of international workshops under the leadership of ROB, a revision of the sunspot number time series was published. The major change of the revised time series (V2) compared to the original time series (V1), is the correction of a discontinuity of the order of 20 % around 1947. In the revised time series, a 'Modern Grand Maximum' no longer appears.

Total Solar Irradiance is continuously monitored with space radiometers since 1978. The occurrence of a dark sunspot causes an instantaneous decrease of the TSI. A sunspot is small and has a relatively short lifetime, of the order of weeks to months. The sunspot decays into large and long-lived regions -with a lifetime of months to years- which are slightly brighter than the solar background. These regions are called facula, and they cause a long-term increase of the TSI. At the annual mean level, the facular TSI increase is stronger than the sunspot TSI decrease, and there is a strong positive correlation between TSI, facula and sunspots. Using the space age TSI observations, it is possible to calibrate the relation between annual mean TSI and annual mean sunspot number, and reconstruct the TSI backwards in time before the space age thanks to the long-term sunspot observations. The results are shown in Figure 17, where the orange curve is the annual mean TSI observed from space, and the purple curve is the reconstructed TSI based on the long-term sunspot observations. These results have been published in Remote Sensing (Dewitte et al. - 2022).

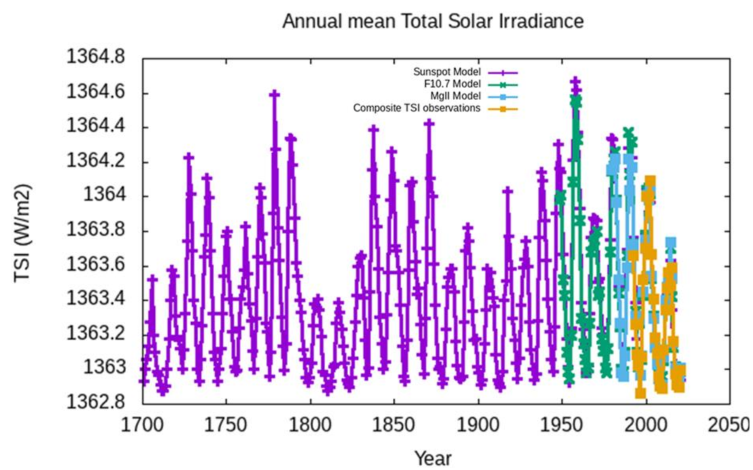

Figure 17: By using the long-term sunspot observations, the TSI van be reconstructed backwards in time before the space age. The orange curve represents the composite TSI space observations, the purple curve the backward TSI reconstruction based on sunspot observations.

Solar wind observed close to the Sun by Parker Solar Probe

The mission Parker Solar Probe (PSP), launched by NASA on 12 August 2018, completed its 14th solar orbit in December 2022. It has a perihelion under 15 solar radii where no spacecraft could fly before, which provides invaluable new insight into the fundamental mechanisms of the acceleration of the solar wind. Some years ago, BIRA-IASB's "Solar wind" team showed that the presence of suprathermal particles, and especially of an enhanced population of electrons (eV to several keV) in the low corona, can explain the coronal heating and the acceleration of the fast solar wind. Suprathermal particles are charged ions and electrons that move at speeds two to hundreds of times faster than the thermal plasma of the solar wind.

The consequences of such energetic particles, and especially halo electrons in the direction perpendicular to the magnetic field, were determined using also previous space missions like HELIOS, CLUSTER and ULYSSES (Pierrard et al., 2022a). The presence of power law tails for the escaping electrons increases the electric potential and accelerates the wind to values observed in the high-speed solar wind, keeping realistic temperatures in the solar corona. The presence of suprathermal tails close to the Sun is confirmed by the observations of PSP that can measure the velocity distribution functions of the solar particles at radial distances lower than 15 Rs (solar radii) in 2022. In 2024, the orbit of PSP will even reach distances lower than 10 Rs.

Figure 18: Parker Solar Probe mission launched in 2018 and exploring distances from the Sun lower than 15 solar radii in 2022. (Credits: NASA)

The new PSP observations also detected broadband electrostatic waves in the near-Sun solar wind (Zhao et al., 2022a). The occurrence of various electron-driven instabilities in the solar wind, expected and observed to change under different solar wind conditions and at different heliocentric distances, have been reviewed (Verscharen et al., 2022). The Alfvén-mode wave was especially analyzed to quantify wave-particle interactions in collisionless plasmas (Zhao et al., 2022b).

Plasmasphere-Radiation belts interactions

Space assets can easily be damaged by high-energy particles during strong geomagnetic storms driven by events at the Sun heading towards the Earth, like Coronal Mass Ejections (CMEs) or Corotating Interaction Regions (CIRs). To build a prototype service contributing to the safety of space assets against the natural hazards of space weather, a combination of different numerical models from the Sun to the Van Allen radiation belts of the Earth has been achieved. BIRA-IASB was involved in the plasmasphere part of this modeling chain. The plasmasphere is a region of the Earth's inner magnetosphere, filled with dense, low energy plasma of ionospheric origin, forming a toroidal region around the Earth. Its outer boundary is called the plasmapause.

We have reviewed existing plasma density models, including ionospheric source models, empirical density models, physics-based and machine-learning density models in the context of radiation belt physics and space weather codes (Ripoll et al., 2022). These models serve to complement satellite observations of the electron plasma density when data are lacking, are for most of them commonly used in radiation belt physics simulations, and can improve our understanding of the plasmasphere dynamics.

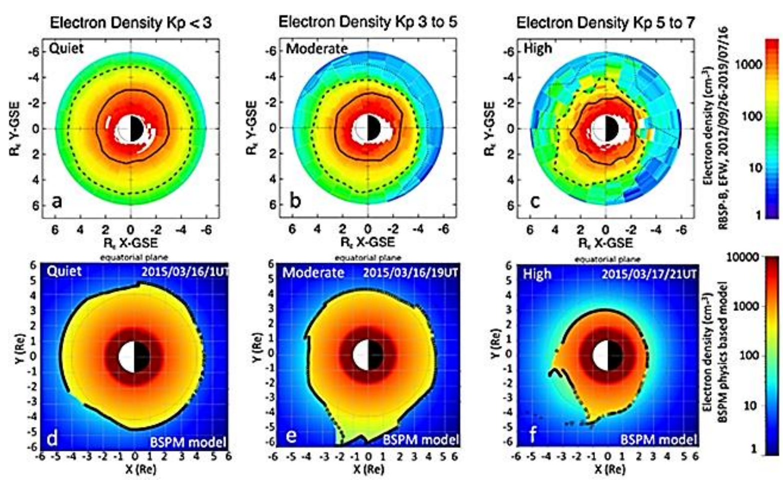

Figure 19: (A-C) Statistics of the electron plasma density (log_{10} of the density in units cm^{-3}) from Van Allen Probes B during the whole mission (09/2012-07/2019) for 3 K_p bins of geomagnetic activity. (D-F) The physics-based Belgian SWIFF Plasmasphere Model (BSPM) model of the electron density (colour scale) and the plasmapause (black circles) during times of (D) quiet, (E) substorm, and (F) storm activity.

The BIRA-IASB 3D kinetic dynamic model of the plasmasphere coupled to the empirical International Reference Ionosphere model provides the density of the particles and the plasmapause position. Using measurements of Van Allen Probes in the plasmasphere and our 3D dynamic plasmasphere model, we were able to calculate the diffusion coefficients contributing to the loss of energetic electrons (Dahmen et al., 2022). The radiation belt modelling was improved through the incorporation of processes and parameters that are of major importance to radiation belt dynamics. The plasmapause position obtained from the plasmasphere model serves as input for the wave-particle interaction models and the density data as input for the data assimilation. The ultimate result is a sophisticated model of the electron radiation belt and a space weather service prototype with tailored radiation belt environment indicators, which provides space weather forecasts for three different typical orbits (LEO, MEO, GEO) with lead times of 4 days.

The electron fluxes in the outer radiation belt during and after the intense geomagnetic storm of 23 June 2015 were investigated both at polar LEO (Low Earth Orbit) and Geostationary Transfer Orbit (GTO) (Pierrard et al., 2022b). We used our EPT (Energetic Particle Telescope) instrument on board the ESA PROBA-V satellite at LEO at an altitude of 820 km and compared with simultaneous observations of the instrument MagEIS on board the NASA Van Allen Probes circulating on a low inclination elliptical GTO orbit ranging from 600 to 30.600 km.

In addition, we used the Electric Field and Waves (EFW) instrument and the Electric and Magnetic Field Instrument Suite and Integrated Science (EMFISIS) to compile both the strength of the whistler waves associated to the storm dynamics and the cold electron density of the plasmasphere and plasma trough where the main wave-particle interactions (WPI) occur. We found that the equatorial trapped electron fluxes observed at GTO are generally higher than at LEO, but with magnitudes depending on the energy. Below 1 MeV, maximal fluxes differ by about 2 orders of magnitude. During the storm, the dropout and flux increase observed at LEO and GTO present very similar shapes in McIlwain parameter L and energy versus time, but with different intensities.

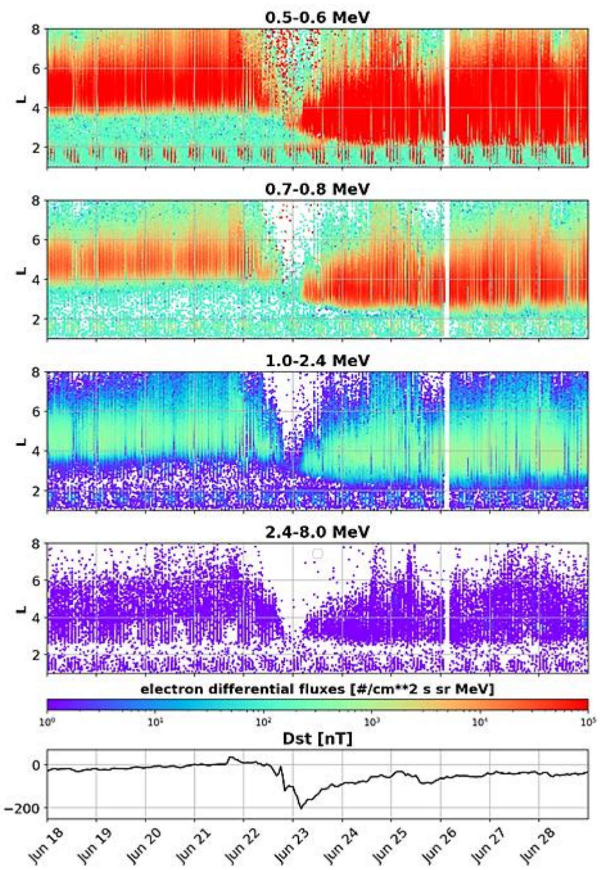

Figure 20: Electron fluxes observed by PROBA-V/EPT at LEO from 18 to 28 June 2015, as a function of the McIlwain parameter L expressed in Earth radii (vertical axis) and time (horizontal axis) for 4 electron energy channels. The V-shaped dropouts are clearly visible at all energies during the magnetic storm. Bottom panel: Disturbed Storm Time Dst index in nT. (Pierrard et al., 2022b)

Ionospheric effects of the Hunga volcano eruption

On 15 January 2022 a major eruption occurred at the Hunga volcano in Tonga. This was the climax of a series of smaller eruptions that started in December 2021, and destroyed most of the island. For the relatively modest size of the eruption, it had an exceptionally large explosive power: the largest since the 1883 Krakatoa eruption. This is explained by the interaction of the magma with the ocean water, since most of the eruption took place underwater. Because of the immense power of this explosion, the resulting shock-wave was able to travel (multiple times) around the world, and to be detected even in the ionosphere, at 300 km altitude. This wave was tracked travelling over Europe by detecting its arrival at different ionospheric observatories. Figure 21 shows the wave first seen in the atmospheric air pressure at ground level, and sometime later in the ionosphere (Verhulst et al., 2022). This demonstrates that the ionospheric disturbances are the result of the shock-wave propagating at lower altitudes, rather than directly propagating through the ionosphere itself. The two different disturbances indicated correspond to the shock wave travelling in both directions along the great circle. The antipode of the eruption was close to this observatory, so the waves travelling in both direction arrive shortly after each other.

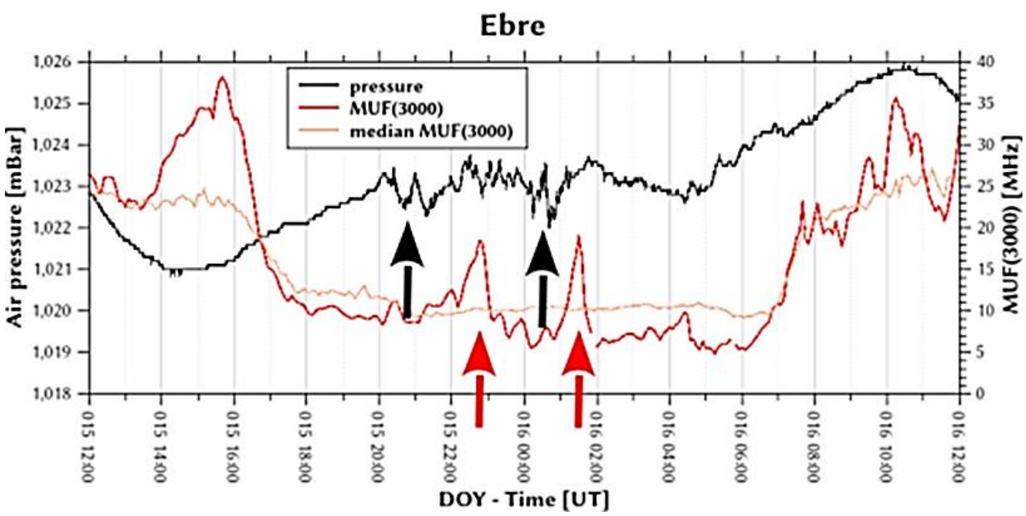

Figure 21: Ground level air-pressure (black) and ionospheric MUF (red) measured at the Ebre observatory in Spain (40.8°N, 0.5°E) on 15-16 January 2022. (Verhulst et al., 2022)

The global spatiotemporal variability of integrated water vapor

Atmospheric water vapor plays a prominent role in climate change and atmospheric, meteorological, and hydrological processes. Because of its high spatiotemporal variability, precise quantification of water vapor is challenging. Therefore, in a study, Van Malderen et al. (2022) combined Integrated Water Vapor (IWV) retrievals at 118 globally distributed Global Positioning System (GPS) sites with IWV ultraviolet (UV) / visual (VIS) satellite retrievals by GOME, SCIAMACHY, and GOME-2 (denoted as GOMESCIA below), and IWV output of a Numerical Weather Prediction model reanalysis (ERA-Interim). The length of study period (1995-2010) is limited by the availability of a consistent GPS data reprocessing for this time period only.

For comparison of the different IWV datasets, GPS IWV was chosen as the reference dataset. We found that the ERA-Interim monthly mean IWVs agree better with GPS IWV (the average r^2 is equal to 0.985) than GOMESCIA (r^2 of 0.878), with correlations at all sites being statistically significant. The lowest correlations are obtained for island and coastal sites where the spatial (horizontal) representation of the IWV field at the site location by the GOMESCIA ground pixel (320 km east-west) and surrounding ERA-interim model grids (80 km) is highly problematic for direct comparison.

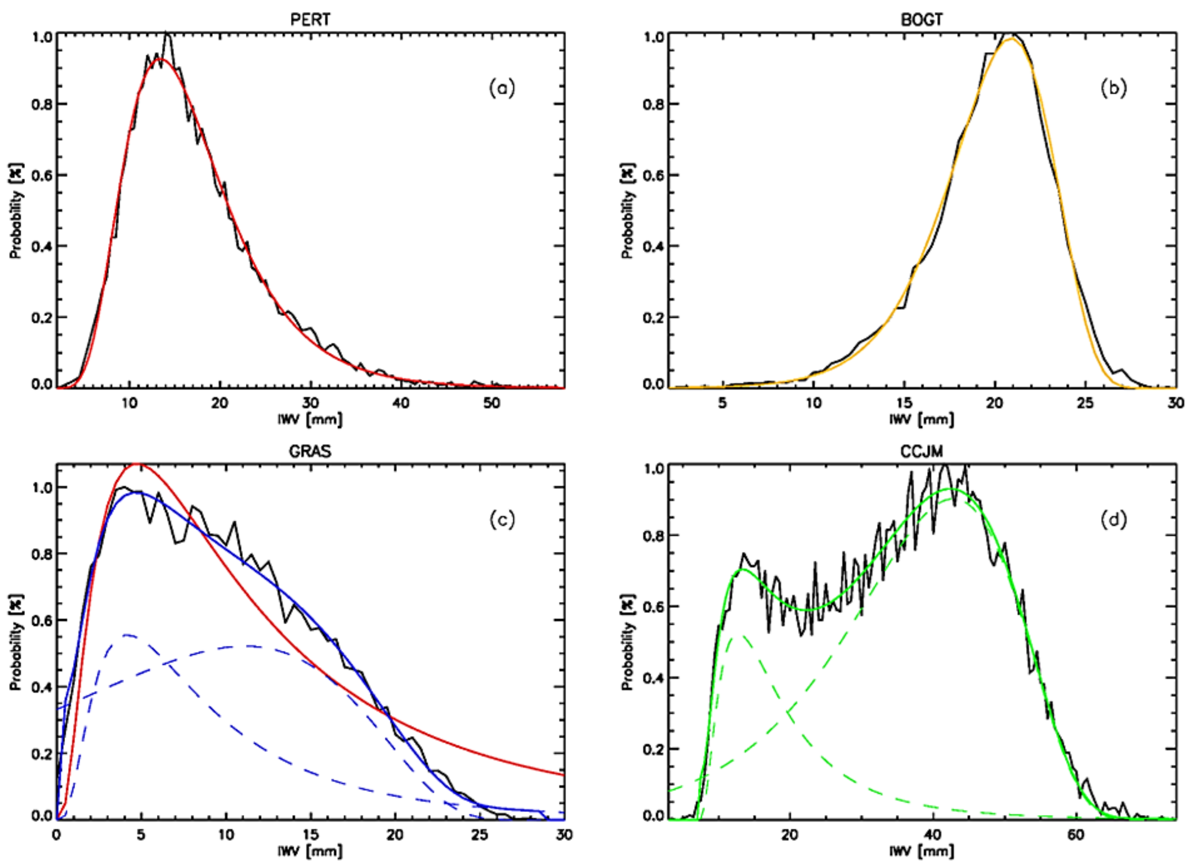

Figure 22: Examples of the different categories of frequency distribution functions for the GPS IWV distribution at 4 GPS sites: (a) the standard lognormal distribution (fit in red) at PERT (Perth, Australia), (b) the reverse lognormal distribution (fit in orange) at BOGT (Bogota, Colombia), (c) the shouldered lognormal distribution (in blue, with the two contributing lognormal distributions in dashed blue) at GRAS (Caussols, France), and, for illustration, the best fit of a single lognormal distribution in red, and (d) the bimodal lognormal distribution (fit in green) at CCJM (Ogasawara, Japan) with its contributing lognormal distributions in dashed lines.

For 60% of stations the GOMESCIA IWV was found to have a negative (dry) bias compared to GPS IWV, most likely due to the selection of cloud-free observations for the GOMESCIA IWV retrieval, inherent to the UV/VIS technique requiring direct sunlight. ERA-Interim IWV has a small positive (moist) bias of 0.5 mm compared to GPS IWV for about 70% of the stations, mostly in the extra-tropics, and a slight dry bias in the tropics when compared to GPS. The standard deviation is, on average, smaller between GPS and ERA-interim (0.8 mm) than between GPS and GOMESCIA (2.7 mm). The three datasets also agree very well in terms of the seasonal behavior, with GOMESCIA deviating more from the other two, especially for some Northern Hemisphere sites.

We found that the frequency distributions of the IWV time series are best fitted with lognormal distributions. This can be a single standard lognormal IWV distribution, like almost all the Australian sites (see the Perth example in Figure 22a), or a reverse lognormal distribution (Bogota, see Figure 22b). Sites in Europe and around half of all North American sites have histograms that are best represented by a leading lognormal distribution for the lower component (dry season), added with another, reverse lognormal distribution for the upper component (wet season), see the French Caussols station in Figure 22c. These two components can consequently be explained by seasonal IWV behavior. For subtropical sites and sites in East Asia (see the Japanese site Ogasawara in Figure 22d), two distinct lognormal distributions are however required, where strong seasonality related to the monsoon prescribes a bimodal lognormal density distribution.

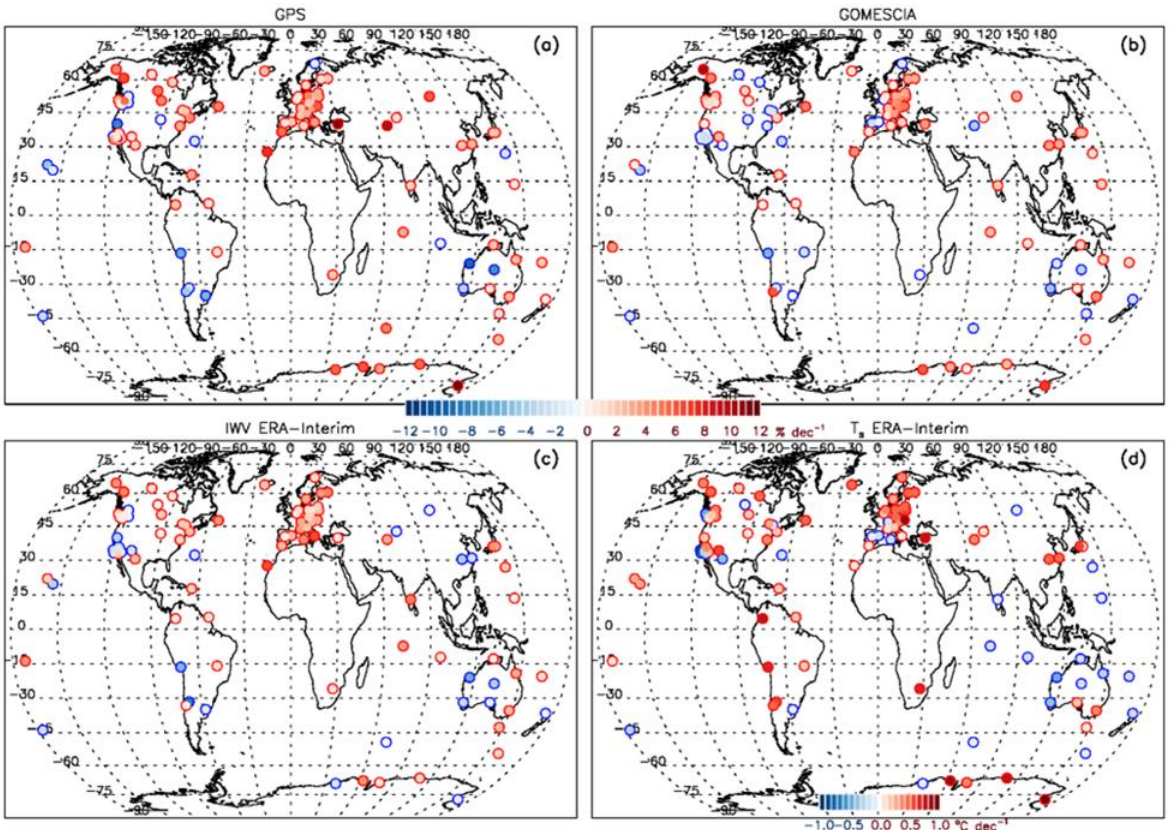

Figure 23: IWV trends in % per decade (% dec^{-1}) for GPS (a), GOMESCIA (b), and ERA-Interim (c) for the period January 1996-December 2010. For illustration, panel (d) shows the ERA-Interim surface temperature trends for the same period in °C per decade (°C dec^{-1}).

Of course, the length of the time series is, in combination with the auto-correlation and variability of the IWV monthly anomalies, too short to detect a quoted trend of 0.2-0.3 mm per decade. If we however concentrate on the geographical consistency of the sign of the linear trends among the different datasets (see Figure 23), then we can conclude that IWV is increasing over Europe and the Indian Ocean, while there is a drying trend over Western Australia. The IWV trend sign pattern above North America is less consistent, especially for the GOMESCIA retrieval. Remaining inhomogeneities in the datasets (e.g., due to instrument changes at some GPS sites, changes in the data assimilation sources in ERA-Interim, and when combining the measurements of the individual instruments to build up the GOMESCIA time series) might impact the results. However, this study highlights that combining information from three distinct IWV datasets enables the consistent characterization of IWV variability and its relationship with surface temperature and precipitation. For instance, over Europe and Western Australia, the respective moistening and drying are associated with surface warming and cooling, respectively. Moreover, the spatial pattern of the sign of the precipitation trends in those regions follows these IWV and surface temperature trend signs with positive trends over continental Europe and negative trends in Western Australia.

No less than 4 colleagues successfully defended their PhD thesis in 2022: Dana Talpeanu, Christine Verbeke, Evangelia Samara and Alexandros Koukras, the latter seeming to be very happy with his newly acquired diploma. Congratulations to all! (Credits: Dana Talpeanu)

Instrumentation and experiments

The Starlink incident as observed by PROBA2/LYRA

On 3 February 2022, SpaceX launched 49 Starlink satellites into staging orbits at 210 km above sea level, prior to raising them to their operational altitudes of 550 km. The launch took place during the recovery phase of a minor geomagnetic storm. Such mild storms usually have a very limited impact on satellites, and the Starlink operators did not anticipate any problem. However, they soon realized that the satellites were experiencing an excessive drag compared to previous launches and they commanded them into a low-drag configuration in an attempt to decrease altitude loss rates. Despite this mitigation, 38 of the 49 satellites re-entered the atmosphere and burned up within the next few days. The importance of the drag increase at the level of low Earth orbits (LEO) caused by such a minor storm was not predicted by models and was therefore totally unexpected. It highlighted the poor knowledge of the effects of space weather on the Earth's atmosphere for altitudes below 500 km, where very few measurements are available.

Figure 24: Starlink satellites re-entering the atmosphere over Puerto Rico on 7 February 2022. Credits: the Sociedad de Astronomia del Caribe

The LYRA radiometer, on board the PROBA2 spacecraft, measures the solar irradiance in four passbands of the UV-EUV spectral range with a sub-second acquisition cadence. It is primarily devoted to the study of solar phenomena, such as eruptions. However, from October to February, the orbit of the spacecraft crosses the shadow of Earth, reproducing an eclipse configuration. For a short period, when entering and getting out of the eclipse zone, the instrument sees the Sun through the Earth's atmosphere, which absorbs part of the light. Analyzing the alteration of the input signal provides us with a way to determine the density profile of the main constituents of the Earth's thermosphere, namely O and N_2, at an altitude ranging between 150 and 350 km.

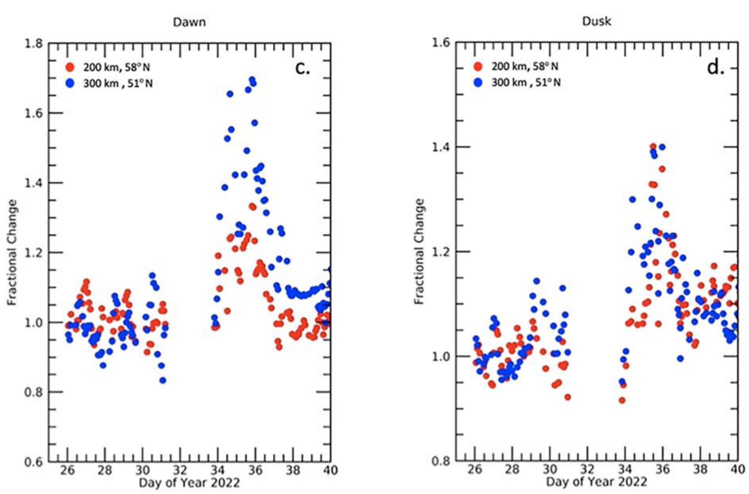

Figure 25: Thermospheric total number density measured by LYRA between day of the year (DOY) 25 to 40, i.e. from 25 January to 9 February 2022. The geomagnetic storm started on 3 February (DOY 34). The left and right panels correspond to measurements in resp. the dawn and dusk sectors.

As the storm happened during its eclipse season, LYRA observations could be used to provide an estimate of the density increase caused by the minor solar storm at the altitude of the Starlink orbits. They highlighted that density enhancements due to the geomagnetic storm starting on 4 February increased rapidly with altitude, reaching 90% at 330 km in the dawn sector and 40% at 330 km in the dusk sector.

These results were submitted in 2022 to the Space Weather journal from the American Geophysical Union (Berger et al. - 2023). They point out the importance of monitoring space weather to the space sector, especially with respect to the increasing number of small low-cost satellites evolving on low Earth orbits. They also highlight the lack of observations to complement models in that range of altitude.

Flight Acceptance Review of the Science Operations Centre for PROBA-3/ASPIICS

PROBA-3 is the next mission in the PROBA (PRoject for On-Board Autonomy) line of small satellites developed by the European Space Agency (ESA). It is primarily a mission dedicated to the in-flight demonstration of technologies for precise formation flying. For PROBA-3, this means that its two small spacecraft will be flying together in formation, along a highly elliptical orbit around the Earth. The formation of two spacecraft will produce a giant solar coronagraph called ASPIICS, which stands for the Association of Spacecraft for Polarimetric and Imaging Investigation of the Corona of the Sun.

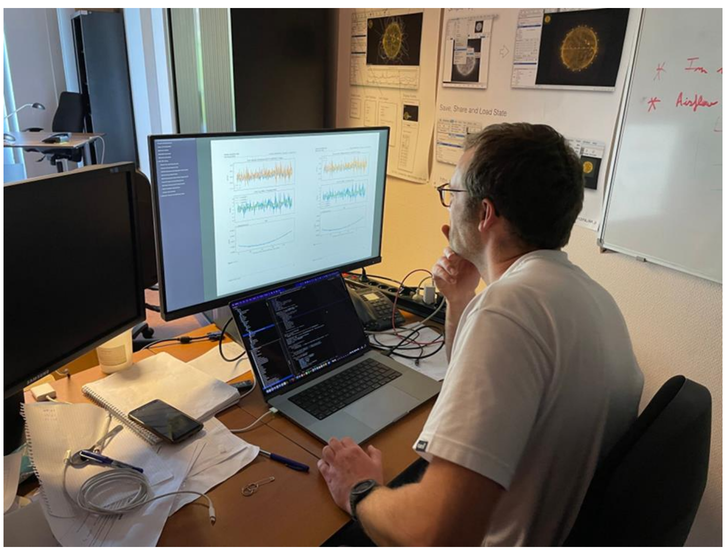

Figure 26: PROBA-3 Science Operations Centre in development.

A coronagraph is a telescope that can observe the solar corona, the tenuous outer atmosphere of the Sun that is usually seen only under total solar eclipse conditions. During a total eclipse, the Moon completely covers the bright disc of the Sun, allowing the dim corona to be seen. The ASPIICS coronagraph will consist of two PROBA-3 spacecraft flying in formation, with one spacecraft carrying the optical telescope, and the second spacecraft carrying the circular occulter that plays the role of the Moon. The inter-spacecraft distance of around 145 meters will allow observing the corona close to the solar limb with unprecedentedly low parasitic light coming from the bright solar disc. Such conditions will be similar to those encountered during a total eclipse. In order to accomplish this task, the two spacecraft have to be aligned with the precision of a few millimeters.

PROBA-3, to be launched in May 2024, will not only demonstrate advanced technologies but is also a mission in the Science Programme of ESA. The scientific objectives of ASPIICS include the investigation of the structure and the dynamics of the quiescent solar corona and of CMEs, huge eruptions of plasma and magnetic fields that may arrive at the Earth and produce geomagnetic storms.

Since 2017, the Solar Influences Data analysis Center (SIDC) of ROB has been developing the Science Operations Centre (SOC) of ASPIICS. After the mission launch, the SOC will be tasked with creating observation programs for the desired science operations of ASPIICS, sending them to the PROBA-3 Mission Operations Centre in Redu (Belgium), as well as receiving and processing the acquired coronal images. The SOC is developed by a team of software engineers and scientists at SIDC, which has been supported by the SOC international partners from Germany, Italy, Poland, and Romania. An important aspect of the SOC is that it has to take into account the particular nature of this innovative mission, namely the presence of two precisely aligned spacecraft. The SOC will have to calculate the influence of dynamically changing positions and orientations of the two spacecraft on the resulting coronal images.

A committee consisting of experts in software development, space mission operations, and science was appointed by ESA to follow the SOC development and to review it at regular intervals. The Flight Acceptance Review was the last in the series of reviews. It had to certify that the SOC is built following the pre-defined scientific and technical requirements. The committee has thoroughly inspected the SOC software and associated documentation. In April 2022, it concluded that the SOC satisfies all the requirements and the Flight Acceptance Review of the ASPIICS SOC is successfully closed.

SIMBA completes its mission

CubeSats are very small satellites built using cubes with sides of 10 cm as building blocks and offer a (relatively) low-cost possibility to do research in space. SIMBA was a small satellite (three cubes big) with a big ambition: to measure one of the fundamental drivers of climate change. Based on measurements from the 30 cm long satellite, the aim was to calculate the total energy budget of our planet.

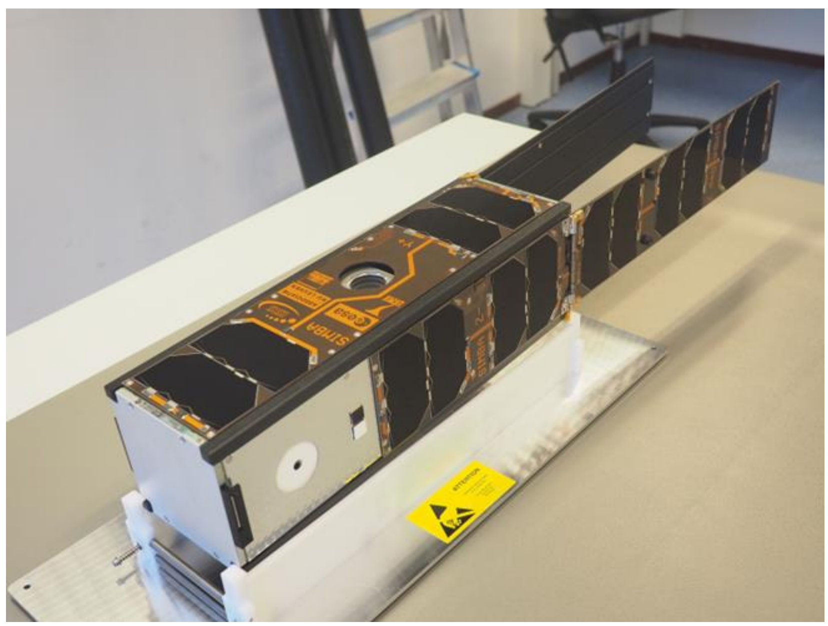

Figure 27: The finished satellite with open solar panels as it flew in space. Only the antennas are stowed away.

SIMBA stands for 'Sun-earth IMBAlance', which means the difference in the amount of incoming and outgoing radiation at the top of the atmosphere. To measure the radiation, the satellite was equipped with a radiometer. The aim was to determine whether it is possible to measure both the incoming radiation from the Sun and the outgoing radiation from the Earth with the same instrument, which has never been done before.

By subtracting the outgoing radiation from the incoming solar radiation, we get a figure for the Earth's radiation balance - the amount of energy our planet retains rather than reflects or radiates away.

The SIMBA mission pioneered the use of CubeSats as full-fledged scientific instruments. The cost reduction compared to big satellites allows for a constellation to be launched, which can then be upgraded with each new generation. This will result in unprecedented ground coverage, and imply a huge step forward in measuring the radiation balance - one of the most important parameters of climate change.

In December 2022 the SIMBA mission, initially set for 6 months but extended to more than 2 years, came to an end. After 28 months in space, 600.700 data points were generated during 3350 hours of data acquisition. 13.000 orbits around the Earth were completed and its orbit degraded by 30 km since its launch. The team at RMIB continued working on the mission and on the data generated by the instrument. The year 2023 will see the last results from the mission both as a data set and as scientific publications.

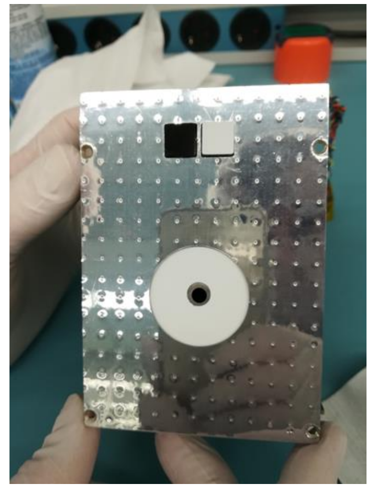

Figure 28: The sensors of SIMBA. The black and white squares are absorbers to provide a discrimination between the Earth's emitted thermal and reflected solar radiation. Behind the white disk with opening is the cavity radiometer instrument.

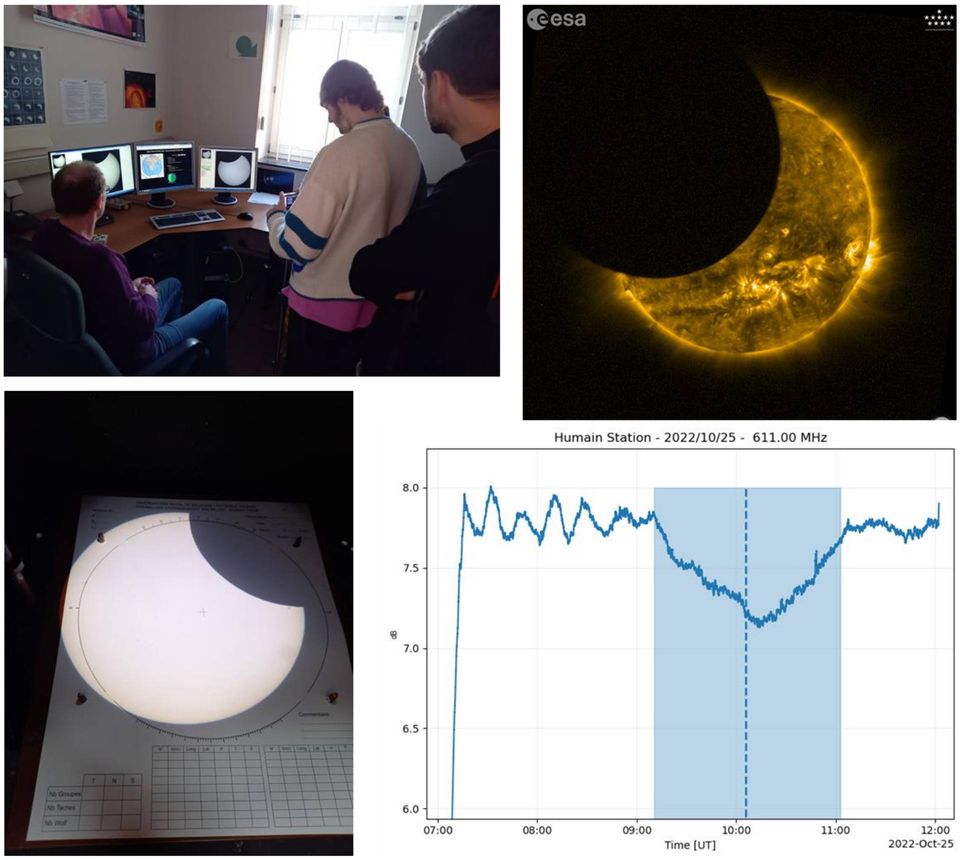

A partial solar eclipse was visible in Belgium on 25 October 2022. It was well attended by the media (upper left), with dedicated websites developed by SILSO and the ROB. The eclipse was nicely followed by the solar telescopes of USET (Uccle Solar Equatorial Table; lower left), the instruments on board the PROBA2 satellite (upper right), and the radio telescopes in Humain showing a dip in the radio intensity at 611 MHz during the eclipse period (lower right).

Applications, modeling and services

FARSUN: Findability and Accessibility of historical Raw SUnspot Numbers

The sunspot record is the primary means by which the solar variability over the last 400 years is known and constitutes a benchmark in solar/stellar variability studies and especially the Earth's climate. While this record has recently been improved via new or updated observations, data, and methodologies, these improvements need now to be made accessible to the many researchers and users outside of the sunspot community.

At the beginning of 2022, a team from the department of Solar Physics led by L. Lefèvre from the World Data Center SILSO (WDC-SILSO) submitted a project aimed to gather and make FAIR (Findability, Accessibility, Interoperability, and Reusability) all available raw historical sunspot number data. The project was selected in July 2022 and started officially in March 2023.

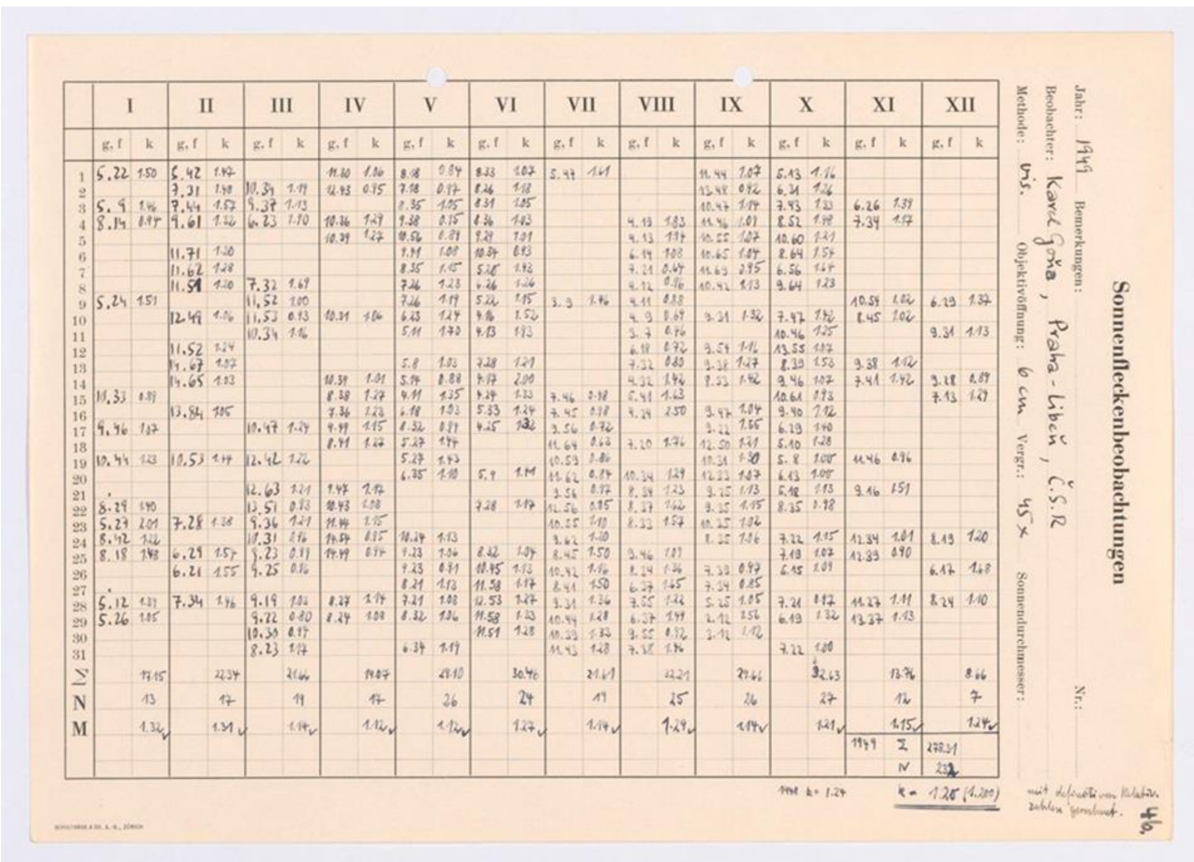

Figure 29: Table of observations from the Czech Republic in 1949

FARSUN will make the raw historical sunspot data (1610-1980) of national and international origin, on which the WDC SILSO deploys its expertise, Findable and Accessible for all users. The project gathers, interprets and valorizes the data, where the latter includes data pre-processing, quality assessment and standardization, as well as to advocate these data to end users. A detailed statistical study will provide quality criteria for these historical data, and the most pertinent criteria will be included in metadata describing the dataset.

This project extends across multiple fields through its network of participants:

- the WDC SILSO expertise as curator of the International Sunspot Number,
- the statistical expertise from the Université Catholique de Louvain, the Université libre de Bruxelles and the Université d'Orléans,
- the expertise on historical datasets from partners at the University of Extremadura, at the Leibniz-Institut für Astrophysik Potsdam and at the University of Nagoya,
- Virtual Observatory (VO) expertise from Observatoire de Paris,
- the time-series expertise from our colleagues of the University of Colorado's LASP (USA)
- solar modeling expertise from the Université de Montréal
- expertise in optical characters recognition from a team of the University of Innsbruck (Transkribus).

The Transkribus tool will help with a novel aspect of the project: exploiting tables of numbers of sunspots and groups observations compiled by the Zurich team from 1945 to 1979. These observations were mentioned in the original Zurich Journals created by Professor Rudolf Wolf, the Mittheilungen, but not included and remained inaccessible for a long time. Following their recent digitization at the ETH Zurich, they are now available through e-manuscripta. An example is shown in Figure 29 for observations by a station in the Czech Republic in 1949.

Over the period 1945 to 1979, there are about 2000 tables to digitize (i.e. transform into machine readable tables), and the Transkribus tool has also developed the capacity to learn from the first character extractions in order to minimize extraction time and maximize efficiency.

The output of this project will be a compilation of historical sunspot numbers that will be made available via standard VO-tools defined by the International Virtual Observatory Alliance (IVOA), and more specifically via an EPN-TAP (Europlanet-Table Access Protocol) service. This will allow this catalog to be Findable (via the IVOA Registry) and Accessible by query from a variety of TAP clients. In addition, the standardization of this VO tool allows other tools (graphical viewers, editors,…) to easily access the data, making them Interoperable while the rich catalog metadata will allow the data to be Reusable, i.e. the data will be FAIR-compliant.

Making these validated historical sunspot data collections FAIR will allow solar physicists, Earth-climate modelers, experts in statistics, or anyone with a keen interest in solar variability, to analyze this unique natural record, increase public awareness about the effects of solar variability on Earth, and thus feed future science in the service of society.

PITHIA-NRF

ROB, RMI and BIRA are taking part in the European Horizon 2020 project PITHIA-NRF: “Plasmasphere Ionosphere Thermosphere Integrated Research Environment and Access services: a Network of Research Facilities”.

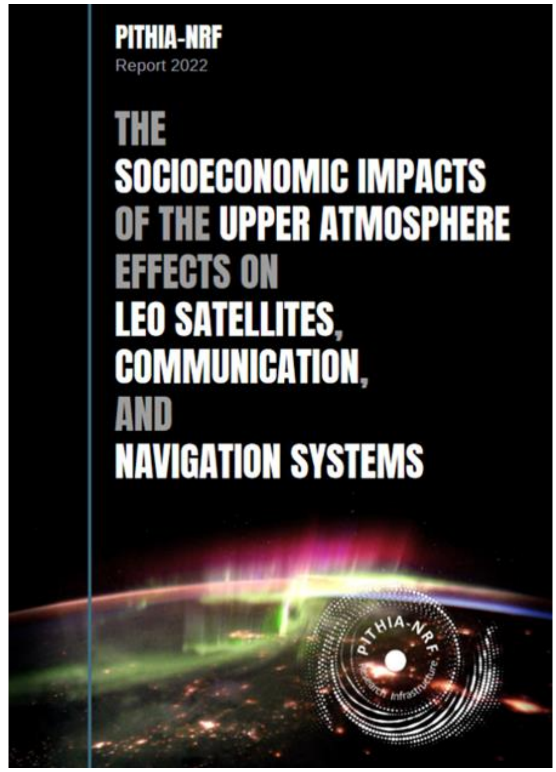

Figure 30: Frontpage of the PITHIA-NRF 2022 report reaching out to the general public and the private stakeholders.

With its consortium of 23 European partners, the PITHIA-NRF project aims at building a European distributed network gathering observing facilities, data processing tools and prediction models dedicated to ionosphere, thermosphere and plasmasphere research. This community building aims at developing synergies in the upper atmosphere research and application fields and maintain strong links with the academic, operational sectors and policy makers. It encourages collaboration by opening access to the best European research infrastructures and facilities, FAIR data, training and innovation services. The project facilitates research advances in the field of space weather, and promotes these advances through communication and public outreach.

ROB, RMI and BIRA are actively participating in the management of the project, provide data, communicate within and outside of the consortium. Due to the Covid-19 restrictions, the first in-person meeting of the consortium since its beginning in 2021 took place in 2022. During these meetings, the First Innovation Day of PITHIA-NRF took place in Rome, bringing together 80 persons from various industries and civil organizations, with the PITHIA-NRF experts in upper atmospheric research to exchange ideas, share knowledge, and explore new avenues of collaboration. In addition, PITHIA-NRF reaches out to the public and private sectors by providing information on “The Socioeconomic Impacts of the Upper Atmosphere Effects on LEO Satellites, Communication and Navigation Systems” (leaflet and report).

Figure 31: A picture taken during the First Innovation Day of PITHIA-NRF on 21 June 2022.

The progress of the PITHIA-NRF project was evaluated in December 2022, with a positive overall assessment. The project fully achieves its objectives and milestones since it started in 2021 and despite the Covid-19 difficulties. Next stages of the project are to enhance its visibility, its training and collaboration opportunities, and the release of the E-Science centre to the public which will provide access to the upper atmosphere data and models and stimulate collaborations.

T-FORS: Forecasting of Travelling Ionospheric Disturbances

A new Horizon project has started, bringing together various European partners, with the goal of developing a forecasting system for TIDs. Travelling ionospheric disturbances (TIDs) are a specific type of space weather disturbance that could compromise the performance of critical space and ground infrastructure by disrupting operations and communications in multiple sectors. T-FORS (Travelling Ionospheric Disturbances Forecasting System) aims at providing new models able to interpret a broad range of observations of the solar corona, the interplanetary medium, the magnetosphere, the ionosphere and the atmosphere, and to issue forecasts and warnings for TIDs several hours ahead.

Machine Learning techniques are used to train the models based on existing databases developed in the frames of past Horizon 2020 projects, to estimate the occurrence probability of medium scale TIDs and to forecast the occurrence and propagation of large scale TIDs. Prototype services are developed based on specifications from the users' community and following harmonized standards and quality controls similar to the best practices of meteorological services. On ground demonstration tests are organized, by aerospace and civil protection agencies, to validate the performance of the T-FORS prototype services. A comprehensive architectural concept is proposed, including the densification of ground instrument networks, new space missions, and possible future adjustments in order to develop a real-time operational service fully compliant and complementary to the ESA Space Weather services.

The EU-funded T-FORS project will develop improved models that could aid in issuing forecasts and warnings for TIDs several hours ahead, exploiting a broad range of observations of the solar corona, the interplanetary medium, the magnetosphere, the ionosphere and the atmosphere. Machine learning algorithms will be used to forecast the occurrence and propagation of large-scale TIDs. What is more, statistical models will be applied to estimate the occurrence probability and propagation pattern of medium-scale TIDs.

[E-SWAN](), the European Space Weather and Space Climate Association, is an international non-profit association established in 2022. It held its first General Assembly during the European Space Weather Week in Zagreb, Croatia. The image above is from this meeting and shows the majority of the E-SWAN [founders](). Its main mission is to unite, sustain and develop space weather and space climate activities in Europe. To this purpose, several committees and working groups have been established. The STCE is strongly supporting and participating in all of the E-SWAN activities.

Publications

This overview of publications consists of three lists: the peer-reviewed articles, the presentations and posters at conferences, and the public outreach talks and publications for the general public. It does not include non-refereed articles, press releases, the daily, weekly and monthly bulletins that are part of our public services,… These data are available at the [STCE website]() or upon request.

Authors belonging to the STCE have been highlighted in the list of peer-reviewed articles.

Peer reviewed articles

1. Alfonsi, L.; **Bergeot, N.**; Cilliers, P. J.; … ; **Pottiaux, E.**; … ; **Van Malderen, R.**; … and 33 co-authors
Review of Environmental Monitoring by Means of Radio Waves in the Polar Regions: From Atmosphere to Geospace
Surveys in Geophysics, 43, 6, 1609-1698, 2022, DOI: 10.1007/s10712-022-09734-z

2. Alipour, N.; Safari, H.; **Verbeeck, C.**; **Berghmans, D.**; … ; **Dolla, L.**; … ; **Gissot, S.**; … ; **Katsiyannis, A.C.**; … ; **Zhukov, A.N.**; and 18 co-authors
Automatic detection of small-scale EUV brightenings observed by the Solar Orbiter/EUI
Astronomy & Astrophysics, 663, A128, 2022, DOI: 10.1051/0004-6361/202243257

3. Ancellet, G.; Godin-Beekmann, S.; Smit, H.G.J.; Stauffer, R.M.; **Van Malderen, R.**; Bodichon, R.; Pazmiño, A.
Homogenization of the Observatoire de Haute Provence electrochemical concentration cell (ECC) ozonesonde data record: comparison with lidar and satellite observations
Atmospheric Measurement Techniques, 15, 10, 3105-3120, 2022, DOI: 10.5194/amt-15-3105-2022

4. Barczynski, K.; Meyer, K.A.; Harra, L.K.; Mackay, D.H.; Auchère, F.; **Berghmans, D.**
A Statistical Comparison of EUV Brightenings Observed by SO/EUI with Simulated Brightenings in Nonpotential Simulations
Solar Physics, 297, 141, 2022, DOI : 10.1007/s11207-022-02074-6

5. Bemporad, A.; Andretta, V.; Susino, R.; … ; **Mierla, M.**; **Berghmans, D.**; **D'Huys, E.**; **Zhukov, A.N.**; **Talpeanu, D.-C.**; … ; and 21 co-authors
Coronal mass ejection followed by a prominence eruption and a plasma blob as observed by Solar Orbiter
Astronomy & Astrophysics, 665, A7, 2022, DOI: 10.1051/0004-6361/202243162

6. Chang, K.-L.; Cooper, O.R.; Gaudel, A.; … ; **Van Malderen, R.**; … ; and 11 co-authors
Impact of the COVID-19 economic downturn on tropospheric ozone trends: An uncertainty weighted data synthesis for quantifying regional anomalies above western North America and Europe
AGU Advances, 3, 2, 2022, DOI: 10.1029/2021AV000542

7. Chitta, L. P.; Peter, H.; Parenti, S.; **Berghmans, D.**; … ; **Kraaikamp, E.**; … ; **Rodriguez, L.**; … ; **Verbeeck, C.**; **Zhukov, A.N.**; … ; and 14 co-authors
Solar coronal heating from small-scale magnetic braids
Astronomy & Astrophysics, 667, A166, 2022, DOI: 10.1051/0004-6361/202244170

8. Dahmen, N.; Sicard, A.; Brunet, A.; Santolik, O.; **Pierrard, V.; Botek, E.; Darrouzet F.**; Katsavrias, C.
FARWEST: Efficient computation of wave-particle interactions for a dynamic description of the electron radiation belt diffusion
Journal of Geophysical Research: Space Physics, 127, 10, e2022JA030518, 2022, DOI: 10.1029/2022JA030518

9. **Dewitte, S.**; Cornelis, J.; Meftah, M.
Centennial Total Solar Irradiance Variation
Remote Sensing, 14, 5, 1072, 2022, DOI: 10.3390/rs14051072

10. Erdélyi, R.; Damé, L.; Fludra, A.; … ; **Bolsée, D.**; … ; **Dewitte, S.**; … ; and 25 co-authors
HiRISE - High-Resolution Imaging and Spectroscopy Explorer - Ultrahigh resolution, interferometric and external occulting coronagraphic science
Experimental Astronomy, 54, 227-256, 2022, DOI: 10.1007/s10686-022-09831-2

11. Franci, L.; Papini, E.; **Micera, A.**; Lapenta, G.; Hellinger, P.; Del Sarto, D.; Burgess, D.; Landi, S.
Anisotropic electron heating in turbulence-driven magnetic reconnection in the near-Sun solar wind
The Astrophysical Journal, 936, 27, 2022, DOI: 10.3847/1538-4357/ac7da6

12. Godin-Beekmann, S.; Azouz, N.; Sofieva, V.F.; … ; **Van Malderen, R.**; … ; and 24 co-authors
Updated trends of the stratospheric ozone vertical distribution in the 60° S-60° N latitude range based on the LOTUS regression model
Atmospheric Chemistry and Physics, 22, 17, 11657-11673, 2022, DOI: 10.5194/acp-22-11657-2022

13. Hosteaux, S.; **Rodriguez, L.**; Poedts, S.
Analysis of Voyager 1 and Voyager 2 in situ CME observations
Advances in Space Research, 70, 6, 1684-1719, 2022, DOI: 10.1016/j.asr.2022.03.005

14. Kahil, F.; Hirzberger, J.; Solanki, S.; … ; **Berghmans, D.**; **Verbeeck, C.**; **Kraaikamp, E.**; **Gissot, S.**; and 52 co-authors
The Magnetic drivers of campfires seen by the Polarimetric and Helioseismic Imager (PHI) on Solar Orbiter
Astronomy & Astrophysics, 660, A143, 2022, DOI: 10.1051/0004-6361/202142873

15. Koji, A.K.; **Van Malderen, R.; Pottiaux, E.; Van Schaeybroeck, B.**
Understanding the Present-Day Spatiotemporal Variability of Precipitable Water Vapor over Ethiopia: A Comparative Study between ERA5 and GPS
Remote Sensing, 14, 3, 686, 2022, DOI: 10.3390/rs14030686

16. López, R.A.; **Micera, A.**; Lazar, M.; Poedts, S.; Lapenta, G.; **Zhukov, A.N.**; Boella, E.; Shaaban, S.M.
Mixing the Solar Wind Proton and Electron Scales. Theory and 2D-PIC Simulations of Firehose Instability
The Astrophysical Journal, 930, 158, 2022, DOI: 10.3847/1538-4357/ac66e4

17. Maharana, A.; Isavnin, A.; Scolini, C.; Wijsen, N.; **Rodriguez, L.**; **Mierla, M.**; **Magdalenic, J.**; Poedts, S.
Implementation and validation of the FRi3D flux rope model in EUHFORIA
Advances in Space Research, 70, 6, 1641-1662, 2022, DOI: 10.1016/j.asr.2022.05.056

18. Makrantoni, P.; Tezari, A.; Stassinakis, A.N.; Paschalis, P.; Gerontidou, M.; Karaiskos, P.; Georgakilas, A.G.; Mavromichalaki, H.; Usoskin, I.G.; **Crosby, N.**; **Dierckxsens, M.**
Estimation of Cosmic-Ray-Induced Atmospheric Ionization and Radiation at Commercial Aviation Flight Altitudes
Applied Sciences, 12, 11, 5297, 2022, DOI: 10.3390/app12115297

19. Mandal, S.; Chitta, L. P.; Antolin, P.; … ; **Berghmans, D.**; **Zhukov, A.N.**; … ; **Verbeeck, C.**; **Kraaikamp, E.**; … ; **Rodriguez, L.**; … ; and 14 co-authors
What drives decayless kink oscillations in active region coronal loops on the Sun?
Astronomy & Astrophysics, 666, L2, 2022, DOI: 10.1051/0004-6361/202244403

20. Mandal, S.; Chitta, L.P.; Peter, H.; Solanki, S.K.; Aznar Cuadrado, R.; Teriaca, L.; Schühle, U.; **Berghmans, D.**; Auchère, F.
A highly dynamic small-scale jet in a polar coronal hole
Astronomy & Astrophysics, 664, A28, 2022, DOI: 10.1051/0004-6361/202243765

21. Mathieu, S.; **Lefèvre, L.**; von Sachs, R.; **Delouille, V.**; Ritter, C.; **Clette, F.**
Nonparametric monitoring of sunspot number observations
Journal of Quality Technology, 55, 1, 104-118, 2022, DOI: 10.1080/00224065.2022.2041376

22. Mavromichalaki, H.; Paschalis, P.; Gerontidou, M.; Papailiou, M.-C.; Paouris, E.; Tezari, A.; Lingri, D.; Livada, M.; Stassinakis, A.N.; **Crosby, N.**; **Dierckxsens, M.**
The Updated Version of the A.Ne.Mo.S. GLE Alert System: The Case of the Ground-Level Enhancement GLE73 on 28 October 2021
Universe, 8, 7, 378, 2022, DOI: 10.3390/universe8070378

23. Mettig, N.; Weber, M.; Rozanov, A.; … ; **Van Malderen, R.**; … ; and 15 co-authors
Combined UV and IR ozone profile retrieval from TROPOMI and CrIS measurements
Atmospheric Measurement Techniques, 15, 9, 2955-2978, 2022, DOI: 10.5194/amt-15-2955-2022

24. **Mierla, M.**; **Zhukov, A.N.**; **Berghmans, D.**; … ; **Janssens, J.**; **Kraaikamp, E.**; **Nicula, B.**; … ; **Talpeanu, D.-C.**; **D'Huys, E.**; **Dolla, L.**; **Gissot, S.**; **Magdalenic, J.**; **Rodriguez, L.**; **Shestov, S.**; **Stegen, K.**; **Verbeeck, C.**; … ; and 12 co-authors
Prominence Eruption Observed in He II 304 Å up to >6 $R_\odot$ by EUI/FSI aboard Solar Orbiter
Astronomy & Astrophysics, 662, L5, 2022, DOI: 10.1051/0004-6361/202244020

25. **Mierla, M.**; Inhester, B.; **Zhukov, A.N.**; **Shestov, S.**; Bemporad, A.; Lamy, P.; Koutcmy, S.
Polarimetric Studies of a Fast Coronal Mass Ejection
Solar Physics, 297, 78, 2022, DOI: 10.1007/s11207-022-02018-0

26. Mrak, S.; Zhu, Q.; Deng, Y.; **Dammasch, I.E.**; **Dominique, M.**; Drob, D.; Hairston, M.R.; Nishimura, Y.; Semeter, J.
Modeling Solar Eclipses at Extreme Ultra Violet Wavelengths and the Effects of Nonuniform Eclipse Shadow on the Ionosphere-Thermosphere system
Journal of Geophysical Research: Space Physics, 127, e2022JA031058, 2022, DOI: 10.1029/2022JA031058

27. Papaioannou, A.; Vainio, R.; Raukunen, O.; Jiggens, P.; Aran, A.; **Dierckxsens, M.**; Mallios, S.A.; Paassilta, M.; Anastasiadis, A.
The probabilistic solar particle event forecasting (PROSPER) model
Journal of Space Weather and Space Climate, 12, A24, 2022, DOI: 10.1051/swsc/2022019

28. **Pierrard, V.**; Lazar, M.; Stverak, S.
Implications of the Kappa Suprathermal Halo of the Solar Wind Electrons
Frontiers in Astronomy and Space Sciences, 9, 2022, DOI: 10.3389/fspas.2022.892236

29. **Pierrard, V.; Winant,A.; Botek, E.;** Ripoll, J.-F.; Cosmides, M.; Malaspina, D.M.; Reeves, G.D.; Thaller, S.A.
Simultaneous Observations of the 23 June 2015 Intense Storm at Low Earth Orbit and Geostationary Transfer Orbit
URSI Radio Science Letters, 4, 16, 2022, DOI: 10.46620/22-0016

30. Podladchikova, T.; Jain, S.; Veronig, A.M.; Sutyrina, O.; Dumbović, M.; **Clette, F.**; Pötzi, W.
Maximal growth rate of the ascending phase of a sunspot cycle for predicting its amplitude
Astronomy & Astrophysics, 663, A88, 2022, DOI: 10.1051/0004-6361/202243509

31. Quintero Noda, Q.; Schlichenmaier, R.; Bellot Rubio, L.R.; … ; **Berghmans, D.**; … ; **Vansintjan, R.**; … ; and 276 co-authors
The European Solar Telescope
Astronomy & Astrophysics, 666, A21, 2022, DOI: 10.1051/0004-6361/202243867

32. Ripoll, J.-F.; Thaller, S.; Hartley, D.; Cunningham, G.S.; **Pierrard, V.**; Kurth, W.; Kletzing, G.C.; Wygant, J.
Statistics and empirical models of the plasmasphere boundaries from the Van Allen Probes for radiation belt physics
Geophysical Research Letters, 49, 21, e2022GL101402, 2022, DOI: 10.1029/2022GL101402

33. Rochus, P.; Auchère, F.; **Berghmans, D.**; … ; **BenMoussa, A.**; … ; **Bonte, K.**; … ; **Delouille, V.**; **Dolla, L.**; … ; **Giordanengo, B.**; **Gissot, S.**; … ; **Hochedez, J.-F.**; … ; **Kraaikamp, E.**; … ; **Mampaey, B.**; … ; **Nicula, B.**; **Parenti, S.**; … ; **Pylyser, E.**; … ; **Rodriguez, L.**; … ; **Seaton, D.B.**; … ; **Stegen, K.**; … ; **Verbeeck, C.**; … ; **West, M.J.**; … ; **Zhukov, A.N.** and 128 co-authors
The Solar Orbiter EUI instrument: The Extreme Ultraviolet Imager (Corrigendum)
Astronomy & Astrophysics, 665, C1, 2022, DOI: https://doi.org/10.1051/0004-6361/201936663e

34. **Rodriguez, L.**; Barnes D.; Hosteaux, S.; … ; **Willems, S.**; … ; **Berghmans, D.**; … ; **Magdalenic, J.**; **Mierla, M.**; … ; and 11 co-authors
Comparing the HELCATS manual and automatic catalogues of CMEs using STEREO-HI data
Solar Physics, 297, 23, 2022, DOI: 10.1007/s11207-022-01959-w

35. **Samara, E.**; **Magdalenic, J.**; **Rodriguez, L.**; Heinemann, S.G.; Georgoulis, M.K.; Hofmeister, S.J.; Poedts, S.
Influence of mid-latitude coronal hole morphology on the solar wind speed at Earth
Astronomy & Astrophysics, 662, A68, 2022, DOI: 10.1051/0004-6361/202142793

36. **Samara, E.**; Laperre, B.; Kieokaew, R.; Temmer, M.; **Verbeke, C.**; **Rodriguez, L.**; **Magdalenic, J.**; Poedts, S.
Dynamic Time Warping as a means to assess solar wind time series
The Astrophysical Journal, 927, 187, 2022, DOI: 10.3847/1538-4357/ac4af6

37. **Schifano, L.**; Vervaeke, M.; Rosseel, D.; Verbaenen, J.; Thienpont, H.; **Dewitte, S.**; Berghmans, F.; Smeesters, L.
Freeform Wide Field-of-View Spaceborne Imaging Telescope: From Design to Demonstrator
Sensors, 22, 21, 8233, 2022, DOI: 10.3390/s22218233

38. **Schifano, L.**; Berghmans, F.; **Dewitte, S.**; Smeesters, L.
Optical Design of a Novel Wide-Field-of-View Space-Based Spectrometer for Climate Monitoring
Sensors, 22, 15, 5841, 2022, DOI: 10.3390/s22155841

39. **Shestov, S.**; **Voitenko, Y.**; **Zhukov, A.N.**
Initiation of Alfvénic turbulence by Alfvén wave collisions: A numerical study
Astronomy & Astrophysics, 661, A93, 2022, DOI: 10.1051/0004-6361/202142362

40. Stauffer, R.M.; Thompson, A.M.; Kollonige, D.E.; … ; **Van Malderen, R.**; … ; and 9 co-authors
An Examination of the Recent Stability of Ozonesonde Global Network Data
Earth and Space Science, 9, 10, e2022EA002459, 2022, DOI: 10.1029/2022EA002459

41. Talha, M.; Ahmed, N.; Ayyaz Ameen, M.; **Sapundjiev, D.**; Murtaza, G.
Equinoctial asymmetry during solar minima at low to mid latitude
Advances in Space Research, 70, 10, 2941-2952, 2022, DOI: 10.1016/j.asr.2022.07.073

42. **Talpeanu, D.-C.**; Poedts, S.; **D’Huys, E.**; **Mierla, M.**
Study of the propagation, in situ signatures, and geoeffectiveness of shear-induced coronal mass ejections in different solar winds
Astronomy & Astrophysics, 658, A56, 2022, DOI: 10.1051/0004-6361/202141977

43. **Talpeanu, D.-C.**; Poedts, S.; **D'Huys, E.**; **Mierla, M.**; Richardson, I.G.
Interaction of coronal mass ejections and the solar wind - A force analysis
Astronomy & Astrophysics, 663, A32, 2022, DOI: 10.1051/0004-6361/202243150

44. Telloni, D.; Zank, G.P.; Stangalini, M.; … ; **Berghmans, D.**; … ; **Kraaikamp, E.**; … ; **Rodriguez, L.**; … ; **Verbeeck, C.**; **Zhukov, A.N.**; and 53 co-authors
Observation of a Magnetic Switchback in the Solar Corona
The Astrophysical Journal Letters, 936, L25, 2022, DOI: 10.3847/2041-8213/ac8104

45. Tezari, A.; Paschalis, P.; Stassinakis, A.; Mavromichalaki, H.; Karaiskos, P.; Gerontidou, M.; Alexandridis, D.; Kanellakopoulos, A.; **Crosby, N.**; **Dierckxsens, M.**
Radiation Exposure in the Lower Atmosphere during Different Periods of Solar Activity
Atmosphere, 13, 2, 166, 2022, DOI: 10.3390/atmos13020166

46. Tezari, A.; Stassinakis, A.N.; Paschalis, P.; Mavromichalaki, H.; Plainaki, C.; Kanellakopoulos, A.; **Crosby, N.; Dierckxsens, M.**; Karaiskos, P.
Radiation Dosimetry Estimations in the Venusian Atmosphere during Different Periods of Solar Activity
Universe, 8, 12, 637, 2022, DOI: 10.3390/universe8120637

47. Tiwari, S.K.; Hansteen, V.H.; De Pontieu, B.; Panesar, N.K.; **Berghmans, D.**
SolO/EUI Observations of Ubiquitous Fine-scale Bright Dots in an Emerging Flux Region: Comparison with a Bifrost MHD Simulation
The Astrophysical Journal, 929, 103, 2022, DOI: 10.3847/1538-4357/ac5d46

48. Triantafyllou, I.; **Katsiyannis, A.C.**; Papadopoulos, G.A.
Historical earthquakes, tsunamis, volcanic eruptions and comets in the eastern Mediterranean and the Sina sub-plate: evidence from two little-known Greek documents
Natural Hazards, 116, 4, 1711-1733, 2022, DOI: 10.1007/s11069-022-05736-7

49. **Van Malderen, R.; Pottiaux, E.;** Stankunavicius, G.; Beirle, S.; Wagner, T.; **Brenot, H.; Bruyninx, C.;** Jones, J.
Global Spatiotemporal Variability of Integrated Water Vapor Derived from GPS, GOME/SCIAMACHY and ERA-Interim: Annual Cycle, Frequency Distribution and Linear Trends
Remote Sensing, 14, 4, 2022, DOI: 10.3390/rs14041050

50. **Van Malderen, R.**; Santos, M.; Zhang, K.
Editorial for the Special Issue "Climate Modelling and Monitoring Using GNSS"
Remote Sensing, 14, 17, 4371, 2022, DOI: 10.3390/rs14174371

51. **Verbeke, C.**; Baratashvili, T.; Poedts, S.
ICARUS, a new inner heliospheric model with a flexible grid
Astronomy & Astrophysics, 662, A50, 2022, DOI: 10.1051/0004-6361/202141981

52. **Verhulst**, T.G.W.; Altadill, D.; Barta, V.; … ; and 12 co-authors
Multi-instrument detection in Europe of ionospheric disturbances caused by the 15 January 2022 eruption of the Hunga volcano
Journal of Space Weather and Space Climate, 12, A35, 2022, DOI: 10.1051/swsc/2022032

53. **Verhulst, T.G.W.**; **Stankov, S.M.**
The Changing Shape of the Ionosphere During a Solar Eclipse
URSI Radio Science Letters, 4, 68, 2022, DOI: 10.46620/22-0068

54. Verscharen, D.; Chandran, B.D.G.; Boella, E.; Halekas, J.; Innocenti, M.E.; Jagarlamudi, V.K.; **Micera, A.**; **Pierrard, V.**; Stverak, S.; Vasko, I.Y.; Velli, M.; Whittlesey, P.L.
Electron-driven instabilities in the solar wind
Frontiers in Astronomy and Space Sciences, 9, 951628, 2022, DOI: 10.3389/fspas.2022.951628

55. Wauters, L.; Dominique, M.; Milligan, R.; Dammasch, I.E.; Kretzschmar, M.; Machol, J.
Observation of a Flare and Filament Eruption in Lyman-α on 8 September 2011 by the PRoject for OnBoard Autonomy/Large Yield Radiometer (PROBA2/LYRA)
Solar Physics, 297, A36, 2022, DOI: 10.1007/s11207-022-01963-0

56. West, M.J.; Seaton, D.B.; **D'Huys, E.**; **Mierla, M.**; Laurenza, M.; Meyer, K.A.; **Berghmans, D.**; Rachmeler, L.; **Rodriguez, L.**; **Stegen, K.**
A Review of the Extended EUV Corona Observed by the Sun Watcher with Active Pixels and Image Processing (SWAP) Instrument
Solar Physics, 297, A136, 2022, DOI: 10.1007/s11207-022-02063-9

57. Ying, B.; Feng, L.; Inhester, B.; **Mierla, M.**; Gan, W.; Lu, L.; Li, S.
Three-dimensional analyses of an aspherical coronal mass ejection and its driven shock
Astronomy & Astrophysics, 660, A23, 2022, DOI: 10.1051/0004-6361/202142797

58. Zhao J., Lee L., Xie H., Yao Y., Wu D., **Voitenko Y., Pierrard V.**
Quantifying Wave-particle Interactions in Collisionless Plasmas: Theory and Its Application to the Alfvén-mode wave
The Astrophysical Journal, 930, 95, 2022, DOI: 10.3847/1538-4357/ac59b7

59. Zhao, J.; Malaspina, M.D.; Dudok De Wit, T.; **Pierrard, V.; Voitenko, Y.;** Lapenta, G.; Poedts, S.; Bale, S.D.; Kasper, J.C.; Larson, D.; Livi, R.; Whittlesey, P.
Broadband Electrostatic Waves in the Near-Sun Solar Wind Observed by the Parker Solar Probe
The Astrophysical Journal Letters, 938, L21, 2022, DOI: 10.3847/2041-8213/ac92e3

60. Zhong, S.; Nakariakov, V.M.; Kolotkov, D.Y.; **Verbeeck, C.**; **Berghmans, D.**
Two-spacecraft detection of short-period decayless kink oscillations of solar coronal loops
Monthly Notices of the Royal Astronomical Society, 516, 4, 5989-5996, 2022, DOI: 10.1093/mnras/stac2545

Presentations and posters at conference

1. Alonso Tagle, M.L.; Maggiolo, R.; Gunell, H.; Cessateur, G.; De Keyser, J.; Lapenta, G.; Pierrard, V.; Vandaele, A.C.
A semi-empirical model of the dependency of atmospheric escape on the planetary magnetic moment
44th COSPAR Scientific Assembly, Athens (Greece), 16-24 July 2022

2. Alonso Tagle, M.L.; Maggiolo, R.; Gunell, H.; Cessateur, G.; De Keyser, J.; Lapenta, G.; Pierrard, V.; Vandaele, A.C.
A semi-empirical model of atmospheric escape dependency on the planetary magnetic moment and solar wind pressure
CmPA retrospective in honor of Prof. Poedts, Leuven (Belgium), 6-9 September 2022 (poster)

3. Alonso Tagle, M.L.; Maggiolo, R.; Gunell, H.; De Keyser, J.; Cessateur, G.; Lapenta, G.; Pierrard, V.; Vandaele, A.C.
Atmospheric Erosion for the Terrestrial Planets: A Semi-Empirical Model
BNCGG Study Day, Brussels (Belgium), 4 November 2022 (poster)

4. Alonso Tagle, M.L.; Maggiolo, R.; Gunell, H.; De Keyser, J.; Cessateur, G.; Lapenta, G.; Pierrard, V.; Vandaele, A.C.
Atmospheric erosion in rocky planets: A semi-empirical model
AGU Fall Meeting, Chicago (Illinois, USA) and online, 12-16 December 2022

5. Anastasiadis, A.; Papaioannou, A.; Vainio, R.; … and 12 others
The SAWS-ASPECS Solar Energetic Particle (SEP) Advanced Warning System
44th COSPAR Scientific Assembly, Athens (Greece), 16-24 July 2022

6. Auchère, F.; Berghmans, D.; Rochus, P.; … and the EUI team
Solar Orbiter/EUI/FSI very wide field observations of the EUV corona
Solar Orbiter 8, Belfast (Northern Ireland, UK) and online, 12-15 September 2022

7. Auchère, F.; Berghmans, D.; Rochus, P.; … and 27 others
Pre-flight calibration of the full sun channel of the Extreme Ultraviolet Imager on board Solar Orbiter
Solar Orbiter 8, Belfast (Northern Ireland, UK) and online, 12-15 September 2022 (poster)

8. Barczynski, K.; Harra, L.K.; Schwanitz, C.; … and 16 others
Slow solar wind sources - high-resolution observations with a stereoscopic view
AGU Fall Meeting, Chicago (Illinois, USA) and online, 12-16 December 2022

9. Bechet, S.
DigiSun: a software dedicated to scientific measurements of sunspots drawings
SCOSTEP 15th Quadrennial Solar-Terrestrial Physics Symposium (STP-15), Alibag (India), 21-25 February 2022

10. Belehaki, A.; and the PITHIA-NRF consortium
Global coordination in space weather and interfacing with user groups
44th COSPAR Scientific Assembly, Athens (Greece), 16-24 July 2022

11. Bemporad, A.; Andretta, V.; Susino, R.; … and 26 others
A Coronal Mass Ejection followed by a prominence eruption and a plasma blob as observed by Solar Orbiter
Solar Orbiter 8, Belfast (Northern Ireland, UK) and online, 12-15 September 2022

12. Bergeot, N.; Habarulema, J.B.; Chevalier, J.-M.; Matamba, T.; Pinat, E.; Cilliers, P.J.; Burešová, D.
Inter-hemispheric comparison of the ionosphere-plasmasphere system at mid-latitudes during quiet and disturbed periods
3rd URSI AT-AP-RASC meeting, Gran Canaria (Spain), 29 May-4 June 2022

13. Berghmans, D.; Antolin, P.; Auchère, F.; Barczynski, K.; … 15 others and the EUI team
First Perihelion of EUI
Solar Orbiter 8, Belfast (Northern Ireland, UK) and online, 12-15 September 2022

14. Berghmans, D.
First Perihelion of EUI on Solar Orbiter
CmPA retrospective in honor of Prof. Poedts, Leuven (Belgium), 6-9 September 2022 (invited talk)

15. Berghmans, D.
Lessons Learned from Solar Orbiter/EUI/FSI for future monitoring EUV imagers
ESA SWE Service Network Workshop 2022, Darmstadt (Germany) and online, 10-12 May 2022

16. Botek, E.; Pierrard, V.
Prediction of electron fluxes in the outer radiation belts using neural networks with PROBA-V/EPT data

ESWW18, Zagreb (Croatia) and online, 24-28 October 2022

17. Brenot, H.; Theys, N.; De Donder, E.; … and 17 others
Decrease of anthropogenic emission from aviation and detection of natural hazards with potential application in geosciences using satellite sensors, ground-based networks and model forecasts in the context of the SACS/ALARM early warning system
EGU General Assembly 2022, Vienna (Austria) and online, 23-27 May 2022

18. Brunet, A.; Dahmen, N.; Santolik, O.; Katsavrias, C.; Maget, V.; Sicard, A.; Aminalragia-Giamini, S.; Pierrard, V.; Botek, E.; Darrouzet, F.; Daglis, I.A.
Electron radiation belt data-assimilation in the SafeSpace project
44th COSPAR Scientific Assembly, Athens (Greece), 16-24 July 2022 (poster)

19. Bruyninx, C.; Bamahry, F.; Legrand, J.; Fabian, A.
Update on the GNSS component of the European Plate Observing System
EUREF Symposium 2022, Online, 31 May-3 June 2022

20. Bruyninx, C.; Legrand, J.; Bamahry, F.; Miglio, A.; Fabian, A.
Modernization of the EPN Historical Data Center
EUREF Symposium 2022, Online, 31 May-3 June 2022

21. Calders, S.; Lamy, H.; Sterken, M.; Anciaux, M.; Lefever, K.; Kolenberg, K.; Coeckelberghs, H.
MOMSTER, a Europlanet-funded STEAM education project
Europlanet Science Congress 2022, Granada (Spain), 18-23 September 2022

22. Chevalier, J.-M. ; Dantepal, J. ; Bergeot, N. ; Defraigne, P. ; Amale, K.
GPS Flex Power Monitoring
EGNOS Service Performance Monitoring Support Final Meeting Consortium, 21 June 2022

23. Clette, F.; Lefèvre, L.; Bhattacharya, S.
Sunspot number, group number and F10.7: new insights
Space Climate 8 Symposium, Krakow (Poland), 19-22 September 2022 (invited talk)

24. Clette, F.
The F10.7cm radio flux revisited
2022 Sun-Climate Symposium, Madison (Wisconsin, USA), 16-20 May 2022

25. Cuadrado, R.A.; Schühle, U.; Teriaca, L.; Heerlein, K.; Berghmans, D.; Auchère, F.; Gissot, S.; Kraaikamp, E.; Harra, L.; Long, D.; Stegen, K.; Verbeeck, C.; Gottwald, A.; and the EUI Team
The Pre-flight Calibration of the HRILYA telescope of EUI on-board Solar Orbiter
Solar Orbiter 8, Belfast (Northern Ireland, UK) and online, 12-15 September 2022 (poster)

26. Daglis I.A.; and the SafeSpace team
Advanced Prediction of the Outer Van Allen Belt Dynamics and a Prototype Service: the H2020 SafeSpace project
EGU General Assembly 2022, Vienna (Austria) and online, 23-27 May 2022 (invited talk)

27. Daglis, I.A.; and the SafeSpace team
Improving the predictions of the outer Van Allen belt dynamics
44th COSPAR Scientific Assembly, Athens (Greece), 16-24 July 2022

28. Dahmen, N.; Sicard, A.; Santolik, O.; Pierrard, V.; Brunet, A.; Darrouzet, F.
The impact of a dynamic diffusion frame on radiation belt physical codes and space weather prediction tools
44th COSPAR Scientific Assembly, Athens (Greece), 16-24 July 2022

29. Dammasch, I.E.; Dominique, M.
Monitoring space weather with PROBA2/LYRA after 12 years in space
ESWW18, Zagreb (Croatia) and online, 24-28 October 2022 (poster)

30. De Donder, E.; Messios, N.; Calders, S.; Calogera, A.; Mezhoud, S.; Heynderickx, D.; Pavano, G.; Clucas, S.; Evans, H.
The Space Environment Information System
SEESAW 2022, Laurel (Maryland, USA) and online, 12-16 September 2022

31. De Donder, E.; Messios, N.; Calders, S.; Calogera, A.; Mezhoud, S.; Heynderickx, D.; Pavano, G.; Clucas, S.; Evans, H.
Assessing the Space Environment and its Effects on Space Missions with SPENVIS
73rd IAC, Paris (France), 18-22 September 2022

32. Delouille, V.; Bello Gonzalez, N.
ESCAPE VO Impact on the European Solar Telescope ESFRI
ESCAPE consortium meeting, Brussels (Belgium), 25-26 October 2022 (invited talk)

33. D'Huys, E.; Vanlommel, P.; Janssens, J.; Van der Linden, R.
Come fly with us: services provided by the Space Weather Education Centre
4th Symposium on Space Educational Activities, Barcelona (Spain), 27-29 April 2022

34. Dierckxsens, M.; Vasalos, G.; Papaioannou, A.; Anastasiadis, A.; Jiggens, P.
Validation Approach of the SAWS-ASPECS Tool

44th COSPAR Scientific Assembly, Athens (Greece), 16-24 July 2022 (invited talk)

35. Dominique, M.; Dolla, L.; Zhukov, A.; … and 12 others
How can SOLAR-C/SOSPIM contribute to the understanding of quasi-periodic pulsations in solar flares?
44th COSPAR Scientific Assembly, Athens (Greece), 16-24 July 2022

36. Dominique, M.
Detection of QPPs in Lyman-a: What are the interest and current limitations of such observations?
1st ISSI meeting, Bern (Switzerland) and online, 19-23 September 2022

37. Dominique, M.; Thiemann, E.; Berger, T.; … and 12 others
How can SOSPIM contribute to the monitoring of thermospheric densities and their fluctuations with solar activity?
ESWW18, Zagreb (Croatia) and online, 24-28 October 2022 (poster)

38. Dominique, M.; Wauters, L.; Heinzel, P.; Milligan, R.
Flare and Filament Observations in Lyman-Alpha
AGU Fall Meeting, Chicago (Illinois, USA) and online, 12-16 December 2022 (poster)

39. Fernandes, R.; Bruyninx, C.; Crocker, P.; Socquet, A.; Vergnolle, M.; and the members of EPOS-GNSS
EPOS-GNSS - Current status of service implementation for European GNSS data and products
EGU General Assembly 2022, Vienna (Austria) and online, 23-27 May 2022

40. Fuller, N.; Blanchard, C.; Amarouche, N.; Degret, G.; Ortiz, M.; Briend, R.; Fernandez, I.; Musset, S.; Klein, K.L.; Sapundjiev, D.
Recent maintenance operations on French neutron monitors and ongoing
44th COSPAR Scientific Assembly, Athens (Greece), 16-24 July 2022

41. Girgis, K.M.; Hada, T.; Yoshikawa, A.; Matsukiyo, S.; Lemaire, J.; Pierrard, V.; Samwel, S.
How do the geomagnetic storms affect the LEO proton flux distribution during Solar Energetic Particle events ?
SGEPSS 2022, Sagamihara city (Kanagawa, Japan) and online, 3-7 November 2022

42. Girgis, K.M.; Hada, T.; Yoshikawa, A.; Matsukiyo, S.; Lemaire, J.; Pierrard, V.; Samwel, S.
LEO Proton Flux Modeling due to Solar Proton Injections during Geomagnetic Storms
AGU Fall Meeting, Chicago (Illinois, USA) and online, 12-16 December 2022 (poster)

43. Gissot, S.; Berghmans, D.; Auchère, F.; … and 16 others
Performance of the Extreme Ultraviolet Imager (EUI) High-Resolution EUV Imager (HRI-EUV) telescope: from pre-flight calibration to first in-flight images
Solar Orbiter 8, Belfast (Northern Ireland, UK) and online, 12-15 September 2022 (poster)

44. Giunta, A.; Grundy, T.; Andretta, V.; … 34 others
Calibrating the VUV instruments of Solar Orbiter with stars: first results from the EUI and SPICE observations
Solar Orbiter 8, Belfast (Northern Ireland, UK) and online, 12-15 September 2022 (poster)

45. Godin-Beekmann, S.; Azouz, N.; Sofieva, V.; … and 25 others
Updated trends of the stratospheric ozone vertical distribution in the 60S-60N latitude range based on the LOTUS regression model
LOTUS side meeting at the Trends Workshop, Helsinki (Finland), 30 May-3 June 2022

46. Gul, B.; Verhulst, T.; Ayyaz Ameen, M.
Correlation between foEs and zonal winds over mid-latitude stations using Horizontal Wind Model (HWM14) during solar cycle 23-24
44th COSPAR Scientific Assembly, Athens (Greece), 16-24 July 2022

47. Harra, L.K.; Alberti, A.; Berghmans, D.; … and 28 others
A spectral solar irradiance monitor (SoSpIM) on the JAXA Solar-C (EUVST) space mission
44th COSPAR Scientific Assembly, Athens (Greece), 16-24 July 2022

48. Harra, L.; Barczynski, K.; David Berghmans, D.; … and 15 others
High spatial imaging of coronal upflows in the quiet Sun - sources of solar wind?
Solar Orbiter 8, Belfast (Northern Ireland, UK) and online, 12-15 September 2022

49. Harra, L.; Barczynski, K.; Mandrini, C.; … and 19 others
Intriguing coronal upflows at the edge of a sunspot - what causes it and can it become part of the solar wind?
Solar Orbiter 8, Belfast (Northern Ireland, UK) and online, 12-15 September 2022 (poster)

50. Jain, S.; Podladchikova, T.; Veronig, A.; Sutyrina, O.; Dumbovic, M.; Clette, F.; Pötzi, W.
Prediction of solar cycle amplitude with the maximal growth rate in ascending phase
44th COSPAR Scientific Assembly, Athens (Greece), 16-24 July 2022 (poster)

51. Kahil, F.; Chitta, L.P.; Peter, H.; … 14 others, the PHI team, and the EUI team

The magnetic drivers of EUI campfires seen by SO/PHI
Solar Orbiter 8, Belfast (Northern Ireland, UK) and online, 12-15 September 2022 (invited talk)

52. Kauristie, K.; Andries, J.; Beck, P.; … and 32 others
ICAO space weather advisories: Experiences gathered by the PECASUS service
3rd URSI AT-AP-RASC meeting, Gran Canaria (Spain), 29 May-4 June 2022

53. Koukras, A.; Keppens, R.; Dolla, L.
Estimating uncertainties in the back-mapping of the fast solar wind
44th COSPAR Scientific Assembly, Athens (Greece), 16-24 July 2022

54. Koukras, A.; Keppens, R.; Dolla, L.
Estimating uncertainties in the back-mapping of the fast solar wind
Solar Orbiter summer school 2022: a multi-instruments mission to the Sun, Sète (France), 30 May-3 June 2022

55. Koukras, A.; Keppens, R.; Dolla, L.
Estimating uncertainties in the back-mapping of the fast solar wind
EGU General Assembly 2022, Vienna (Austria) and online, 23-27 May 2022

56. Koukras, A.; Keppens, R.; Dolla, L.
Estimating uncertainties in the back-mapping of the fast solar wind
SHINE 2022 workshop, Waikiki (Hawaii, USA), 27 June-1 July 2022 (poster)

57. Koukras, A.
Understanding the acceleration of the fast solar wind by linking remote sensing and in situ observations
Thesis, Public PhD Defense, Heverlee (Belgium) and Online, 19 December 2022

58. Koza, J.; Bemporad, A.; Mierla, M.; Berghmans, D.; Zhukov, A.
Bayesian analysis of a prominence eruption observed by the Solar Orbiter EUI/FSI imager and at the Mauna Loa Solar Observatory
Solar Orbiter 8, Belfast (Northern Ireland, UK) and online, 12-15 September 2022 (poster)

59. Kraaikamp, E.; Berghmans, D.; Verbeeck, C.; Stegen, K.; Gissot, S.; Auchère, F.; Schühle, U.; and the EUI Team
The highest resolution full disc EUV corona image ever
Solar Orbiter 8, Belfast (Northern Ireland, UK) and online, 12-15 September 2022 (poster)

60. Li, X.; Butala, M.; Valliappan, S.P.; Magdalenic, J.; Delouille, V.; Rodriguez, L.; Shukhobodskaia, D.
Transfer-Solar-GAN- Generation of Input Sources for Solar Wind Models with Deep Learning
Machine learning in Heliophysics, Boulder (Colorado, USA) and online, 21-25 March 2022

61. Long, D.; Chitta, L.P.; Baker, D.; Hannah, I.G.; Ngampoopun, N.; Berghmans, D.; Zhukov, A.N.
The Energetics of a Solar Jet in a Polar Coronal Hole
Solar Orbiter 8, Belfast (Northern Ireland, UK) and online, 12-15 September 2022

62. Magdalenic, J.; Valliappan, S.P.; Rodriguez, L.
How the fast solar wind develops on its way from the Sun to Earth
CmPA retrospective in honor of Prof. Poedts, Leuven (Belgium), 6-9 September 2022 (poster)

63. Magdalenic, J.; Valliappan, S.P.; Rodriguez, L.
Studying dynamics of the fast solar wind, through observations and modelling
ESWW18, Zagreb (Croatia) and online, 24-28 October 2022

64. Magdalenic, J.; Valliappan, S.P.; Rodriguez, L.
Origin of the solar wind observed by the PSP
EGU General Assembly 2022, Vienna (Austria) and online, 23-27 May 2022 (invited talk)

65. Maget, V.; Bourdarie, S.; Ferlin, A.; and 14 others
A new Earth Radiation Belt Forecast And Nowcast (RB-FAN) Framework based on the Salammbô data assimilation codes
ESWW18, Zagreb (Croatia) and online, 24-28 October 2022 (poster)

66. Maggiolo, R.; Alonso Tagle, M.L.; Gunell, H.; Cessateur, G.; Darrouzet, F.; De Keyser, J.; Pierrard, V.; Vandaele, A.C.
Semi-empirical modelling of atmospheric escape as a function of the planetary magnetic moment and of the solar wind pressure: implication for the Martian atmospheric loss
44th COSPAR Scientific Assembly, Athens (Greece), 16-24 July 2022

67. Makrantoni, P.; Tezari, A.; Stassinakis, A.N.; Paschalis, P.; Gerontidou, M.; Mavromichalaki, H.; Usoskin, I.G.; Crosby, N.; Dierckxsens, M.
Atmospheric Cosmic Ray Induced Ionization and Radiation affecting aviation
NMDB@Athens symposium, Athens (Greece) and online, 26-30 September 2022

68. Malandraki, O.; Karavolos, M.; Kokkinis, G.; Milas, N.; Crosby, N.; Dierckxsens, M.
Solar Particle Radiation Storms Forecasting and Analysis within ESA/SSA- The HESPERIA SEP Real-Time Forecasting products
ESWW18, Zagreb (Croatia) and online, 24-28 October 2022

69. Mandal, S.; Chitta, L.P. ; Peter, H.; Solanki, S.K.; Aznar Cuadrado, R.; Teriaca, L.; Schühle, U.; Berghmans, D.; Auchère, F.
A highly dynamic small-scale jet in a polar coronal hole
Solar Orbiter 8, Belfast (Northern Ireland, UK) and online, 12-15 September 2022 (poster)

70. Martínez Picar, A.
Narrow pass-band filtering technique for radio meteor automatic detection
International Meteor Conference 2022, Poroszló (Hungary), 29 September-2 October 2022

71. Mavromichalaki, H.; Paschalis, P.; Tezari, A.; Paouris, E.; Lingri, D.; Stassinakis, A.; Crosby, N.; Dierckxsens, M.; Gerontidou, M.
The first Ground Level Enhancement (GLE73) of the Solar Cycle 25
44th COSPAR Scientific Assembly, Athens (Greece), 16-24 July 2022

72. Mierla, M.; the EUI team, and the EUI consortium
Eruptions observed by EUI/FSI onboard Solar Orbiter
Solar Orbiter 8, Belfast (Northern Ireland, UK) and online, 12-15 September 2022 (invited talk)

73. Moeller, G.; Adavi, Z.; Wilgan, K.; Brenot, H.; Hanna, N.; Kamm, B.; Schenk, A.; Pottiaux, E.; Shehaj, E.; Zhang, W.; Trzcina, E.; Rohm, W.
Tomographic fusion strategies for the reconstruction of small-scale structures in the lower atmosphere
1st Workshop on Data Science for GNSS Remote Sensing, Potsdam (Germany), 13-15 June 2022 (poster)

74. Moraux, A.; Dewitte, S.; Munteanu, A.
A deep learning multimodal method for precipitation estimation: case study of the extreme rainfall from July 2021
EGU General Assembly 2022, Vienna (Austria) and online, 23-27 May 2022

75. Nasi, A.; Katsavrias, C.; Aminalragia-Giamini, S.; … and 19 others
Investigating the dependency of acceleration mechanism signatures on electron populations following consecutive CIRs, through observations and simulations
AGU Fall Meeting, Chicago (Illinois, USA) and online, 12-16 December 2022

76. Natras, R.; Soja, B.; Schmidt, M.; Dominique, M.; Türkmen, A.
Machine Learning Approach for Forecasting Space Weather Effects in the Ionosphere with Uncertainty Quantification
EGU General Assembly 2022, Vienna (Austria) and online, 23-27 May 2022

77. Niembro, T.; Reeves, K.K. ; Seaton, D.B. ; Hess, P.; Berghmans, D.; Andretta, V.
Following a prominence eruption from the Sun to Parker Solar Probe with multi-spacecraft observations
Solar Orbiter 8, Belfast (Northern Ireland, UK) and online, 12-15 September 2022 (poster)

78. Niemela, A.; Sarkar, R.; Wijsen, N.; Aran, A.; Rodriguez, L.; Magdalenic, J.; Poedts, S.
Modelling the SEP Event of 11 April 2013
44th COSPAR Scientific Assembly, Athens (Greece), 16-24 July 2022 (poster)

79. Niemela, A.; Wijsen, N.; Rodriguez, L.; Aran, A.; Magdalenic, J.; Poedts, S
Simulating the gradual SEP event of 15 March 2013 with PARADISE
44th COSPAR Scientific Assembly, Athens (Greece), 16-24 July 2022

80. Niemela, A.; Wijsen, N.; Rodriguez, L.; Aran, A.; Magdalenic, J.; Poedts, S.
Simulating the gradual SEP event of 15 March 2013 with PARADISE
CmPA retrospective in honor of Prof. Poedts, Leuven (Belgium), 6-9 September 2022

81. Niemela, A.; Wijsen, N.; Aran, A.; Rodriguez, L.; Magdalenic, J.; Poedts, S.
Analysis of the CME and associated gradual SEP event of March 2013
EGU General Assembly 2022, Vienna (Austria) and online, 23-27 May 2022

82. Niemela, A.; Wijsen, N.; Rodriguez, L.; Aran, A.; Magdalenic, J.; Poedts, S.
Gradual SEP modelling with PARADISE: March and April 2013 events
SHINE 2022 workshop, Waikiki (Hawaii, USA), 27 June-1 July 2022

83. Niemela, A.; Wijsen, N.; Aran, A.; Rodriguez, L.; Magdalenic, J.; Poedts, S.
Simulating the gradual SEP event of 15 March 2013 with PARADISE
ESWW18, Zagreb (Croatia) and online, 24-28 October 2022

84. Pacheco, D.; Papaioannou, A.; Kouloumvakos, A.; … and 30 others
Analysis of a Multi-Spacecraft Event During the First Solar Orbiter Perihelion: the 21 March 2022 SEP event
AGU Fall Meeting, Chicago (Illinois, USA) and online, 12-16 December 2022

85. Papaioannou, A.; Vainio, R.; Raukunen, O.; Jiggens, P.; Aran, A.; Dierckxsens, M.; Paassilta, M.; Mallios, S.; Anastasiadis, A.

The Probabilistic Solar Particle Event foRecasting (PROSPER) Model
44th COSPAR Scientific Assembly, Athens (Greece), 16-24 July 2022

86. Petrova, E.; Magyar, N.; Van Doorsselaere, T.; Berghmans, D.
High frequency oscillations in Solar Orbiter/EUI observations
Solar Orbiter 8, Belfast (Northern Ireland, UK) and online, 12-15 September 2022 (invited talk)

87. Pierrard, V.; Botek, E.; Ripoll, J.-F.; Reeves, G.; Thaller, S.A.
Observations of Electron Fluxes in the Radiation Belts with PROBA-V/EPT at Polar Low Earth Orbit and Van Allen Probes/MAGEIS at Near Equatorial Elliptical Orbit
3rd URSI AT-AP-RASC meeting, Gran Canaria (Spain), 29 May-4 June 2022

88. Pierrard, V.
Influence of Kappa suprathermal tails on the solar wind characteristics
44th COSPAR Scientific Assembly, Athens (Greece), 16-24 July 2022 (invited talk)

89. Pierrard V.
Characteristics of the suprathermal particles in the solar wind and their consequences
Parker Solar Probe electrons seminars, Online, 27 September 2022 (invited talk)

90. Pierrard, V.
The dynamics of the plasmasphere and its links with the radiation belts
Los Alamos National Laboratory seminar, Online, 16 February 2022 (invited talk)

91. Pierrard, V.
Influence of the solar activity on the boundaries in the magnetosphere: plasmapause, radiation belts, auroral oval
BNCGG Study Day, Brussels (Belgium), 4 November 2022 (poster)

92. Pottiaux, E.
Recent GNSS-Meteorology Activities at ROB
E-GVAP Annual Symposium, Online, 10 March 2022

93. Pottiaux, E.; Bruyninx, C.
GNSS-based remote sensing of atmospheric water vapor at ROB for meteorology and climate: Status, perspectives, and challenges
BNCGG Study Day, Brussels (Belgium), 4 November 2022 (poster)

94. Ripoll, J.-F.; Thaller, S.; Hartley, D.; Cunningham, G.; Pierrard, V.; Kurth, W.S.; Kletzing, C.; Wygant, J.R.
Plasmapause and dense outer edge of the plasmasphere from Van Allen Probes EFW and EMFISIS measurements for radiation belt modeling
AGU Fall Meeting, Chicago (Illinois, USA) and online, 12-16 December 2022

95. Rodriguez, L.; Warmuth, A.; Andretta, V.; … and 33 others
The eruption of 22 April 2021 as observed by Solar Orbiter, STEREO and Earth bound instruments
Solar Orbiter 8, Belfast (Northern Ireland, UK) and online, 12-15 September 2022

96. Rodriguez, L.
Highlights of CME and space weather projects shared with Stefaan Poedts
CmPA retrospective in honor of Prof. Poedts, Leuven (Belgium), 6-9 September 2022 (invited talk)

97. Rodriguez, L.; … and the EUI team
Using EUI to link EPD events back to the Sun
EPD co-Is meeting, 23 March 2022 (invited talk)

98. Rodriguez, L.; Shukhobodskaia, D.; Niemela, A.; Maharana, A.; Verbeke, C.; Samara, E.; Magdalenic, J.; Vansintjan, R.; Mierla, M.; Sarkar, R.; Kilpua, E.; Asvestari, E.; Poedts, S.
Validation of the EUHFORIA model for cone and spheromak CME runs
ESWW18, Zagreb (Croatia) and online, 24-28 October 2022 (poster)

99. Samara, E.; Arge, C.N.; Pinto, R.F.; Magdalenic, J.; Rodriguez, L.; Poedts, S.
Calibrating the WSA model in EUHFORIA based on PSP observations: challenges and limitations toward the improvement of solar wind forecasting
SHINE 2022 workshop, Waikiki (Hawaii, USA), 27 June-1 July 2022 (invited talk)

100. Samara, E.; Arge, C.N.; Pinto, R.; Magdalenic, J.; Rodriguez, L.; Poedts, S.
Calibrating the WSA model in EUHFORIA based on PSP observations: challenges and limitations toward the improvement of solar wind forecasting
CmPA retrospective in honor of Prof. Poedts, Leuven (Belgium), 6-9 September 2022

101. Samara, E.; Arge, C.N.; Pinto, R.F.; Magdalenic, J.; Rodriguez, L.; Poedts, S.
Calibrating the WSA velocity in EUHFORIA based on PSP observations
EGU General Assembly 2022, Vienna (Austria) and online, 23-27 May 2022

102. Samara, E.
Understanding and modeling the solar wind: challenges, limitations and solutions towards better predictions

Thesis, Public PhD Defense, Leuven (Belgium) and Online, 7 November 2022

103. Sapundjiev, D.; Stankov, S.M.; Jodogne, J.C.
Gamma-ray bursts detection capabilities of a sudden ionospheric disturbance (SID) detector
27th European Cosmic Ray Symposium, Nijmegen (The Netherlands), 25-29 June 2022

104. Sapundjiev, D.
Status of Space Weather Observatory and Services at the Royal Meteorological Institute of Belgium
ESWW18, Zagreb (Croatia) and online, 24-28 October 2022

105. Sasso, C.; Susino, R.; Liberatore, A.; … and 29 others
Multi-spacecraft Observations of a Prominence Eruption
Solar Orbiter 8, Belfast (Northern Ireland, UK) and online, 12-15 September 2022 (poster)

106. Schwanitz, C.; Harra, L.; Barczynski, K.; … and 17 others
Coronal Up- & and Downflows in Hinode/EIS seen by Solar Orbiter EUI
AGU Fall Meeting, Chicago (Illinois, USA) and online, 12-16 December 2022

107. Shestov, S.; Zhukov, A.N.
Processing of the ASPIICS on-ground calibration data
7th Proba-3 virtual Scientific Working Team meeting, Online, 9 December 2022

108. Smit, H.G.J.; Chen, G.; Groebner, J.; Hall, B.; Kazadzis, S.; Redondas, A.; Steinbacher, M.; Viallon, J.; **Van Malderen, R.;** Zellweger, C.; Takatsuji, S.; Wegener, R.; Wiedensohler, A.; Lehmann, C.
Uncertainty, Stability and Traceability in Global Monitoring of Atmospheric Composition and the Role of WMO/GAW Central Calibration Facilities - Reality and Plans
Metrology for Climate Action Workshop, Online, 26-30 September 2022

109. Smit, H.G.J.; Thompson, A.M.; Johnson, B.J.; … and 17 others
Long Term WMO-GAW Ozonesonde QA/QC and Data Quality Improvements: The 25th Anniversary of the Juelich Ozone Sonde Intercomparison Experiment (JOSIE)
WMO TECO-2022, Paris (France) and online, 10-13 October 2022

110. Sorokina, D.; Van Doorsselaere, T.; Talpeanu, D.-C.; Poedts, S.
MHD modelling of coronal streamers and streamer waves
Solar Orbiter summer school 2022: a multi-instruments mission to the Sun, Sète (France), 30 May-3 June 2022 (poster)

111. Stauffer, R.M.; Thompson, A.M.; Kollonige, D.E.; Tarasick, D.W.; **Van Malderen, R.;** Smit, H.G.J.; Vömel, H.; Morris, G.A.; Johnson, B.J.; Cullis, P.D.
An Examination of Recent Global Ozonesonde Network Data Quality
AGU Fall Meeting, Chicago (Illinois, USA) and online, 12-16 December 2022

112. Talpeanu, D.-C.; Poedts, S.; D'Huys, E.; Mierla, M.; Richardson, I.G.
Interaction of coronal mass ejections and the solar wind. A force analysis
ESWW18, Zagreb (Croatia) and online, 24-28 October 2022 (poster)

113. Talpeanu, D.-C.
Numerical and Observational Study of Stealth and Consecutive Coronal Mass Ejections
Thesis, Public PhD Defense, Heverlee (Belgium) and Online, 20 June 2022

114. Tarasick, D.; Stauffer, R.M.; Smit, H.G.J.; Thompson, A.M.; Davies, J.; **Van Malderen, R.;** Johnson, B.J.; Vömel, H.
Assessing data quality in long-term Canadian ozone sounding records
iCACGP-IGAC 2022 Biannual Science Conference, Manchester (UK) and online, 10-15 September 2022

115. Telloni, D.; Zank, G. P.; ManyOtherAuthors, X; Berghmans, D.; Kraaikamp, E.; Rodriguez, L.; Verbeeck, C.; Zhukov, A. N.
Observation of Magnetic Switchback in the Solar Corona
Solar Orbiter 8, Belfast (Northern Ireland, UK) and online, 12-15 September 2022 (invited talk)

116. Teriaca, L.; Schühle, U.; Aznar Cuadrado, R.; Heerlein, K.; Berghmans, D.; Auchère, F.; Gissot, G.; Kraaikamp, E.; Harra, L.; Long, D.; Stegen, K.; Verbeeck, C.
The radiometric response and performance evolution of the HRILYA telescope of EUI from first light to now
Solar Orbiter 8, Belfast (Northern Ireland, UK) and online, 12-15 September 2022 (poster)

117. Tezari, A.; Stassinakis, A.; Paschalis, P.; Mavromichalaki, H.; Gerontidou, M.; Karaiskos, P.; Kanellakopoulos, A.; Plainaki, C.; Crosby, N.; Dierckxsens, M.
Estimation of the radiation exposure in the atmospheres of Earth, Venus and Mars with the software DYASTIMA
44th COSPAR Scientific Assembly, Athens (Greece), 16-24 July 2022

118. Thiemann, E.; Sewell, R.; Dominique, M.; Pilinski, M.; Sutton, E.; Peck, C.; Seaton, D.B.
Real-Time Operational Measurements of the Thermospheric State: Recent Advances and Future Possibilities

AGU Fall Meeting, Chicago (Illinois, USA) and online, 12-16 December 2022 (poster)

119. Thiemann, E.; Sewell, R.; Woods, T.; Dominique, M.; Greer, K.; Sutton, E.; Piliski, M.; Berger, T.
Solar EUV Photometers as Compact Sensors for Measuring Thermospheric Density, Temperature and Composition
SSWRF II, Laurel (Maryland, USA), 3-7 October 2022

120. Thompson, A.M.; Smit, H.G.J.; Stauffer, R.M.; Kollonige, D.E.; and the **ASOPOS 2.0 Panel**
The 2021 ASOPOS (Assessment of Standard Operating Procedures [SOP] for Ozonesondes) 2.0 WMO GAW 268 report: global ozonesonde best practices
WMO TECO-2022, Paris (France) and online, 10-13 October 2022

121. Valliappan, S.P.; Magdalenic, J.; Rodriguez, L.; Samara, E.
Performance analysis of EUHFORIA at near-Sun distances using PSP observations
CmPA retrospective in honor of Prof. Poedts, Leuven (Belgium), 6-9 September 2022 (poster)

122. Valliappan, S. P.; Magdalenic, J.; Rodriguez, L.
EUHFORIA simulation using AI generated farside magnetogram
ESWW18, Zagreb (Croatia) and online, 24-28 October 2022

123. Valliappan, S.P.; Magdalenic, J.; Rodriguez, L.; Poedts, S.; Samara, E.
Solar wind modelling with EUHFORIA and comparison with the PSP observations
EGU General Assembly 2022, Vienna (Austria) and online, 23-27 May 2022

124. Valliappan, S.P.; Magdalenic, J.; Rodriguez, L.; Poedts, S.; Samara, E.
Employing PSP observations to calibrate near-Sun solar wind modelling by EUHFORIA
44th COSPAR Scientific Assembly, Athens (Greece), 16-24 July 2022

125. Vanden Broeck, G.; Bechet, S.; Clette, F.
Study of the magnetic structures in full-disk solar Ca II K images and sun-like stars connection
Space Climate 8 Symposium, Krakow (Poland), 19-22 September 2022 (poster)

126. Vanden Broeck, G.; Bechet, S.; Clette, F.; Rauw, G.
Study of the magnetic structures in full-disk solar Ca II K images and sun-like stars connection
Cool Stars 21, Toulouse (France), 4-9 July 2022 (poster)

127. Van Malderen, R.; Poyraz, D.; Smit, H.G.J.; … and 29 others
Update of the Homogenization of the Long-Term Global Ozonesonde Records
LOTUS side meeting at the Trends Workshop, Helsinki (Finland), 30 May-3 June 2022

128. Van Malderen, R.; Smit, H.G.J.; Thompson, A.M.; Stauffer, R.M.; Kollonige, D.; Tarasick, D.W.; Johnson, B.J.; Vömel, H.; von der Gathen, P.; Morris, G.; Querel, R.; Davies, J.; Cullis, P.
Panel for the Assessment of Standard Operating Procedures for Ozonesondes (ASOPOS) 2.0: overview and current activities
WMO GAW Scientific Advisory Group on Ozone and Solar UV Radiation Meeting, Geneva (Switzerland), 3-5 October 2022

129. Van Malderen, R.; Smit, H.G.J.; Blot, R.; Vigouroux, C.; Leblanc, T.; Petropavlovskikh, I.; Van Roozendael, M.; Hendrick, F.; Cede, A.; Cooper, O.; and the HEGIFTOM team
Harmonization and Evaluation of Ground-based Instruments for Free Tropospheric Ozone Measurements by TOAR-II Focus Working Group HEGIFTOM
WMO GAW Scientific Advisory Group on Ozone and Solar UV Radiation Meeting, Geneva (Switzerland), 3-5 October 2022

130. Van Malderen, R.; Smit, H.G.J.; Blot, R.; Vigouroux, C.; Leblanc, T.; Petropavlovskikh, I.; Van Roozendael, M.; Hendrick, F.; Cede, A.; Cooper, O.; and the HEGIFTOM team
Harmonization and Evaluation of Ground-based Instruments for Free-Tropospheric Ozone Measurements by TOAR-II Focus Working Group "HEGIFTOM"
GML GMAC-50, Online, 23-27 May 2022

131. Van Malderen, R.; Stauffer, R.
Recent global ozonesonde network data quality underscores the success of homogenization efforts
NDACC Steering Committee Meeting, Paris (France), 26-30 September 2022

132. Van Malderen, R.; De Backer, H.; De Muer, D.; Poyraz, D.; Verstraeten, W.; De Bock, V.; Delcloo, A.; Mangold, A.; Laffineur, Q.; Allaart, M.; Fierens, F.; Thouret, V.
50 years of balloon-borne ozone profile measurements at Uccle, Belgium
GML GMAC-50, Online, 23-27 May 2022

133. Van Malderen, R.; Poyraz, D.; Smit, H.G.J.; … and 29 others
Homogenization of the Long-Term Global Ozonesonde Records
WMO TECO-2022, Paris (France) and online, 10-13 October 2022

134. Verbeeck, C.; Berghmans, D. ; Gissot, S.; Kraaikamp, E.; Bogdan, N.; and the EUI Team
Start analyzing EUI data today!

Solar Orbiter 8, Belfast (Northern Ireland, UK) and online, 12-15 September 2022 (poster)

135. Verbeeck, Cis
Introduction to JHelioviewer
Solar Orbiter 8 Workshop Data Analysis Tutorial Day, Belfast (Northern Ireland, UK) and online, 16 Sept 2022 (invited talk)

136. Verbeke, C.; Andries, J. ; de Patoul, J.; Shukhobodskaia, D.; Rodriguez, L.; Poedts, S; SWOP, Team
Integration of EUHFORIA within the SWOP environment
10th CCMC workshop (2022).CTALKCONT

137. Verbeke, C.
Quantifying the evolution of interplanetary coronal mass ejections by coupling physics-based and data-driven modeling
Thesis, Public PhD Defense, Leuven (Belgium) and Online, 19 September 2022

138. Verhulst, T.G.W.; Altadill, D.; Barta, V.; Belehaki, A.; … and 12 others
Ionospheric disturbances caused by the 2022 Hunga-Tonga volcanic eruption detected over Europe
44th COSPAR Scientific Assembly, Athens (Greece), 16-24 July 2022

139. Verhulst, T.G.W.; Altadill, D.; Barta, V.; … and 12 others
Ionospheric disturbances in Europe caused by the 2022 Hunga-Tonga volcanic eruption
8th IAGA/ICMA/SCOSTEP Workshop on Vertical Coupling in the Atmosphere-Ionosphere System, Sopron (Hungary), 11-15 July 2022

140. Verhulst, T.G.W.; Altadill, D.; Barta, V.; … and 12 others
Multi-instrument detection in Europe of ionospheric disturbances caused by the 15 January 2022 eruption of the Hunga volcano
3rd URSI AT-AP-RASC meeting, Gran Canaria (Spain), 29 May-4 June 2022

141. Verhulst, T.G.W.; Sapundjiev, D.; Stankov, S.
ARTIST-5 automatic scaling of quick-run DPS-4D ionograms
3rd URSI AT-AP-RASC meeting, Gran Canaria (Spain), 29 May-4 June 2022

142. Wauters, L.; Dominique, M.; Dammasch, I.E.
Multi-wavelength observations of filament eruptions
ESWW18, Zagreb (Croatia) and online, 24-28 October 2022

143. Winant, A.; Botek, E.; Pierrard, V.
Comparison of high energy electron fluxes in the outer radiation belt using PROBA-V/EPT and RBSPB/MagEIS
BNCGG Study Day, Brussels (Belgium), 4 November 2022 (poster)

144. Wintoft, P.; Wik, M.; Viljanen, A.; Johnsen, M.G.; Solheim-Thinn, K.; Rodriguez, L.; Setréus, J.
Real-time challenges for space weather predictions: October-November 2021 solar and geomagnetic events for Scandinavia
ESWW18, Zagreb (Croatia) and online, 24-28 October 2022

145. Žigman, V.; Dominique, M.; Grubor, D.; Rodger, C.J.; Clilverd, M.A.
Lower-ionosphere Electron Density from Multi-instrument Satellite Observations and Ground VLF Measurements during Solar Flares
ESWW18, Zagreb (Croatia) and online, 24-28 October 2022

146. Žigman, V.; Dominique, M.; Grubor, D.; Rodger, C.J.; Clilverd, M.A.
Lower-ionosphere Electron Density and Effective Recombination Coefficients from Multi-instrument Observation and Ground VLF Measurements during Solar Flares
10th VERSIM Workshop, Sodankylä (Finland) and online, 7-11 November 2022

147. Zhao, J.; Lee, L.C.; Xie, H.; Yao, Y.; Wu, D.-J.; Pierrard, V.; Voitenko, Y.
Quantifying Wave-particle Interactions in Collisionless Plasmas: the Alfvén-mode Wave
AOGS 2022, Online, 1-5 August 2022 (invited talk)

148. Zychova, L.; Lefever, K.; Crosby, N.
A Touch of Space Weather - Outreach project for visually impaired students
EGU General Assembly 2022, Vienna (Austria) and online, 23-27 May 2022

149. Zychova, L.; Lefever, K.; Crosby, N.
A Touch of Space Weather - Outreach project for visually impaired students
CAP2022, Sydney (Australia) and online, 12-16 September 2022

150. Zychova, L.; Lefever, K.; Crosby, N.; Dierckxsens, M.; Calders, S.; Bogaert, P.; Passchyn, K.
A Touch of Space Weather - Outreach project for visually impaired students
Europlanet Science Congress 2022, Granada (Spain), 18-23 September 2022

Public Outreach: talks and publications for the general public

1. Berghmans, D.
Het weer in de ruimte
Space Week @ Planetarium, Belgium, 20 October 2022

2. Berghmans, D.
Eerste resultaten van de Extreme Ultraviolet Imager op Solar Orbiter
Astropolis Voordrachten, Oostende, 28 April 2022

3. Berghmans, D.; D'Huys, E.
EUV beelden van de zonnecorona
URANIA Seminar series, Belgium, 26 April 2022

4. Calders, S.
Space weather effects on space flight
Public observatory Cozmix, Brugge, 23 November 2022

5. Cessateur, G.
Les aurores dans le système solaire
Open Door Days, Space Pole Uccle, 25 September 2022

6. Chabrillat, S.
L'urgence climatique: de la crise à l'espoir
Open Door Days, Space Pole Uccle, 25 September 2022

7. Chevalier, J.-M.
GNSS basics and the effect of space weather on GNSS
Internship of young students, 22 February 2022 and 29 March 2022

8. Clette, F.
Le Soleil et nous
Éditions Favre, Lausanne ; Paris, 2022 ; EAN : 9782828918910

9. Clette, F.
Le Soleil et nous: Météo et climat spatial
Groupe d'Astronomie de Spa, Belgium, 28 October 2022)

10. Clette, F.
Le Soleil et nous: Météo et climat spatial
Université de Mons, Belgium, 28 September 2022

11. Clette, F.
Le Soleil et nous: météo et climat spatial
Euro Space Center, Redu (Belgium), 11 August 2022

12. Clette, F.
Le cycle instable des taches solaires. Quel mécanisme et quels impacts sur Terre?
Open Door Days, Space Pole Uccle, 25 September 2022

13. Clette, F.
Un cycle qui recycle: aux sources de l'activité magnétique solaire
Rencontres des Observateurs du Soleil, Serbannes Vichy (France), 25 June 2022

14. Crosby, N.
Weather and Climate in Space
Open Door Days, Space Pole Uccle, 25 September 2022

15. Defraigne, P.
Combien de temps dure une seconde ?
Open Door Days, Space Pole Uccle, 24 September 2022

16. De Kemper, E.
Comment sonder la couche d'ozone à l'aide des étoiles ?
Open Door Days, Space Pole Uccle, 24-25 September 2022

17. de Patoul, J.
Space weather and the daily work of a forecaster
Open Door Days, Space Pole Uccle, 24 September 2022

18. de Patoul, J.
La météorologie spatiale et le travail quotidien des prévisionnistes
Open Door Days, Space Pole Uccle, 24 September 2022

19. Dewitte, S.
Klimaatsverandering meten vanuit de ruimte
Open Door Days, Space Pole Uccle, 24 September 2022

20. D'Huys, E.
Alarm, een zonnestorm op komst!
Open Door Days, Space Pole Uccle, 25 September 2022

21. D'Huys, E.
Alarm, een zonnestorm op komst!
Summer Space festival, Brussels, 25 June 2022

22. D'Huys, E.
Alarm, een zonnestorm op komst!
Wetenschapsbattle, Gent, 22 March 2022

23. D'Huys, E.
Alarm, een zonnestorm op komst!
Dag van de Wetenschap, Planetarium, Brussels, 27 November 2022

24. D'Huys, E.; Berghmans, D.; Vanlommel, P.
De koninklijke sterrenwacht op reis naar de zon
Zonnekijkdag, Cosmodroom Genk, 3 July 2022

25. Dils, B.
Hoe werken broeikasgassen?
Open Door Days, Space Pole Uccle, 25 September 2022

26. Errera, Q.
La couche d'ozone
Open Door Days, Space Pole Uccle, 24 September 2022

27. Hamdi, R.
Le réchauffement global : les dernières nouvelles du rapport du GIEC AR6
Open Door Days, Space Pole Uccle, 25 September 2022

28. Janssens, J.
De kunst van het zonnewaarnemen
Lecture for Astronomy Course at MIRA Public Observatory, Grimbergen, 7 September 2022

29. Janssens, J.
De activiteit van onze Zon
Heelal (Sterrenkijkkrant), pp. 3-5, November 2022

30. Janssens, J.
Best of 2021
STCE YouTube channel, 12 April 2022

31. Maggiolo, R.
Les champs magnétiques planétaires protègent-t-ils les atmosphères ?
Open Door Days, Space Pole Uccle, 25 September 2022

32. Marqué, C.
Observations radioastronomiques - Station de Humain
IBPT visit at BIRA-IASB, 9 December 2022

33. Meeus, F.; Berghmans, D.
MIRA Ceti sprak met... David Berghmans
Volkssterrenwacht MIRA interviews, 2022-03

34. Merlaud, A.
Pourquoi faire confiance aux modèles du climat?
Open Door Days, Space Pole Uccle, 25 September 2022

35. Pierrard V.; Botek E.; Darrouzet F.
Qu'est-ce que la plasmasphère terrestre et comment l'étudier?
Ciel et Terre, 138, 3, 79, 2022

36. Pierrard, V.; Botek, E.; Darrouzet F.; Fratta, S.
What is the Earth's plasmasphere and how do we study it in Belgium?
BIRA-IASB Aeronomy YouTube channel, 15 April 2022

37. *SWIC - Space Weather Introductory Course*
D'Huys, E.; Janssens, J.; Vanlommel, P.; STCE collaborators (Marqué, C.; Martinez, A.; Clette, F.; Bechet, S.; Dierckxsens, M.; De Donder, E.; Chevalier, J.-M.; de Patoul, J.; SIDC/RWC; B.USOC) and international partners (Doornbos E. (KNMI); Sievers, K. (KSAW))
Lectures, Exercises, Visits, Quiz, Dedicated courses

- SWIC 2022/1 on 14-15-17-18 February 2022 (online)
- SWIC 2022/2 on 14-15-16 March 2022
- SWIC 2022/3 on 13-14-15 June 2022
- SWIC 2022/4 on 21-22-23 November 2022
- SWIC 2022/5 on 5-6-8-9 December 2022 (online)

38. Vanlommel, P.; D'Huys, E.; Janssens, J.
STCE Newsletter
Weekly newsletter, 51 issues, 2022

39. Vanlommel, P.
Noorderlicht: hemelse wetenschap
Open Door Days, Space Pole Uccle, 24 September 2022

40. Vanlommel, P.
When the Sun vanishes
STCE YouTube channel, 4 November 2022

41. Verbeeck, C.
Bijzonder beroep: zonnefysicus Cis Verbeeck
Bekend in Nijlen, pp. 18-21, 8 March 2022

42. Verhoelst, T.; Keppens, A.
De ozonlaag
Open Door Days, Space Pole Uccle, 24 September 2022

43. Walsh, R.; Rinsler, A.; D'Huys, E.; Vanlommel, P.
SUNatRMCA timelapse
STCE YouTube channel, 13 April 2022

44. Zychova, L.
Space Weather and its role in history
The Sisyfos club, the Charles University, Prague, The Czech republic, 18 February 2022

45. Zychova, L.
Solar Storm 1967: Us and Them
Cosmo Tea, Masaryk University, Brno, The Czech Republic, 25 February 2022

46. Zychova, L.
Women in Space, an online discussion
American Centre, US Embassy in Prague, The Czech republic, 7 March 2022

47. Zychova, L.
Space Weather and you
Czech Liaison Office for Education and Research in Brussels (CZELO), 8 March 2022

48. Zychova, L.
Universe, will you kill us?
Nerdland festival, Wachtebeke, 4 June 2022 (selected talk)

49. Zychova, L.
Humanism in science
Opening of the ‘I want to be a human’ exhibition in the Planetarium, Brussels, 22 September 2022

50. Zychova, L.
Science & humanism
Masaryk University, The Czech Republic, 7 October 2022

51. Zychova, L.
A Touch of Space Weather workshop
Open Doors at Space Pole, Uccle 24-25 September 2022

52. Zychova, L.
A Touch of Space Weather workshop
Astropolis, Oostende, 19-20 July 2022

53. Zychova, L.
A Touch of Space Weather workshop
De Kade, Brugge, 17 May 2022

54. Zychova, L.
A Touch of Space Weather workshop
Bogaert International School, Uccle, 14 December 2022

55. Zychova, L.
A Touch of Space Weather workshop
IRSA, Uccle, 15 June 2022

Thou shalt understand!… Space weather experts explaining to each other the fine details of plasma cloud propagation using hands, feet, doodles, a coffee thermos, and a USB power cable. Yeah, seriously!

List of abbreviations

~	About, proportional to
Δ	Delta (difference)
//	Parallel
⊥	Perpendicular
% dec^{-1}	change (percentage) per decade
1D, 2D, 3D,…	One, two, three,… dimensional
Å	Ångstrom (0.1 nm)
A	Article
AAS	American Astronomical Society
ACE	Advanced Composition Explorer
AGU	American Geophysical Union
AIA	Atmospheric Imaging Assembly (SDO)
ALARM	multi-hAzard monitoring and earLy wARning systeM
AM	Amplitude Modulation
AMS	American Meteorological Society
ANeMoS	Athens Neutron Monitor Station
AOGS	Asia Oceania Geosciences Society
APS	(1) American Physical Society ; (2) Active Pixel System (PROBA2)
AR	(1) Active Region ; (2) Annual Report
ARASE	Nickname of the ERG satellite (JAXA)
ARCAS	Augmented Resolution Callisto Spectrometer
ARTIST	Automatic Real-Time Ionogram Scaler with True height (software)
ASGARD	An educational space programme for schools (no acronym)
ASL	Above Sea Level
ASOPOS	Assessment of Standard Operating Procedures for OzoneSondes
ASPECS	Advanced Solar Particle Event Casting System
ASPIICS	Association of Spacecraft for Polarimetric and Imaging Investigation of the Corona of the Sun (PROBA-3)
AT-AP-RASC	ATlantic / Asia-Pacific Radio SCience meeting
AU, au	Astronomical Unit; about 150 million km
B	Magnetic field (strength)
B_0	Heliographic latitude of the central point of the solar disk (The range of B_0 is ±7.23°)
BE	Belgium
BE-WISSDOM	Belgian Web Incessant Screening for SDO Mission
BELSPO	Belgian Science Policy Office
BeNELux	Belgium, The Netherlands, and Luxembourg
BIRA	Koninklijk Belgisch Instituut voor Ruimte-Aëronomie
BIRA-IASB	Royal Belgian Institute for Space Aeronomy
BISA	Royal Belgian Institute for Space Aeronomy
BNCGG	Belgian National Committee for Geodesy and Geophysics
BRAIN-be	Belgian Research Action through Interdisciplinary Networks (BELSPO)
BRAMS	Belgian RAdio Meteor Stations
B.RCLab	Belgian Radiometric Characterization Laboratory
BSPM	Belgian SWIFF Plasmasphere Model
BUKS	Belgium, UK, and Spain
B.USOC	Belgian User Support and Operation Centre
Bz	Component of the IMF perpendicular to the ecliptic ("north-south" component)
°C	Degrees Celsius
°C dec^{-1}	°C per decade
C1, C2, C3	Coronagraphs of LASCO (SoHO)
C-class flare	Common x-ray flare
C/N_0	Carrier-to-Noise
CA	COST Action (COST)
Ca II H	A blue line in the solar spectrum at 396.85 nm
Ca II K	A blue line in the solar spectrum at 393.37 nm
CACTus	Computer Aided CME Tracking software
CALLISTO	Compound Astronomical Low frequency Low-cost

	Instrument for Spectroscopy and Transportable Observatory
CAP	Communicating Astronomy with the Public
CCMC	Community Coordinated Modeling Center
CESRA	Community of European Solar Radio Astronomers
CH	Coronal Hole
CH_4	Methane
CH_4TIR	CH4 Thermal InfraRed
CIR	Co-rotating Interaction Region
Cluster	ESA/NASA mission to study the Earth's magnetosphere (no acronym)
cm, cm^2, cm^3	centimeter, square centimeter, cubic centimeter
CME	Coronal Mass Ejection
CMOS	Complementary Metal-Oxide-Semiconductor
CmPA	Center for mathematical Plasma-Astrophysics
CNES	Centre national d'études spatiales (France)
CNRS	Centre national de la recherche scientifique (France)
Co.	Cooperation
CO_2	Carbon Dioxide
co-Is	co-investigators
COMESEP	COronal Mass Ejections and Solar Energetic Particles
COPUOS	COmmittee on the Peaceful Uses of Outer Space (UN)
COR (1/2)	Coronagraph (Inner/Outer) onboard STEREO
CORS	Continuously Operating Reference Stations (GNSS)
COSPAR	COmmittee on SPAce Research
COST	(European) COoperation in Science & Technology
COTS	Commercial off-the-shelf
COVID-19	Coronavirus disease 2019
CR	Carrington Rotation
CRAF	Committee on Radio Astronomy Frequencies
CrIS	Cross-track Infrared Sounder (Suomi National Polar-orbiting Partnership)
CROM	A type of pyrheliometer developed by D. Crommelynck (RMI)
CSL	Centre Spatial de Liège
CubeSat	A small satellite measuring 10cm x 10cm x 10cm
dB-Hz	decibel-Hertz (bandwidth relative to 1 Hz)
DeMeLab	Detector Measurements Laboratory (aka STCL)
Digisonde	Digitally Integrating Goniometric IonoSONDE
DIGISUN	A software application for digitization of scanned sunspot drawings
DLR	German Aerospace Center
dm, dm^2, dm^3	decimeter, square decimeter, cubic decimeter
DOI	Digital Object Identifier
DOU	Dourbes (Intermagnet)
DoY	Day of Year
DPS	(1) Division for Planetary Sciences (EPSC) ; (2) Digital Portable Sounder
Dr.	Doctor
DRBS	Dourbes (Belgium, NMDB)
DSCOVR	Deep Space Climate Observatory
Dst	Disturbance Storm Time index (geomagnetic)
DYASTIMA	Dynamic Atmospheric Shower Tracking Interactive Model Application
E	East
E, E_- , E_+	Energy, Ingoing energy, Outgoing energy
e.g.	exempli gratia (example given)
e-Callisto	extended Compact Astronomical Low-cost Low-frequency Instrument for Spectroscopy and Transportable Observatory
EC	European Commission
ECC	Electrochemical Concentration Cell
ECMWF	European Centre for Medium-range Weather Forecasts
ed.	Edition
Eds.	Editors
EFW	Electric Field and Waves instrument (Van Allen probes)

EGNOS	European Geostationary Navigation Overlay Service
EGNSS	European GNSS
EGU	European Geosciences Union
E-GVAP	EUMETNET GNSS water Vapour Programme
EIS	EUV imaging spectrometer (Hinode)
EISCAT	European Incoherent SCATter scientific association
EIT	Extreme ultraviolet Imaging Telescope (SOHO)
ELF	Extreme Low frequency (3-30 Hz)
EM	(1) Electromagnetic (2) Engineering Model
EMFISIS	Electric and Magnetic Field Instrument Suite and Integrated Science (Van Allen Probes)
ENVISAT	Environmental Satellite (ESA)
EPD	Energetic Particle Detector
EPN	(1) EUREF Permanent Network (2) Europlanet
EPOS	European Plate Observing System
E-PROFILE	EUMETNET Profiling Programme
EPS	European Physical Society
EPSC	European Planetary Science Congress
EPT	Energetic Particle Telescope (PROBA-V)
ERA	ECMWF re-analysis
ERAI , ERA5	ERA-Interim, 5th ERA
erg	10^{-7} Joule
ERG	Exploration of energization and Radiation in Geospace (now called ARASE ; JAXA)
Es	Sporadic E-layer (ionosphere)
ES	Earth System (Science and Environmental Management (COST)
ESA	European Space Agency
ESAC	European Space Astronomy Centre
ESC	Expert Service Centre (SSCC)
ESD	ElectroStatic Discharge
ESCAPE	(1) European SpaceCraft for the study of Atmospheric Particle Escape (2) European Science Cluster of Astronomy & Particle physics ESFRI research infrastructures
ESERO	European Space Education Resource Office
ESFRI	European Strategy Forum on Research Infrastructures
ESOC	European Space Operations Centre
ESPD	European Solar Physics Division (EPS)
ESPM	European Solar Physics Meeting
ESTEC	European Space Research and Technology Centre
E-SWAN	European Space Weather and Space Climate Association
ESWW	European Space Weather Week
et al.	et alii (and other)
etc.	et cetera (and so forth)
ETH	Eidgenössische Technische Hochschule Zürich
EU	European Union
EUHFORIA	European Heliospheric Forecasting Information Asset
EUI	Extreme-Ultraviolet Imager (Solar Orbiter)
EUMETNET	Network of European Meteorological Services
EUMETSAT	European Organisation for the Exploitation of Meteorological Satellites
EUREF	EUropean Reference Frame
EUV	Extreme Ultraviolet
EUVST	EUV High-throughput Spectroscopic Telescope (Solar-C ; Jaxa)
EUVI	Extreme Ultraviolet Imager (STEREO/SECCHI; LGRRS)
eV	electron volt (1 eV = 1.602 × 10^{-19} joules)
EVE	Extreme ultraviolet Variability Experiment (SDO)
ExoMars	Exobiology on Mars (ESA, Roscosmos)
$F_{10.7}$, $F_{10.7\ cm}$	Solar radio flux at 10.7 cm wavelength
F_2	Main ionospheric layer
FAIR	Findable, Accessible, Interoperable, and Re-usable
FARWEST	FAst Radiation diffusion with Waves ESTimator

FARSUN	Findability and Accessibility of historical Raw SUnspot Numbers
Fe IX-X	8 respectively 9 times ionized iron
FITS	Flexible Image Transport System
FM	(1) Flight Model (2) Frequency Modulation
FMI	Finnish Meteorological Institute
FNRS	Fonds National de la Recherche Scientifique
foE	Critical frequency E-layer
foEs	Sporadic E critical frequency
foF2	Critical frequency F2-layer
FOV	Field-Of-View
FP7	Framework Programme 7 (EU)
Fri3D	Flux Rope in 3D
FRS	Fonds de la Recherche Scientifique
FSI	Full Sun Imager (Solar Orbiter / EUI)
ft	foot or feet (1 ft = 30,48 cm)
FTE	Full-Time Equivalent
ftp	file transfer protocol
FUV	Far Ultraviolet
G, GB	Gigabyte (10^9 bytes)
Galileo	European GNSS
GASS	General Assembly and Scientific Symposium
GAW	Global Atmospheric Watch (WMO)
GBO	Ground-Based Observatory
GCR	Galactic Cosmic Rays
GEANT-4	GEometry ANd Tracking (simulation platform)
GEO	A circular geosynchronous orbit 35,786 km in altitude
GeV	Giga electronvolt (10^9 . 1.6 . 10^{-19} Joule)
GFZ	Deutsches GeoForschungsZentrum (German Research Centre for Geosciences)
GHz	Gigahertz (10^9 Hz)
GLE	Ground Level Enhancement
GLONASS	GLObal NAvigation Satellite System (Russia)
GMAC	Global Monitoring Annual Conference
GML	Global Monitoring Laboratory
GNSS	Global Navigation Satellite System
GOES	Geostationary Operational Environmental Satellite
GOME	Global Ozone Monitoring experiment (SCIAMACHY)
GOMESCIA	GOME/SCIAMACHY/GOME-2
GONG	Global Oscillation Network Group
GPS	Global Positioning System (USA)
GRAPE	GNSS Research and Application for Polar Environment
GSE	Geocentric Solar Ecliptic system
GSFC	Goddard Space Flight Center
GTO	Geostationary Transfer Orbit
h	(1) hour ; (2) Planck's constant (6.62607004 × 10^{-34} m^2 kg / s)
H	(1) Hydrogen ; (2) Heat flux
H-alpha (Hα)	A red visible spectral line at 656.28 nm created by Hydrogen
H2020	Horizon 2020 (EU)
He, He II	Helium, ionized Helium
HEGIFTOM	Harmonization and Evaluation of Ground-based Instruments for Free Tropospheric Ozone Measurements
HEK	Heliophysics Events Knowledgebase
Helios 1, 2	Two joint German-American space missions in the 1970s (no acronym)
HESPERIA	High Energy Solar Particle Events foRecastIng and Analysis
HF	High Frequency (3-30 MHz)
HI	(1) Neutral atomic Hydrogen ; (2) Heliospheric Imager (STEREO)
Hinode	A JAXA/NASA solar mission : Solar-B satellite ("sunrise")
h_mF_2	peak density height of F_2-layer
HMI	Heliospheric and Magnetic Imager (SDO)
hPa	hectopascal (atmospheric pressure)

HRI	High Resolution Imager (Solar Orbiter / EUI)
HRIEUV	High Resolution Imager in the EUV (Solar Orbiter / EUI)
HRILYA	High Resolution Imager in Ly-α (Solar Orbiter / EUI)
HSRS	Humain Solar Radio Spectrograph
HSS	High Speed Stream
HuRAS	Humain Radio Astronomy Station
HWM	Horizontal Wind Model
HXR	Hard x-rays
Hz	Hertz (per second)
i	The index in a counter or series
I	Current
I-V	Current-Voltage
IAC	International Astronautical Congress
IAG	International Association of Geodesy
IAGA	International Association of Geomagnetism and Aeronomy
IAS	Institut d'Astrophysique Spatiale (France)
IASB	Institut royal d'Aéronomie Spatiale de Belgique
IASC	International Arctic Science Committee
IAU	International Astronomical Union
iCACGP	international Commission on Atmospheric Chemistry and Global Pollution
ICARUS	a new inner heliospheric model for the simulation of a steady background solar wind and the propagation and evolution of superposed CMEs (KUL; no acronym)
ICAO	International Civil Aviation Organization
ICCC	Inter-Commission Committee on "Geodesy for Climate Research"
ICMA	International Commission on the Middle Atmosphere
ICME	Interplanetary CME
ICSO	International Conference on Space Optics

ICT	Information and Communication Technologies
IDL	Interactive Data Language
i.e.	"id est" (that is)
IEEE	Institute of Electrical and Electronics Engineers
IGAC	International Global Atmospheric Chemistry project
IGS	International GNSS Service
IMC	International Meteor Conference
IMF	Interplanetary Magnetic Field
IMO	International Meteor Organization
INGV	Istituto nazionale di geofisica e vulcanologia (Italy)
INSPIRE	(1) International Satellite Program in Research and Education (2) Infrastructure for Spatial Information in the European Community (EU)
IOP	Institute of Physics
IPAG	Institut de Planétologie et d'Astrophysique de Grenoble
IPC	International Pyrheliometer Comparison
IQR	InterQuartile Range
IR	Infrared
IRAP	Institut de Recherche en Astrophysique et Planétologie (France)
IRI	International Reference Ionosphere
IRIS	Interface Region Imaging Spectrograph (NASA)
IRM(B)	Institut Royal Météorologique (de Belgique)
IRSA	Institut Royal pour Sourds et Aveugles (Brussels, Belgium)
ISAS	Institute of Space and Astronautical Science
ISC	(1) International Science Council; (2) International Steering Committee
ISN	International Sunspot Number
ISO	International Organization for Standardization
ISS	International Space Station
ISSI	International Space Science Institute

ISSS	(1) International School of Space Science; (2) International School/Symposium for Space Simulations
ISWAT	International Space Weather Action Teams (COSPAR)
IT	Information Technology
IUGG	International Union of Geodesy and Geophysics
IVOA	International Virtual Observatory Alliance
IWV	Integrated Water Vapour
JAXA	Japan Aerospace Exploration Agency
JGR	Journal of Geophysical Research
jHV	jHelioViewer
JOSIE	Jülich Ozone Sonde Intercomparison Experiment
JPEG	Joint Photographic Experts Group
JSON	JavaScript Object Notation
JSWSC	Journal of Space Weather and Space Climate
JUICE	JUpiter ICy moons Explorer
k	wave number
K	(1) Local K index: A 3-hour geomagnetic index, ranging from 0 (quiet) to 9 (extremely severe storm); (2) degrees Kelvin
K*	Local 1-minute resolution K index
Ka-band	"Kürz above": Radio frequency band from 27-40 GHz
KAW	Kinetic Alfvén Waves
KBEL	Local K index for Belgium
keV	kilo electronvolt ($10^3 . 1.6 . 10^{-19}$ Joule)
kHz	kilo Hertz (10^3 /second)
KI	Potassium iodide
km, km^2	kilometer, square kilometer
km/s	kilometers per second
KMI	Koninklijk Meteorologisch Instituut
KNMI	Koninklijk Nederlands Meteorologisch Instituut
K_p	"planetarische Kennziffer", a geomagnetic index, ranging from 0 (quiet) to 9 (extremely severe storm)
KSO	Kanzelhöhe Solar Observatory
KSB	Koninklijke Sterrenwacht van België
KUL, KULeuven	Katholieke Universiteit Leuven
kV	kiloVolt (10^3 Volt)
λ	wavelength
λ_e	electron inertial length
l/m^2	Liter per square meter
L-class	Large class satellite (ESA)
L	Letter (manuscript)
L*	Set of Earth's magnetic field lines which cross the Earth's magnetic equator at * earth radii from the centre of the Earth (e.g. L = 2); also known as McIlwain parameter
L_0	Heliographic longitude of the central point of the solar disk
L1, … , L5	First, … , fifth Lagrangian point
L1, L2	GPS frequencies: L1 = 1575.42 MHz, L2 = 1227.60 MHz
LASCO	Large Angle Spectrometric Coronagraph (SOHO); small (C2) and wide (C3) field of view
LASP	Laboratory for Atmospheric and Space Physics
Lat	Latitude
LATMOS	Laboratoire ATmosphères, Milieux, Observations Spatiales (France)
LBL	line-by-line
LDE	Long Duration Event
LEO	Low Earth Orbit (below 2000 km ASL)
LIDAR	LIght Detection And Radar
LIEDR	Local Ionospheric Electron Density profile Reconstruction
LMSAL	Lockheed Martin Solar and Astrophysics Laboratory
LOC	Local Organising Committee
LOFAR	Low-Frequency Array
Lon	Longitude
LOTUS	Long-term Ozone Trends and Uncertainties in the Stratosphere
LPV-200	Localizer Performance with Vertical guidance until the aircraft is 200 ft above the runway
Ls	Solar longitude

LT	Local Time
Ly-α	Lyman-alpha, a spectral line in the VUV at 121.6 nm
LYA	Ly-α
LYRA	Large Yield Radiometer, formerly called Lyman Alpha Radiometer (PROBA2)
LWS	Living With a Star
µm	micrometer (10^{-6} meter)
M-class	Medium class satellite (ESA)
M-class flare	Medium x-ray flare
m, m^2, m^3	Meter, square meter, cubic meter
MAB	Manhay (Intermagnet)
MACH	Magnetic fields, Atmospheres, and the Connection to Habitability
MagEIS	MAGnetic Electron Ion Spectrometer (Van Allen probes)
MAJIS	Moons And Jupiter Imaging Spectrometer (JUICE)
MAPLD	Military and Aerospace Programmable Logic Devices
MB	Megabyte (10^6 bytes)
mbar	millibar
MEO	Medium Earth Orbit (between 2000 and 35,786 km ASL)
METIS	Multi Element Telescope for Imaging and Spectroscopy (SolO)
MeV	Mega electronvolt (10^6 . 1.6 . 10^{-19} Joule)
MHD	Magnetohydrodynamics
MHz	Megahertz (10^6/s)
MImOSA	Magnetic imaging of the outer solar atmosphere
MIT	Massachusetts Institute of Technology
MJD	Modified Julian Day
MLH	mixing layer height
MLT	Magnetic Local Time
mm, mm^2	millimeter (10^{-3} meter), square mm
Mm	Megameter (10^6 meter)
mm/s	millimeter per second
MOC	Mission Operations Center
MOMA	Multi-wavelength Observations and Modelling of Aurora
MoMo	Model of Mars Ionosphere
MOMSTER	MObile Meteor STation for Education & outreach
MPPC	Max Planck-Princeton Center
MPS	Max Planck Institute for Solar System Research
ms	millisecond (10^{-3} second)
MUF, MUF3000	Maximum Usable Frequency, the maximum radio frequency which can be reflected by the ionosphere for a given distance of transmission e.g. 3000 km
MUV	Mid Ultraviolet
ν	Frequency
N	North
N-S	North-South
N_2	Nitrogen
N_2O	Nitrous oxide (“laughing gas”)
nA	nano Ampère (10^{-9} meter)
NASA	National Aeronautics and Space Administration
NASU	National Academy of Sciences of Ukraine
NATO	North Atlantic Treaty Organization
Nc, Ns, Ng	the number of spots Ns, the number of groups Ng, and the composite Nc = Ns + 10Ng
NDACC	Network for the Detection of Atmospheric Composition Change
NeQuick	Electron density Quick calculation model (ionospheric model)
Net-TIDE	Pilot Network for Identification of Travelling Ionospheric Disturbances in Europe
NIR	Near IR
NL	The Netherlands
NM	Neutron Monitor
nm	nanometer (10^{-9} meter)
NMDB	Neutron Monitor DataBase
N_mF_2	peak density of F_2-layer
No.	Number of
NO_2	Nitrogen dioxide
NOAA	National Oceanic and Atmospheric Administration
NOMAD	Nadir and Occultation for MArs Discovery (ExoMars)
NRT	Near Real Time
ns	nanosecond (10^{-9} second)

NSO	National Solar Observatory
nT	nano-Tesla (10^{-9} Tesla)
NUV	Near Ultraviolet
NV/SA	Naamloze Vennootschap / Société Anonyme
NWC	Northwest Cape of Australia
NWP	Numerical Weather Prediction
O	Oxygen
O_3	Ozone
O3S	Ozone Sonde
O3S-DQA	O3S Data Quality Assessment
ODC	On Duty Center (PECASUS)
ORB	Observatoire Royal de Belgique
ORFEES	Observation Radio Fréquences pour l'Etude des Eruptions Solaires
P	The position angle between the geocentric north pole and the solar rotational north pole measured eastward from geocentric north. The range in P is $\pm$26.3°
P2SC	PROBA2 Science Center
PARADISE	Particle Radiation Asset Directed at Interplanetary Space Exploration
PB	Petabyte (10^{15} bytes)
PBC	Primary Backup-Center (PECASUS)
PC	Personal Computer
PDF	Probability Density Functions
PECASUS	Partnership for Excellence in Civil Aviation Space weather User Services (ICAO) *(original: Pan-European Consortium for Aviation Space weather User Services)*
PFSS	Potential Field Source Surface
pfu	particle (proton) flux unit: the number of particles registered per second, per square cm, and per steradian
PhD	Doctor of Philosophy
PHI	Polarimetric and Helioseismic Imager (Solar Orbiter)
PI	Principal Investigator
PIC	Particle -in-Cell
PICASSO	PICo-satellite for Atmospheric and Space Science Observations
PITHIA-NRF	Plasmasphere Ionosphere Thermosphere Integrated Research Environment and Access services: a Network of Research Facilities (EU)
PRESTO	(1) Fast warning message for important SWx events (2) PREdictability of the Solar-Terrestrial Coupling (SCOSTEP)
PROBA	PRoject for OnBoard Autonomy
PROBA-V	PROBA-Vegetation
PROSPER	PRObabilistic Solar Particle Event foRecasting model
ps	picosecond (10^{-12} second)
PSP	Parker Solar Probe
PTB	Physikalish-Technische Bundesanstalt (Germany)
PWE	Plasma Wave Experiment (ARASE)
px	pixel
Python	Programming language (no acronym)
Q&A	Questions and Answers
QA	Quality Assurance
QC	Quality Control
QE	Quantum Efficiency
QPP	Quasi-periodic pulsation
ρ_T	gyroradius
R	Resistor
$R_\odot$	Solar radius (696.000 km)
r^2	the square of the correlation coefficient
R&D	Research and Development
R-ESC	Space Radiation ESC (SSCC)
RAS	Royal Astronomical Society
RB-FAN	Radiation Belt Forecast And Nowcast
R_e	Earh radius (radii)
RF	Radio Frequency
RHESSI	Reuven Ramaty High Energy Solar Spectroscopic Imager
RMI(B)	Royal Meteorological Institute (of Belgium)
RMS	Root Mean Square
ROADMAP	ROle and impAct of Dust and clouds in the Martian AtmosPhere
ROB	Royal Observatory of Belgium
Roscosmos	Russian Space Agency
RSSB	Royal Statistical Society of Belgium
R_s	Solar radius (radii)
R_{sun}	Solar radius (~ 696.000 km)

RWC	Regional Warning Center
Rx	Receiver
σ	sigma (confidence level)
s	second
S	South
S-band	Radio frequency band from 2-4 GHz
S/C	Spacecraft
S-class	Small class satellite (ESA)
SAA	South Atlantic Anomaly
SACS	Support to Aviation Control System
SANSA	South African National Space Agency
SAR	(1) Superactive region; (2) Synthetic Aperture Radar
SAWS	SEP Advanced Warning System
SBC	Secondary Backup-Center (PECASUS)
SC24, SC25	Solar Cycle 24, Solar Cycle 25
SCAR	Scientific Committee on Antarctic Research
SCIAMACHY	SCanning Imaging Absorption spectroMeter for Atmospheric CHartographY (ENVISAT)
SCK-CEN	Studiecentrum voor Kernenergie - Centre d'Etude de l'Energie Nucléaire
SCOPE	Solar Coronagraph for OPErations
SCOSTEP	Scientific Committee on Solar Terrestrial Physics
SDO	Solar Dynamics Observatory
SECCHI	Sun Earth Connection Coronal and Heliospheric Investigation (STEREO)
SEE	Single Event Effects
SEESAW	Space Environment Engineering and Science Applications Workshop
SEP	Solar Energetic Particle
SEPEM	Solar Energetic Particle Environment Modelling
SEU	Single Event Upset
SFU, sfu	Solar Flux Unit (10^{-22} W m^{-2} Hz^{-1})
SGEPSS	Society of Geomagnetism and Earth, Planetary and Space Science
SHINE	Solar Heliospheric & Interplanetary Environment
SIDC	Solar Influences Data analysis Center
SILSO	Sunspot Index and Long-term Solar Observations (ROB)
SIMBA	Sun-earth IMBAlance
SLP	Sweeping / Segmented / Single/ Split / Spherical Langmuir Probe
SLT	Solar Local Time
SMD	Safety and Metrology Division (Federal Services for Metrology)
SMILE	Solar wind-Magnetosphere-Ionosphere Link Explorer (ESA)
sms	short message service
S_N , SN	(1) Sunspot Number ; (2) Space weather and Near-earth objects ; (3) Standard normal homogenization tests
SO	Solar Orbiter
SOC	Science Operations Centre
SOHO	SOlar & Heliospheric Observatory
Solar-C	Next Generation Solar physics Mission (JAXA)
SOLARNET	European network of solar physics researchers and facilities (H2020)
SOLCON	SOLar CONstant radiometer
SOLIS	Synoptic Optical Long-term Investigations of the Sun (NSO)
SolO	Solar Orbiter
SOP	Standard Operating Procedures
SoSpIM	Spectral Solar Irradiance Monitor (Solar-C)
SOVA	SOlar constant and VAriability
SPADE	Small Phased Array DEmonstrator
SPD	Solar Physics Division (AAS)
SPENVIS (-NG)	SPace ENVironment Information System (- Next Generation)
SPICE	Spectral Imaging of the Coronal Environment (SolO)
SPIE	Society of Photo-optical Instrumentation Engineers
SPOCA	Spatial Possibilistic Clustering Algorithm

SPRING	Solar Physics Research Integrated Network Group (SOLARNET)
SPS	Science for Peace and Security (NATO)
sr	steradian
SRB	Solar Radio Burst
SREM	Standard Radiation Environment Monitor (Integral, Rosetta)
SSA	(1) Space Situational Awareness ; (2) singular spectrum analysis
SSCC	SSA Space Weather Coordination Centre (ESA)
SSI	Solar Spectral Irradiance
SSN	SunSpot Number
SSWRF II	2nd international workshop on Small Satellites for Space Weather Research and Forecasting
STCE	Solar-Terrestrial Centre of Excellence
STCL	Space Technology & Calibration Laboratories
STEM	Science, Technology, Engineering, Mathematics
STEAM	Science, Technology, Engineering, Arts, Mathematics
STEREO	Solar-TErrestrial RElations Observatory
STM	Structural Model
SunPy	software library for solar physics based on Python
SUVI	Solar Ultraviolet Imager (GOES)
SVO	Solar Virtual Observatory
SW	Space Weather (journal)
SWAP	Sun Watcher using APS detector and image Processing (PROBA2)
SWAVES	STEREO WAVES
SWE	Space Weather
SWEC	Space Weather Education Center
SWEK	Space Weather Event Knowledgebase
SWIC	Space Weather Introductory Course
SWIFF	Space Weather Integrated Forecasting Framework
SWOP	Space Weather OPerations
SWPC	Space Weather Prediction Center (USA)
SWT	Science Working Team
SWx	Space weather
SXR	Soft x-rays
SZA	Solar Zenith Angle
τ, t	Time
T, TB	Terabyte (10^{12} bytes)
TAP	Table Access Protocol
TEC	Total Electron Content
Tech-TIDE	Warning and Mitigation Technologies for TIDs Effects
TECO	Technical Conference on Meteorological and Environmental Instruments and Methods of Observation
TECu	TEC unit ($10^{16} e^{-} m^{-2}$)
T-FORS	Travelling ionospheric disturbances FORecasting System
TID	Travelling Ionospheric Disturbance
TIR	Thermal InfraRed
TOAR	Tropospheric Ozone Assessment Report
TROPOMI	TROPOspheric Monitoring Instrument (Sentinel-5 Precursor)
TSI	Total Solar Irradiance
TVAC	Thermal-VACuum chamber
Tx	Transmitter
UCAR	University Corporation for Atmospheric Research
UCL, UCLouvain	Université Catholique de Louvain
UFO	University FOrum (Ghent, Belgium)
UHF	Ultra High Frequency (0.3 - 3 GHz)
UK	United Kingdom
ULB	Université libre de Bruxelles
Ulysses	A joint ESA/NASA/Canada NRL mission to study the Sun (1990-2009; no acronym)
UNCOPUOS	United Nations Committee on the Peaceful Use of Outer Space
URAN	Ukrainian Radio Interferometer of NASU
URL	Uniform Resource Locator

URSI	International Union of Radio Science - Union Radio-Scientifique Internationale
US(A)	United States (of America)
USAF	United States Air Force
usb, USB	Universal Serial Bus
USET	Uccle Solar Equatorial Table
UT(C)	(Coordinated) Universal Time
UV	Ultraviolet
v	Velocity (speed)
V	Volt, voltage
V1, V2, …	Version 1, 2, …
VarSITI	Variability of the Sun and Its Terrestrial Impact
VERSIM	VLF-ELF Remote Sensing of Ionospheres and Magnetospheres
VHF	Very High Frequency (30-300 MHz)
VIP	Very Important Person
VIRGO	Variability of solar IRradiance and Gravity Oscillations (SoHO)
VIS	Visible
VKI	Von Karman Institute
VLF	Very Low Frequency (3-30 kHz)
VO	Virtual Observatory
Vol.	Volume
VSWMC	Virtual Space Weather Modelling Centre
VTEC	Vertical TEC
VUB	Vrije Universiteit Brussel
VUV	Vacuum Ultraviolet
VVS	Vereniging Voor Sterrenkunde (Belgian Astronomical Association)
W	(1) Watt; (2) West
WAAS	Wide Area Augmentation System (GPS/North-America)
W/m^2	Watt per square meter
WAVES	Radio and plasma wave investigation (WIND, STEREO)
WDC	World Data Center
WFOV	Wide Field Of View
WG	Working Group
WHPI	Whole Heliosphere and Planetary Interactions
WMO	World Meteorological Organization
WP	Work Package
WPI	Wave-Particle Interactions
WRC	World Radiation Center
WRR	World Radiometric Reference
WS	Workshop
WSA	Wang-Sheeley-Arge (model for solar wind)
X-band	Radio frequency band from 8-12 GHz
X-class flare	Extreme x-ray flare
XRT	X-Ray Telescope (Hinode)
ZTD	Zenith Total Delay